Western Australian School of Mines: Minerals, Energy and Chemical Engineering

Investigation into mono ethylene glycol and impacts of its degradation on MEG regeneration and reclamation system

Edith A. Ugwumba (Odeigah)

This thesis is presented for the Degree of

Doctor of Philosophy

of

Curtin University

November 2022

Declaration

To the best of my knowledge and belief, this contains no materials previously published by any other person except where due acknowledgement has been made.

This thesis contains no material which has been accepted for the award of any other degree or diploma in any university.

Signed:…….

Date:…….

Acknowledgement

My special thanks to Curtin University and the Australian government for the opportunity to undertake this PhD study under the Curtin Research Training Program Scholarships; this opportunity is greatly appreciated.

My sincere thanks go to my supervisors, Franca Jones, Rolf Gubner and Moses Tade. I appreciate the help and support I received from all members of the Curtin corrosion Engineering and Industry centre, especially Ibukun, Ammar, Marissa, Hoda, Yu Long, Adam, Sami and Samer

Thank you to my lovely kids (Chika, Chigo and Oluchi), my father (Mr S. G. Odeigah), my brothers (Tony and Mark Odeigah) and all my family and friends for your love, understanding and support.

Lastly, but most importantly, my most sincere thanks go to the almighty God and two people without whom I will not have a thesis. First, my husband, Hyginus Chinagorom Ugwumba, thank you for all those numerous times you have had to rearrange plans to accommodate my studies and all the times you have encouraged me to see my studies to completion. Second, my primary Supervisor, Dr Thunyaluk (Kod) Pojtanabuntoeng, thank you for being a reliable academic and emotional support throughout my studies; your numerous 'yes, you can do this' has helped me pull through.

Thank you

List of publications

List of publications included as part of this thesis.

This thesis is assembled as a hybrid consisting of published papers that form the individual chapters listed below:

Chapter 2

Odeigah, E. A., & Pojtanabuntoeng, T. (2022). Regeneration and Reclamation of monoethylene glycol (MEG) Used as a Hydrate Inhibitor: A Review. *American Journal of Chemical Engineering*, *10*(2), 32-45.

Chapter 4

Odeigah, E. A., Pojtanabuntoeng, T., Jones, F., & Gubner, R. (2018). The effect of monoethylene glycol on calcium carbonate solubility at high temperatures. *Industrial & Engineering Chemistry Research*, *57*(46), 15909-15915.

Statement of the contribution of others

I, Edith Anwunli (Odeigah) Ugwumba, as the first author of the individual publications comprising each chapter of this thesis, was primarily involved in planning and conducting the experiments, data analysis and interpretation of the findings and manuscript preparations. Contributions by the co-authors are mentioned below.

Chapter 2

Thunyaluk Pojtanabuntoeng significantly contributed to the review and evaluation of the manuscripts.

Chapter 4

Thunyaluk Pojtanabuntoeng significantly contributed to the conception of experiments, data interpretation, and evaluation of the manuscripts. Rolf Gubner actively participated in the preparation and critical revision of the manuscripts. Franca Jones actively participated in the preparation and critical revision of the manuscripts.

Curtin Corrosion Engineering Industry Centre (CCEIC) under the Curtin University Western Australia School of Mines: Minerals, Energy and Chemical Engineering provided all the facilities for the project to conduct all experiments. The Curtin University Research Training Program (RTP) Scholarship assisted financially in conducting the project.

Author's Statement of Previous Publication

The author has previously published some results of data analyses and approaches discussed in this thesis during the preparation. The ideas and analysis techniques in these publications were developed as a part of the thesis background work by the author before publication. The following list details the previous publications by the author at the time of submission of this thesis.

Journal publication

Soames, A., **Odeigah, E. A.,** Al Helal, A., Zaboon, S., Iglauer, S., Barifcani, A., & Gubner, R. (2018). Operation of a MEG pilot regeneration system for organic acid and alkalinity removal during MDEA to FFCI switchover. *Journal of Petroleum Science and Engineering*, *169*, 1-14.

I assure that I have obtained, where necessary, permission from all the copyright owners to use any third-party copyright material reproduced in the thesis or to use any of my published work in which another party holds the copyright

Acknowledgement of Country

We acknowledge that Curtin University works across hundreds of traditional lands and custodial groups in Australia and with First Nations people around the globe. We wish to pay our most profound respects to their ancestors and members of their communities, past and present, and their emerging leaders. Our passion and commitment to working with all Australians and peoples from across the world, including our First Nations peoples, are at the core of our work, reflective of our institutions' values and commitment to our role as leaders in the Reconciliation space in Australia.

Abstract

Monoethylene glycol (MEG) is used as a hydrate inhibitor to lower the hydrate formation temperatures of gas in deep-water oil and gas production. The recovery and regeneration of MEG make it more economically viable for hydrate inhibition application as it offsets its relatively high purchase cost. The desirable outcome of MEG recovery and regeneration is to reduce salt and water content; however other undesirable outcomes are also being experienced during this process. A significant challenge in this field of study is to minimise fouling and scale formation in the MEG regeneration system while preserving the efficiency of regeneration and reclamation. There is also the issue of substantial MEG losses due to degradation due to chemical interactions during high-temperature regeneration.

One way of tackling these problems is to gain an in-depth understanding of the chemical properties of MEG and how they change during regeneration and reclamation with the aim of using this knowledge to promote desirable outcomes and impede undesirable ones. This work focuses on MEG chemistry changes in the reboiler of the MEG regeneration and reclamation system, with the main aim of contributing a more profound understanding regarding the MEG degradation, interaction with divalent ions and corrosivity with common MEG Recovery Unit (MRU) construction metal. This research was carried out in collaboration with the bench-scale MEG regeneration facility at the Curtin Corrosion Engineering Industry Center (CCEIC). The findings from this work are of enormous significance to the oil and gas industry. They are expected to

contribute to a deeper understanding of the fouling and oxidative thermal degradation chemistry in the MEG system.

This work presents a comprehensive review of the evolution of MEG regeneration systems over the years and introduces recent developments. Test methods for MEG assay using the ion chromatography (IC) technique were developed and validated for accuracy and precision on MRU MEG samples as a relatively lower cost option than other existing test methods. The solubility of calcium carbonate in MEG/water solution at high temperatures and high MEG concentrations is studied, and the effect of MEG on calcium solubility is reported. The oxidative stability of MEG under regeneration conditions in the MRU is investigated. Furthermore, the corrosive behaviour of thermally degraded MEG under MRU conditions is reported with the effects of produced organic acid on the CO_2 corrosion of carbon steel.

Table of content

List of Figures

List of Tables

Chapter 1

Introduction

1.1 Introduction

This work investigates the problems associated with monoethylene glycol (MEG) degradation during recycling for use as a thermodynamic hydrate Inhibitor (THI) in oil and gas production. MEG is an organic colourless liquid with IUPAC name ethane-1,2-diol. Hydrates are crystalline solids where gas molecules are trapped within cages of water molecules, whose formation, stability and decomposition depend on temperature, pressure, composition, and properties of the hydrate-forming gas [1]. Typical gas molecules are carbon dioxide, hydrogen sulphide, methane, ethane, propane or butane [2]. The cage-like structure of a gas hydrate is presented in Figure 1-1.

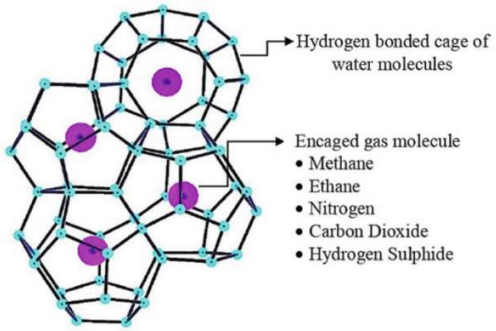

Figure 1-1: Structure of a gas hydrate (copied from [2])

Hydrates are formed when water mixes with gas under certain temperatures and pressures defined by a hydrate phase diagram like the one presented in Figure 1-2 for methane gas hydrate [3]. Hydrates usually form at temperatures much higher than the freezing point of water at a given pressure. Hydrate formation temperature and pressure relative to the freezing point of water are illustrated with points a, b and c in Figure 1-2. As seen in Figure 1-2, the mixture of water and methane gas at 1Mpa is liquid water and methane gas at -1 ^{0}C (point a). When pressure increases to 10 Mpa and the temperature remain at -1 ^{0}C (point b), the same water and methane mixture would exist as a hydrate; as point b falls inside the methane hydrate phase zone. At 10 Mpa, point c on the methane hydrate phase boundary shows hydrate formation onset at 12 ^{0}C. This hydrate onset temperature is much higher than the -0.8 °C freezing point of water at 10 Mpa [4]. Unfortunately, many deepwater oil and gas operations occur in cold weather and fall inside the hydrate forming region of the hydrate phase diagram [1]. Sloan et al. (2007) presents an in-depth description of the formation of natural gas hydrates and is recommended for further reading [5].

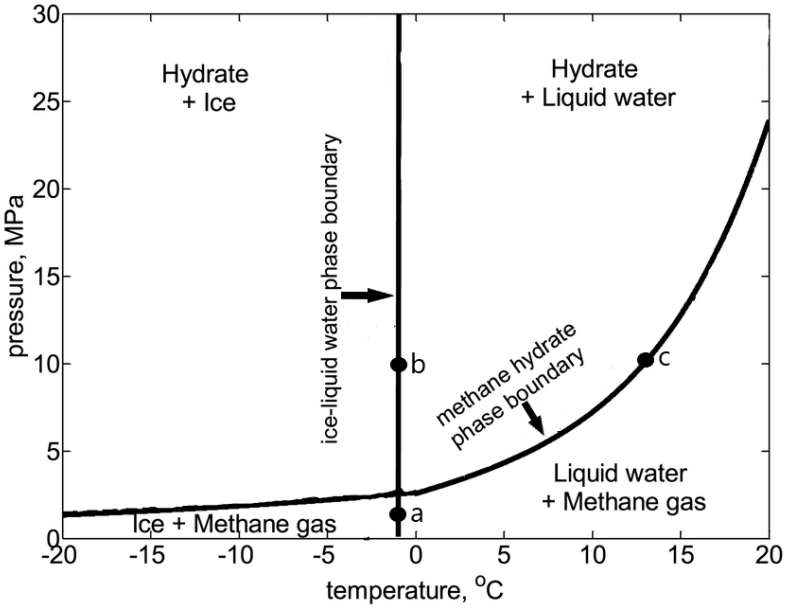

Figure 1-2: Methane Hydrate phase diagram (adapted from [3])

The formation of Hydrates presents critical safety, production, and operational challenges to oil and gas production as hydrates can grow large plugging production pipelines. Hydrate plugs like the ones shown in Figure 1-3 will disrupt pipeline production and are very difficult to remove [6-9]. Removing these hydrates involves lowering the pipeline pressure and slowly allowing the plug to thaw [10]. However, this process of thawing the hydrate only increases safety risks. The hydrate plug is more likely to become projectile during thawing, causing damage to the pipeline and downstream processing vessels. Consequently, preventing hydrate formation in the pipeline remains the best course of action.

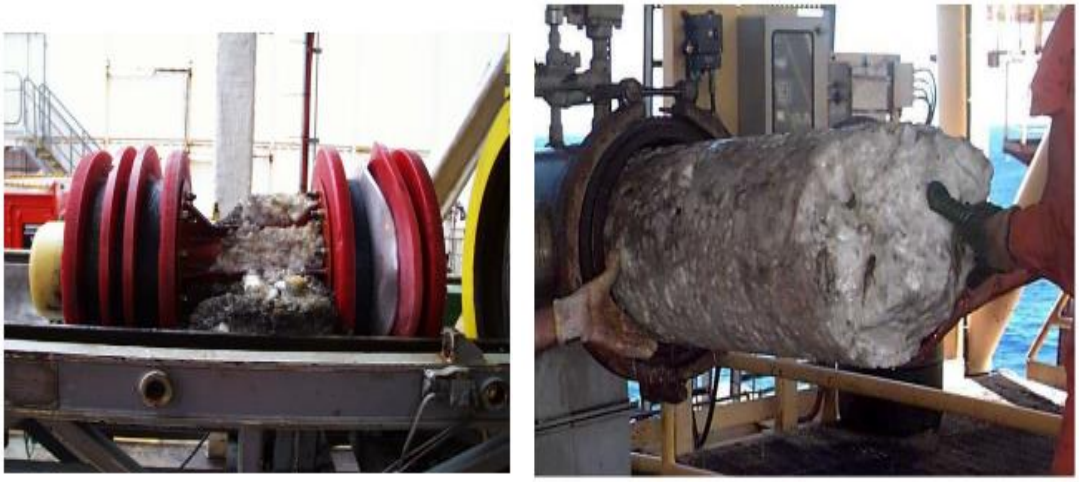

Figure 1-3: Hydrate plugs from oil and gas operations; photos courtesy of Statoil (left) and Petrobras (Right)

Four parameters are required for hydrate formation: water, gas, temperature (in the hydrate stable region) and pressure (in the hydrate stable region). Eliminating of any one of these four parameters will inhibit hydrate formation and form the basis for hydrate inhibition techniques [11]. Heating and insulation of pipelines have been used to eliminate "low temperature" and move operations outside the hydrate stability zone on the hydrate curve [10]. Likewise, operating the pipelines at lower pressures also moves flow outside the hydrate stability zone and inhibits hydrate formation. There is also the dehydration of gas to remove water and move outside the hydrate formation

region. However, removing any of these four parameters is not always practicable or desirable. For instance, it is not practical to dehydrate a gas producing from a subsea reservoir, nor is the cost of heating or insulating long tie-back pipelines desirable [11]. Consequently, the addition of chemicals for hydrate inhibition is often employed. Chemical additives for hydrate inhibition generally work by altering the properties of the water and gas mixture so that hydrate formation is inhibited during operation at temperatures and pressures in the hydrate stability region of the hydrate phase diagram [11].

Chemical additives for hydrate inhibition are generally categorised into low-dose hydrate inhibitors (LDHI) and thermodynamic hydrate inhibitors (THI). LDHI are further categorised as kinetic hydrate inhibitors (KHIs) or anti-agglomerates (AAs) based on their mechanism for hydrate inhibition. As the name implies, LDHIs are chemicals applied at relatively low doses for hydrate inhibition; typical dose rates vary from 500 ppm to 2% of the total volume of water treated [11].

KHIs are typically water-soluble polymers that delay the onset of hydrate nucleation but do not prevent it indefinitely [12]. On the other hand, anti-agglomerates are surfactants that disperse the hydrate crystals into the liquid hydrocarbon phase and prevent the growth of large hydrate blocks [12]. A visual representation of the LDHI mechanism at various stages of hydrate formation and growth is seen in Figure 1-4. While both categories of KHI are effective at preventing hydrate formation in deepwater applications, most chemicals that fall under this group have poor environmental classification. KHIs can also contribute to hydrocarbon-water emulsion stability during processing and have limited effectiveness above 10 ^{0}C subcooling. Subcooling is the difference in pipeline operating temperature and hydrate onset temperature at a given pressure. Also, KHI applications are relatively recent compared to THI and are not as well established as THI applications [12].

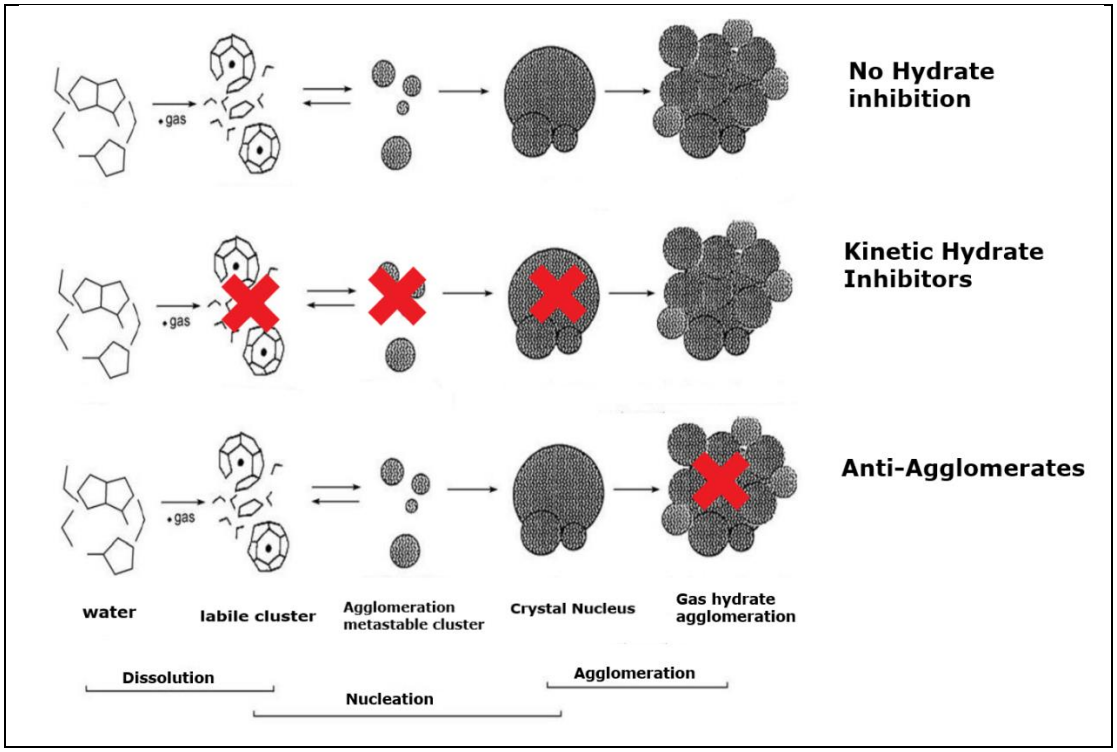

Figure 1-4: Hydrate formation, growth and low-dose hydrate inhibition (adapted from [13])

Thermodynamic hydrate inhibitors are small chain alcohols and glycols that inhibit hydrate formation by changing the chemical potential of water molecules and shifting the hydrate phase boundary towards the left on the hydrate phase diagram [14], as illustrated in Figure 1-5. This shift reduces the hydrate onset temperature at a given pressure, allowing for operating at much greater subcooling temperatures. A reduction in hydrate onset temperature of about 5 ^{0}C from point c to d, on the addition of a THI, is illustrated in Figure 1-5. The effective subcooling achievable with THI increases with the concentration of the THI. Concentrations higher than 60 wt% of the total produced water are usually used. Methanol and MEG are the two most used THIs because of their low cost and availability. Of the two commonly used THIs, though slightly less effective, MEG is less flammable, less toxic, more easily recyclable and partitions less into the hydrocarbon phase [15-16].

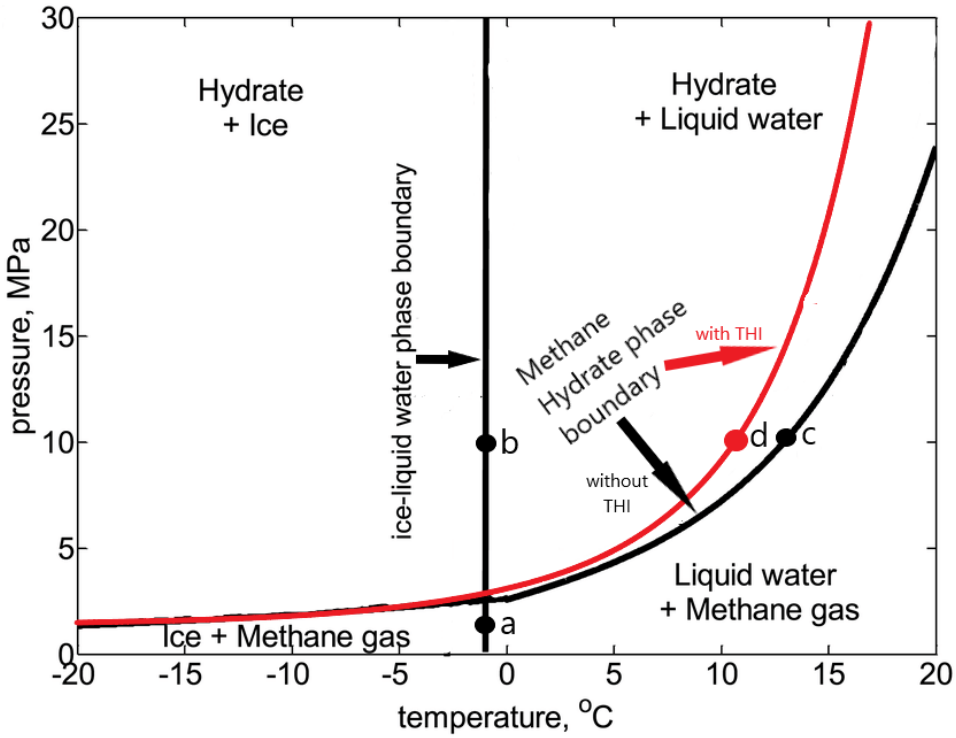

Figure 1-5: Methane Hydrate phase diagram with Thermodynamic Hydrate inhibition (adapted from [3])

The ability to reuse MEG for hydrate inhibition over a couple of pipeline cycles reduces the costs associated with using MEG and is an economic advantage to operators [6-9]. This means less glycol is needed to be bought and transported to the production site. For reservoir gas operations, MEG is injected at the well-head, transported with produced fluids in the pipeline and recovered downstream of production for reinjection into the well-head and another cycle of pipeline flow. During this operation, lean MEG mixes with the produced water from the reservoir. The production fluid containing natural gas, hydrocarbon liquids, produced water, and the injected MEG enters the downstream processing facility, where the fluids undergo phase separation. The produced fluids pass through a slug catcher and are then flashed in a three-phase production separator to separate gas, hydrocarbon liquids, and the produced water and MEG mixture, commonly known as rich MEG. The rich MEG (with about 40 – 60 wt. % water) [6-9] is regenerated in a MEG Recovery Unit (MRU) into a lean (about 10-20 wt% water) MEG for reuse while the

separated salts are sent to disposal. This lean has considerably less salt depending on the efficiency of desalination.

The MRU is designed to recover a much cleaner lean MEG stream with reduced water and salt content from its feed-rich MEG stream. MEG processing in the MRU usually starts with a pre-treatment step, followed by dewatering (or regeneration) and/or desalination (or reclamation), depending on the specific MRU design configuration. The traditional MRU design has only the pre-treatment and dewatering section with a much less defined desalination section. In contrast, more recent MRU designs handle dewatering with full and slipstream desalination. Entrained hydrocarbon is flashed and skimmed off the aqueous MEG stream in the pre-treatment step. Water is removed in the dewatering section of the MRU by heating in a reboiler to boil off water and reconcentrate the MEG. Salt is removed by precipitation in the desalting step. MEG dewatering is commonly referred to as regeneration, and both terms are used interchangeably. Likewise, MEG desalination is commonly referred to as reclamation; both terms are also used interchangeably.

1.2 The research problem

In 2009, the Victorian and Tasmanian sections of the Society for petroleum engineers (SPE) held a technical meeting on MEG regeneration [9]. In this meeting, significant players in the LNG industry came together to identify problems that they are facing with their MRU, and all problems mentioned there could be categorised into three groups:

i. Fouling within the MEG system
ii. Emulsion formation and difficulty of separating MEG from condensate
iii. Health and safety issues associated with MEG degradation products and contaminants

The consensus at this meeting was that more research is required to understand the chemical behaviour of MEG within the regeneration system and thus pave the way for solutions to some of the problems mentioned above.

In 2014, WorleyParsons, a significant engineering consultancy firm, organised a similar meeting titled "Operational Issues and Solutions Regarding the MEG Closed Loop Circuit and the MEG Recovery Unit (MRU)". In this 2014 meeting, references were made to the previous meeting in 2009, and the three major problems remained technical challenges in the operation of the MEG regeneration system. Simply put, all operators of MEG facilities are seeking more understanding of the behaviour of fluids in the MEG system.

Some researchers have devised various operational procedures which may be used to manage these problems [17-18]. Other researchers have developed models that can predict mineral solubility in the presence of MEG [19-20]. With the complex fluid composition, these models can be challenging to apply in industrial conditions. Another research focus has been the scale formation of various ions [21]. However, these studies have not taken a holistic look at the chemical interaction of fluids within the MEG system and how the change in its chemistry contributes to fouling, scale formation and other observed phenomena. Neither has this previous research been applied on a larger scale flow loop to better correlate the actual industry conditions. One way of tackling these problems is to gain an in-depth understanding of exactly how the chemical properties of MEG are changed during regeneration and reclamation and to use this knowledge to promote desirable outcomes while impeding undesirable ones.

This study focuses on the factors contributing to MEG property changes in the reboiler of the MEG regeneration and reclamation system. Findings from this work are of colossal significance to the LNG industry; they will contribute to a

deeper understanding of the fouling and degradation chemistry in the MEG system and methods for solving the related operational challenges. This research was carried out in collaboration with the bench-scale MEG regeneration facility at the Curtin Corrosion Engineering Industry Center (CCEIC). The goal is to foster synergy with its current ongoing research for a better understanding of the MEG regeneration process, with emphasis on the reboiler operation.

1.3 Research Objectives

The objectives for this research are:

1) To develop a robust alternative methodology for assay MEG samples from the MEG regeneration Unit.
2) To investigate the effect of MEG on the solubility and depositing of divalent ions in the MEG regeneration Unit
3) To Investigate the thermal oxidative degradation of MEG during regeneration
4) To investigate the effect of thermal degradation on the CO_2 corrosion of carbon steel in the MEG regeneration unit

1.4 Thesis structure

This work starts with a review of existing literature on the regeneration and reclamation of MEG as a hydrate inhibitor. This review is presented in **Chapter 2** and was published in the American Journal of Chemical Engineering, titled "Regeneration and Reclamation of monoethylene glycol (MEG) Used as a Hydrate Inhibitor: A Review" [22]. The review explored the evolution of MEG regeneration systems over the years. It introduced recent developments,

particularly on process efficiency, MEG quality, corrosion, energy conservation and other technical issues associated with the operation of the MRU. The entire MEG recycle and regeneration process and the various sections and functions are reviewed. The different MRU design configurations, factors that affect the performance of the MRU as well as corrosion and corrosion mitigation in the MRU are discussed. This review shows that the degradation of MEG, amongst other factors, contributes to changes in MEG in the MRU. High-temperature regions of the MRU were seen to be more prone to fouling, and the reboiler was particularly affected because of the high temperature at which it operated. The reboiler is generally operated at temperatures between 120 °C to 145 °C, but MEG starts to degrade at these temperatures causing discolouration and precipitation of degradation products and salts. Consequently, efforts in this work focused on the reboiler, considering that it is the highest temperature region of this MRU.

A significant part of this study included the need to accurately conduct assay on MEG samples in a timely and cost-efficient manner. Methods available for this assay at the time of conducting this study were based on gas chromatography and inductively coupled plasma methods which were expensive to install and implement. There was a need to find a cheaper method for these assays while maintaining the accuracy of results with a reasonable analysis time with possible scale-up for field use. Consequently, **Chapter 3** of this work was commissioned. The work reported in Chapter 3 of this thesis, "Ion chromatography for MEG assay and application to MEG regeneration plant", outlines the method development for the assay MRU MEG sample by ion chromatography. This method development started from choosing the proper IC setup and column for the analyses, then optimising the application for the best separation of analyte ions and good sensitivity in the MRU MEG sample matrix. Lastly, the new method was validated using actual MRU

samples from the CCEIC Pilot MEG plant, which was running as per industry standards for verification of accuracy and robustness. The new IC method was then used for assay in the rest of the work reported here and other published articles [23-24]. With a suitable method for sample assay, efforts were then focused on investigating the behaviour of MEG within the MRU with an emphasis on the reboiler.

As mentioned in the earlier part of this chapter, fouling is frequently reported in MRU operations, mainly at the high-temperature regions of the MRU, of which the reboiler is the hottest, operating at temperatures above 120 °C. Salt build-up is also widespread in MRU operation; one reason for salt build-up is the continuous use of MEG in a recycle loop where, in most cases, not all salt content is stripped from the MEG on every pass through the MRU. The other reason salt can build up is that the salt content of the reservoir fluids eventually ends up in the MEG stream. At this point, it is worth noting that the salt content of MEG is not the sole cause of fouling in the MRU and associated processing units; however, it is well-known that the salt content contributes immensely. Two low-solubility salts which are most frequently reported are carbonate salts of calcium and magnesium. These carbonates are notorious for depositing in and around hot spots in the MRU and topside areas of oil and gas processing facilities. Calcium carbonate is slightly more prevalent than its magnesium counterpart. However, it was noted that while there was much literature on the solubility of these carbonate salts both in water and MEG streams, there was limited data on the solubility of these calcium and magnesium carbonate salts at MRU reboiler conditions of 140 °C, 80 wt. MEG % and low CO_2 partial pressure. **Chapter 4** of this work sought to fill in the gap in this area. Results from these solubility measurements were significant in predicting the behaviour of calcium carbonate in the MRU reboiler operation. An interesting finding from work in Chapter 4 of this work is the effect of degradation on the

solubility of calcium salts. While it was observed that calcium carbonate solubility reduced with temperature to a minimum and then showed a slight increase with increases in temperature from about 120 ^{0}C, the degrading MEG affected the solubility of calcium carbonate, causing an increased solubility. This led to further investigation into the degradation products of MEG under MRU conditions and their effects on carbon steel corrosion.

The investigation into the degradation of MEG under MRU reboiler conditions is reported in **Chapter 5** - Thermal oxidative stability of monoethylene glycol during regeneration. Chapter 5 reports the effect of MRU parameters on the degradation of MEG. The aim was to explore how MEG degrades under these conditions, how fast it was degraded, how its pH changed, and the degradation products. Parameters considered were oxygen content, ionic strength, MEG content and temperature. The distribution of produced organic acids with changes in MEG concentration, oxygen content and ionic species in the degrading MEG solution at 140 °C are detailed in Chapter 5.

The investigation on the degradation of MEG continues into **Chapter 6**, where the influence of thermally degraded MEG on the corrosion of carbon steel as it relates to the MRU material of construction was explored. It was deemed essential to quantify the changes in corrosion rates of carbon steel with thermally degraded MEG compared to the corrosion of carbon steel in fresh MEG with equivalent degradation products added to it. One finding of this investigation is that while there was a similar trend with added organic acids and the thermally degraded MEG, there were differences in the measured corrosion rates. Consequently, the work opens another horizon for research into the differences in corrosion rates and possible causes.

It is acknowledged that the work reported in this thesis does not answer all questions relating to the fouling within the MRU and associated MEG handling

and processing units. It is expected that the results and findings reported here contribute knowledge to a better understanding of the behaviour of MEG in the MRU and, in conjunction with the existing body of research into this topic, will pave the way in optimising the MEG reclamation and regeneration process. This research will advance understanding of the degradation and corrosion in the MEG regeneration and reclamation process. The research has significant industrial implications in terms of process design and optimisation.

References

1. Bai, Y., & Bai, Q. (2018). *Subsea engineering handbook* (2nd ed.): Gulf Professional Publishing.
2. Sahu, C., Sircar, A., Kumar, R., & Sangwai, J. S. (2022). Natural Gas Hydrates: Energy Locked in Cages. In *Status and Future Challenges for Non-conventional Energy Sources Volume 1* (pp. 155-171): Springer.
3. You, K., Flemings, P. B., Malinverno, A., Collett, T., & Darnell, K. (2019). Mechanisms of methane hydrate formation in geological systems. *Reviews of Geophysics, 57*(4), 1146-1196.
4. Brunner, G. (2014). Properties of Pure Water. In G. Brunner (Ed.), *Supercritical Fluid Science and Technology* (Vol. 5, pp. 9-93): Elsevier.
5. Sloan Jr, E. D., & Koh, C. A. (2007). *Clathrate hydrates of natural gases*: CRC press.
6. Boschee, P. (2012). Gas Hydrate Control Using Monoethylene Glycol in the Gulf of Mexico. *Oil and Gas Facilities, 1*(03), 14-18. doi:10.2118/0612-0014-OGF
7. BRUSTAD, S., LOKEN, K., & WAALMANN, J. K. A. (2005). Engineering and Technology Hydrate Prevention using MEG instead of MeOH: Impact of experience from major Norwegian developments on technology selection for injection and recovery of MEG. *S. OTC, 17355*.
8. Ng, H.-J., Chen, C.-J., & Saeterstad, T. (1987). Hydrate formation and inhibition in gas condensate and hydrocarbon liquid systems. *Fluid Phase Equilibria, 36*, 99-106. doi:http://dx.doi.org/10.1016/0378-3812(87)85016-1
9. MEG Regeneration Technical Meeting. (2009). In. Port Campbell, Australia: Society of Petroleum Engineers.
10. Austvik, T., Li, X., & Gjertsen, L. H. (2000). Hydrate plug properties: formation and removal of plugs. *Annals of the New York Academy of Sciences, 912*(1), 294-303.
11. Mokhatab, S., Wilkens, R. J., & Leontaritis, K. (2007). A review of strategies for solving gas-hydrate problems in subsea pipelines. *Energy Sources, Part A, 29*(1), 39-45.
12. Kelland, M. A. (2006). History of the development of low dosage hydrate inhibitors. *Energy & Fuels, 20*(3), 825-847.
13. Othman, E. A. (2014). *Gas Hydrate Equilibrium Measurements for Multi-Component Gas Mixtures and Effect of Ionic Liquid Inhibitors.* (Master's Thesis), Texas A&M University, USA.
14. Xin, Z., Zhengsong, Q., Weian, H., Guowei, Z., & Yongjun, Z. (2015). Inhibition mechanism and optimized design of thermodynamic gas hydrate inhibitors. *Acta Petrolei Sinica, 36*(6), 760.

15. Brustad, S., Løken, K.-P., & Waalmann, J. G. (2005). *Hydrate Prevention using MEG instead of MeOH: Impact of experience from major Norwegian developments on technology selection for injection and recovery of MEG.* Paper presented at the Offshore technology conference.
16. Teixeira, A. M., de Oliveira Arinelli, L., de Medeiros, J. L., & Ofélia de Queiroz, F. A. (2018). Recovery of thermodynamic hydrate inhibitors methanol, ethanol and MEG with supersonic separators in offshore natural gas processing. *Journal of Natural Gas Science and Engineering, 52*, 166-186.
17. Nazzer, C. A., & Keogh, J. (2006). *Advances in Glycol Reclamation Technology*. Paper presented at the Offshore Technology Conference, Houston Texas [online]. https://onepetro.org/OTCONF/proceedings-abstract/06OTC/All-06OTC/29835
18. Khorrami, Z., Karimkhani, B., & Farhadi, F. (2010). *Finding the Best Alternative for Plugging Problem in MEG Regeneration Unit Using AHP Method.* Paper presented at the SPE Russian Oil and Gas Conference and Exhibition.
19. Sandengen, K. (2006). *Prediction of mineral scale formation in wet gas condensate pipelines and in MEG (mono ethylene glycol) regeneration plants.* (PhD Thesis), Norwegian University of Science and Technology, Norway.
20. Kaasa, B., Sandengen, K., & Ostvold, T. (2005). *Thermodynamic predictions of scale potential, pH and gas solubility in glycol containing systems*. Paper presented at the SPE International Symposium on Oilfield Scale, Aberdeen, United Kingdom [online]. https://onepetro.org/SPEOSS/proceedings/05OSS/All-05OSS/SPE-95075-MS/187900
21. Guan, H., Cole, G., & Clark, P. J. (2009). Inhibitor Selection for Iron Scale Control in MEG Regeneration Process. *SPE Prod & Oper, 24*(04), 543 - 549. doi:https://doi.org/10.2118/114059-PA
22. Odeigah, E. A., & Pojtanabuntoeng, T. (2022). Regeneration and Reclamation of Mono-Ethylene Glycol (MEG) Used as a Hydrate Inhibitor: A Review. *American Journal of Chemical Engineering, 10*(2), 32-45.
23. Soames, A., Odeigah, E., Al Helal, A., Zaboon, S., Iglauer, S., Barifcani, A., et al. (2018). Operation of a MEG pilot regeneration system for organic acid and alkalinity removal during MDEA to FFCI switchover. *Journal of Petroleum Science and Engineering, 169*, 1-14. doi:10.1016/j.petrol.2018.05.047
24. Odeigah, E. A., Pojtanabuntoeng, T., Jones, F., & Gubner, R. (2018). The Effect of Monoethylene Glycol on Calcium Carbonate Solubility at High Temperatures. *Industrial & Engineering Chemistry Research, 57*(46), 15909-15915.

Chapter 2

Regeneration and Reclamation of Monoethylene Glycol (MEG) used as a Hydrate Inhibitor: A Review

Published in American Journal of Chemical Engineering

*Edith A. Odeigah**[a], Thunyaluk Pojtanabuntoeng*[a]

[a] WA School of Mines: Minerals, Energy and Chemical Engineering, Curtin University, Bentley, Western Australia 6102, Australia.

2.1 Abstract

The use of monoethylene glycol (MEG) as a hydrate inhibitor in wet gas pipelines is increasingly becoming widespread, especially in deep-water long-tie back pipelines where the use of low dosage hydrate inhibitor (LDHI) is not practical. MEG is a commonly used thermodynamic hydrate inhibitor (THI), and it prevents hydrate formation by lowering hydrate formation temperature. One significant advantage of MEG over other THIs is that MEG can be regenerated and reused, which minimises the cost of chemicals as large volumes of THIs are usually required. Over the years, significant research advances have been made in MEG recovery and the MEG Recovery Unit (MRU) design. This paper presents a comprehensive review of the evolution of MEG regeneration systems over the years and introduces recent developments, particularly on energy conservation. The entire MEG recycle and regeneration process is reviewed as well as the various sections and their functions. The different MRU configuration are discussed and factors that affect the performance of the MRU as well as Corrosion and corrosion mitigation in the MRU. This review shows that there are a number of new improvements in the MRU application that are yet to be fully explored as well as some technical challenges that are yet to be fully understood.

Keywords: Monoethylene glycol, MEG regeneration Unit, Hydrate Inhibitor

2.2 Introduction

Hydrate formation and its prevention remains a technical challenge for flow assurance in wet gas pipelines. Gas hydrates are crystalline solids formed from water and hydrocarbon gases molecules at low temperatures and elevated pressures. Gas hydrates formation starts with a nucleation step where microcrystalline hydrate particles form. They subsequently agglomerate and grow into large structures that may eventually obstruct the flow inside the pipeline. Hence, hydrate prevention and its management is one of the major focuses for flow assurance [1].

A combination of four essential parameters – water, gas, temperature and pressure – must be present within the hydrate stability region, as defined by the hydrate equilibrium curve, for hydrate formation to be initiated [2]. A typical pressure-temperature diagram showing the hydrate stability region and equilibrium curve is shown in Figure 2-1.

Consequently, eliminating one of the four hydrate formation requisites can prevent hydrate formation. However, as the composition of gas produced from the gas wells and the reservoir pressure cannot be controlled, the hydrate onset temperature is the only parameter that can be controlled with the least effect on the production. Operating at temperatures and pressure outside the hydrate stability region can delay the onset of hydrate formation. Still, the ability to operate outside the hydrate stability temperatures and pressured is vastly limited, especially in deep-water, long-distance tie-backs, of which there have been many developments in recent times. The use of thermodynamic hydrate inhibitors (THI) to reduce the hydrate stability region and increasing the window for operation outside the hydrate region is a common approach for hydrate prevention

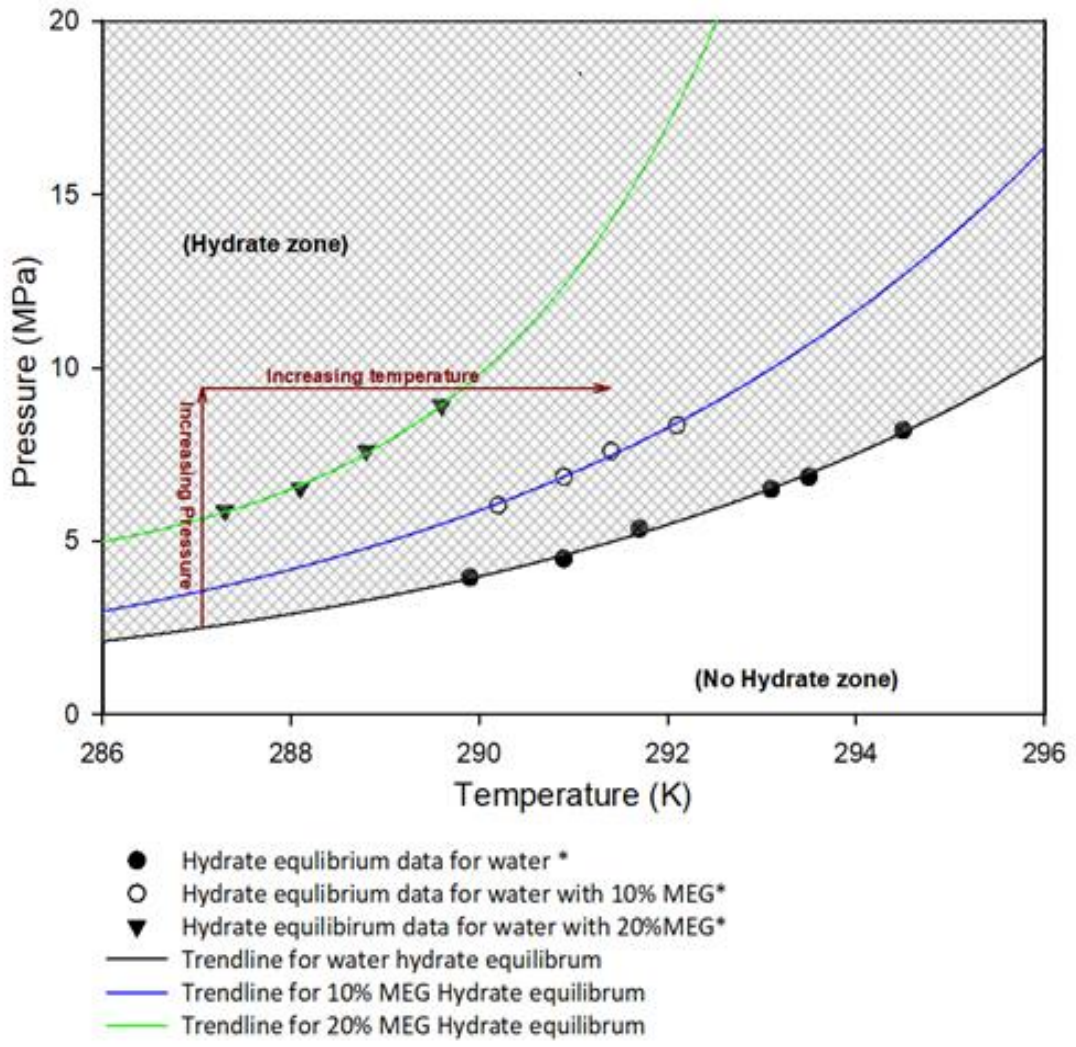

Figure 2-1: Typical Hydrate equilibrium plot * Data from [3] and trendlines were determined by polynomial regression fitting

Additionally, the kinetics of hydrate formation – how fast the hydrates grow and increase in size – can be controlled. There have been positive advances in the application of low dose hydrate inhibitors (LDHI) in the form of kinetic hydrate inhibitors (KHI) and anti-agglomerates (AA) for hydrate management and prevention. KHIs typically have a lactam or caprolactam functional group and they act by suppressing the nucleation and accumulation of gas hydrates [4]. As the name implies, LDHIs are applied in lower dose rates, i.e., between 0.25 to 5 vol. % of the produced water, compared to THIs that are applied in much larger volumes (up to 90 vol%) [5].

While LDHIs have proven effective in hydrate prevention, they are not robust for use across all field applications. The mechanism of hydrate inhibition typically limits the application of AAs to a water cut less than 50 to 75% as they require the presence of a hydrocarbon phase to remain effective [5]. In addition, the efficiency of KHIs appeared to be influenced by the operating pressure. Lederhos et al. (1996) investigated the efficiency of poly(N-vinylcaprolactam) (PVCAP), N-vinylpyrrolidone/N-vinylcaprolactam/N,N-dimethylaminoethyl-methacrylate (VC-713), and N-vinylpyrrolidone- co-N-vinylcaprolactam (VP/VC) at controlling hydrate formation and reported a fivefold increase in hydrate inhibition efficiency when pressure increased from about 6Mpa to 10Mpa while induction times remained unaffected [6]. This study also reported that a reduction in temperature by 8 °C, from 285.6 K to 277 K, rendered some inhibitors inactive and that KHIs were more effective at low dose rates and in water with high salt content, such as with seawater and with formation water breakthrough. Nonetheless, water with high salt content is not favourable in oil and gas production as it increases the corrosivity and complications of fluids separation, resulting in more significant financial implications. On the contrary, Brustad et al. reported that KHIs demonstrated high performance at high pressures [7], highlighting the controversies that still exist in the field of KHI application. Further research effort is needed in this field. AA application also requires further study as they have not been proven to be effective at high pressures [8]. Furthermore, with increasingly strict regulations on global environmental protection, the use of KHI and LDHI are not favoured due to their low biodegradability [9]. Therefore, increasing research focus is now being placed on developing novel “green” LDHIs and KHIs [9, 10].

The application of THIs is much more established as they have been proven effective in other environments, such as antifreeze used in the automotive industry. Research and field experience of THIs in other environment apply to

oil and gas production. THIs are effective in most conditions but require a high inhibitor volume and higher handling cost. However, they remain the most viable option in most cases today.

Low molecular weight alcohols and glycols are effective THIs, with triethylene glycol (TEG) and monoethylene glycol (MEG) being the most commonly used THIs. Although methanol presents a higher sub-cooling per unit volume used compared to TEG and MEG, but the choice of MEG as a THI in wet gas pipelines is largely favoured because MEG can be regenerated and reused over a number of cycles. THIs are generally used in large quantities, as much as 20 vol% of combined pipeline liquid phase [11] (combined pipeline liquid phase here means the combination of MEG, water, and liquid hydrocarbon). Hence, the ability to be recycled and reused provides long term economic advantages, making MEG a highly favoured choice for THI.

THIs also provide other benefits, such as reducing the scale formation tendency and corrosivity of the aqueous phase. Fan et al. (2011) demonstrated that MEG and methanol decreased barite scale induction [12]. MEG at 10 wt.% increased the induction time for barite scale formation by 1.5 times compared to water. However, further increasing MEG concentration in the aqueous phase (MEG- water co-solvent) from 10 wt.% to 30 wt.% had little effect on induction time of barite nucleation. MEG also increases the induction time for the formation of the $CaCO_3$ polymorphs [13]. Methanol at 10 wt.% was also effective in scale inhibition as it increased the scale induction time by 1.4 times compared to water. On the other hand, the efficiency of methanol was highly affected by its concentration in the aqueous phase (Methanol-water cosolvent). An Increase in methanol concentration from 10 wt.% to 30 wt.% resulted in a 35% increase in scale induction time. This study showed that both THIs demonstrated a positive effect on hydrate inhibition and scale inhibition.

While methanol was shown to inhibit hydrate formation more effectively than MEG, MEG offers another benefit, i.e., corrosion rate reduction. The corrosion inhibition property of MEG is considered a great benefit to flow assurance. The corrosion inhibition afforded by MEG is further discussed later in section 4.1.3.

2.3 MEG Recovery Unit (MRU) Operational Sections

The process of recycling MEG is commonly referred to as MEG recovery. Rich MEG returning from pipeline and process facilities enter the MRU with high water and salt content and is processed into lean MEG with lower water and, occasionally, salt content for re-injection into the pipeline near the wellhead. Rich MEG typically has 30-50% water content whereas lean MEG typical has less than 20% water content [15]. The entire MEG recovery process consists of three dominant sections. These are pre-treatment, dewatering and desalination. The dewatering process is commonly referred to as regeneration, while the desalination process is referred to as reclamation. These words may be used interchangeably in the rest of this paper.

2.3.1 Pre-treatment

The aqueous phase returning from the gas pipeline is a mixture of MEG, water, and other water-soluble components. This feeds into the MRU for the recovery of MEG. However, the critical function of the MRU is the separation of MEG from an aqueous phase of water and salts; hence, MRUs are generally not equipped to handle other water-soluble contaminants from the pipeline and process that may partition into the aqueous phase. It is, thus, critical to minimise the quantity of contaminants entering the MRU. For this reason, the

pre-treatment process upstream of the MEG regeneration and reclamation units is required.

The common contaminants found in oil and gas pipelines and process aqueous phase are entrained hydrocarbons, corrosion product scales, and residual pipeline chemical additives such as scale, dissolved ions from produced water and corrosion inhibitors. These contaminants have been reported to cause fouling and MRU process upsets [14]; they can be removed from the rich MEG stream as a first step in the MRU before the dewatering and desalination processes.

The pre-treatment in the MRU starts with the separation of entrained hydrocarbons from rich MEG, which is not typically fully separated in the gas process slug catcher. The presence of emulsion is common due to many reasons. Agitation from high production flow rate or pressure differentials within the flow line can stabilize emulsions of hydrocarbons and MEG. A second factor that facilitates the formation of 'hydrocarbon in MEG' emulsion is the low operating temperature typical of gas pipelines, as reported in a MEG regeneration technical meeting (2009) [15]. Other contaminants like chemical treatment residuals (i.e., corrosion inhibitors), naturally occurring surfactants from the reservoir, and suspended particles also stabilize hydrocarbons in MEG emulsion [14].

The process upsets in the MRU as a result of emulsion is frequently reported [16-20]. If the emulsion phase is not fully separated, light hydrocarbons can flash off during the regeneration process, resulting in a decrease in the system operating temperature and contamination in the MRU water streams [21]. The heavy hydrocarbons, on the other hand, can accumulate in the MRU bottom MEG stream resulting in increased MEG viscosity and fouling in reboilers and heat exchangers [14]. The increase in MEG viscosity can also enhance loading

on MEG recycle pump. The entrained hydrocarbons were reported to stabilise suspended particles in the MEG stream and make it difficult to settle out these particles [22]. Burping in MEG distillation column is also frequently associated with entrained hydrocarbon carryover in MEG [15]. Burping occurs when there is periodic build-up and collapse of a vapour blanket in the distillation column. when built-up, the vapour blanket causes localised increased pressure preventing further boiling until the blanket collapses; these cycle of increase and decrease in pressure results in severe flooding that increased the product loss in the distillate stream [23].

Methods to demulsify hydrocarbon in MEG emulsion and removal of entrained hydrocarbons in MEG are dependent on the type of emulsion formed. According to Latta 2018 [24], fractional interface coalescence efficiency (f_{ice}) is used to determine methods and equipment for minimising hydrocarbon content effluent in the aqueous phase. A high f_{ice} means that the dispersed phase in the emulsion has a high propensity to coalesce and separate from the aqueous phase, and vice versa. Hydrocarbons with higher API gravity generally have a higher f_{ice} and separation can be easily achieved by gravitational separation in a settling tank with minimal residence time. In a series of lab bottle tests, liquid iso-paraffin with API gravity of 53.2 completely separated from MEG-water mixture in under one minute after shearing was stopped [25]. For this type of light hydrocarbon, a settling tank with a skimming pump may be sufficient to remove entrained oil upstream of the MRU; especially when there is the facility to maintain or provide warm temperature as well as baffles/weirs to allow for separation of the hydrocarbon phase in the settling tank. A more difficult case of separation is experience with heavy oil with low API gravity [26], in this case the f_{ice} for the emulsion is low and complete separation requires the use of multiple size exclusion filters.

A second major pre-treatment step in the MRU is the removal of low solubility divalent ion salts from the rich MEG. Common divalent ion salts found in the MRU are carbonate scales of calcium and magnesium ions, which have very low solubility and readily precipitate at high temperatures. As such, there is tendency for carbonate scale precipitation in unfavourable high temperature regions like the reboiler and/or pumps. As MEG is heated, the dissolved CO_2 is removed causing the pH to rise. A one unit increase in pH across the MEG reboiler inlet and outlet has been reported [27]. At these high temperatures and pH, the residual divalent cations can precipitate in the MRU as carbonate scales, which are hard to clean up and can cause fouling and gunking. For this reason, the precipitation of these divalent ion salts is usually controlled so they are easily removed from the system.

Seiersten and Kundu 2018 published an extensive review on the scale management in MEG systems [28]. In brief, rich MEG is slightly heated to about 50-60 °C and dosed with a hydroxide or carbonate alkali to increase its pH to facilitate the precipitation of divalent ions such as calcium, magnesium, iron, and strontium [28]. The precipitates are given time to settle in the settling tank and suspended particles are removed alongside any other particles in the final step, i.e., filtration.

However, most but not all MRUs have this pre-treatment step, If the MRU has other means of handling salt precipitates prior to the dewatering stage, this pre-treatment step may not be required. With other MRU design configurations that do not have a salt handling capability upstream of dewatering in a distillation column, this pre-treatment step is crucial to minimize scaling in the reboiler and associated pumps. Nonetheless, the use of scale inhibitor is recommended for all MRU reboilers [29].

Filtration is the final pre-treatment step to remove any oil wetted fine solid particles that may be suspended in the rich MEG upstream of the MRU, following the alkali treatment of rich MEG to precipitate the divalent ion salts. These particles also include corrosion products accumulated from the pipelines as reported by Soames et al (2019). These particles demonstrate strong tendency to remain afloat when they are oil wetted [22]. Filtration ensures that all these very fine particles do not enter the MRU, where they can cause fouling [26].

2.3.2 MEG Dewatering

A critical function of the MRU is to reduce water content from its feed rich MEG stream to produce a lean MEG stream with much less water content. The rich MEG stream typically holds 40-50 wt.% water while the lean MEG stream typically holds less than 20% water [30]. The dewatering of rich MEG to lean MEG is thus a vital step in the MEG regeneration process. Due to the difference in boiling points of MEG and water (100°C @1 atm for water and 197 °C @ 1 atm for MEG), the dewatering step is achieved by reflux distillation in an atmospheric distillation unit. A typical MRU distillation column operating temperature is about 120 °C. Considering that there is a relatively low vapour load during dewatering, the packed distillation column is the most commonly used as it can maintain a low pressure drop and achieve high efficiency of separation with the expected vapour load [31]. Important factors to consider during MEG dewatering are the windows for operating temperature, pressure and MEG salt loading. The window for operating temperature must be balanced to achieve required separation efficiency with consideration for MEG degradation onset temperature and process energy consumption [32]. MEG losses as a result of thermal oxidative degradation can impact operating cost for regular MEG top-up [32] and cause process upsets due to the reduction in pH as organic acids are degradation products of MEG [27].

The energy requirement for dewatering MEG using the conventional distillation method is significant and can account for up to 60% of the energy consumption of the entire MRU. Reducing energy consumption while achieving efficient dewatering remains a challenge. Pries et al. (2020) compared the Destubcal technology, a falling film distillation method, with conventional distillation [33]. The technology allows uniform temperature distribution along the distillation column, hence more effective energy usage. According to Pries et al. (2020) the Destubcal technology consumed 46.3% less energy than the convention distillation column to concentrate 66 wt.% (rich) MEG to 88.61 wt.% (lean) MEG. Destubcal technology reported by Pries et al. (2020) is a series of distillation tests performed with a single tube falling film distillation column assisted by a thermosyphon system operating at atmospheric pressure [33]. This technology is yet to be deployed commercially and the effects of salt loading and possible fouling of tube walls were not evaluated in this study.

Recent research developments have also investigated the membrane distillation method as another low energy alternative for dewatering MEG [34]. Membrane distillation is a combination of thermal distillation and membrane technology in which volatile vapour is transferred from a hot aqueous distillation bottom through a microporous hydrophilic membrane because of the partial pressure difference created due to the temperature difference on both sides of the membrane [35]. In 1999, Rincon et al. confirmed the feasibility of the membrane distillation for water-MEG separation from used coolant liquid [36]. Later in 2005, Mohammadi T. and Akbarabadi M. used vacuum membrane distillation to reconcentrate MEG from used coolant solution using a flat-sheet polypropylene membrane [37]. Vacuum is applied to create the required vapour pressure difference across the membrane to drive a flux during distillation. With this process, Mohammadi T. and Akbarabadi M. distilled water (with less than 1 wt.% MEG) from 60 wt.% MEG solution at 60

°C. The vacuum membrane distillation technology demonstrated promising results in recovering used coolant liquid but much research is still required to apply this technology in the THI application where a high salt loading is expected.

In 2019, Ajdar et al. explored the use of air gap membrane distillation to dewater MEG. In this technique, a stagnant air gap between the membrane and a condensation surface inside the distillation unit generates the flux required to drive the separation [34]. One major advantage of the air gap membrane distillation over other types of membrane distillation is that there is no contact of the permeate (i.e., top distillate) with the membrane, thus resulting in a relatively higher flux, less fouling tendency, and less heat loss [38]. The permeate is the vapour that passes through the membrane and is recovered as a top distillate and the permeate flux is the quantity of the permeate produced per unit time and unit membrane area [39]. Ajdar et al. used a polysulfone hollow fibre membrane surface coated with polydimethylsiloxane to improve hydrophobicity and was able to achieve a 26 kg/(m^2h) permeate flux rate. Energy consumption figures were not published for this membrane distillation technology as it is yet to be scaled up for commercial application.

2.3.3 MEG Desalination

After the pre-treatment and dewatering steps, the lean MEG stream generally has low water contents (<20 wt.% on a salt free basis) and low divalent salts. However, in some cases where the pre-treatment step is absent before the dewatering step, divalent salts concentration can still be considerable. Prior to reinjecting the lean MEG into the pipelines, these salts need to be removed to below acceptable limits. The final process of the MRU is the desalination.

The desalination of MEG in the MRU is the removal of salts from MEG, commonly achieved by the difference in volatilities of the salts and MEG. The

desalination process is classified into monovalent and divalent cation salts removal. The principles of divalent salts removal have already been discussed in the pre-treatment section. When the concentrations of divalent ions are low and do not reach the saturation points of carbonate scales, the scaling tendency is low. In this case, divalent ion salts can be removed together with the monovalent ion salts in the desalination step. Otherwise, the removal of the divalent ions is usually accomplished as part of the MRU pre-treatment section, where the mono-valent ion removal is usually stand-alone in the desalination unit.

Monovalent ion salts (most commonly sodium and potassium chlorides) are usually very soluble with less tendency to cause fouling in the system. However, regardless of solubility, they need to be removed from the MEG stream to avoid build-up.

The conventional desalination process involves the recovery of a solvent by boiling. While the boiling point of pure MEG at one atmosphere is 197 °C; the onset of thermal oxidative degradation varies significantly depending on ionic content and exposure time to high temperature. Thermal oxidative degradation for neat MEG is reported to start at 162 °C [40]. Consequently, heating MEG to its boiling point of 197 °C is not a viable option as this can lead to MEG losses due to degradation and adverse effects from the degradation products, which are volatile fatty acids. Additionally, raising MEG temperature to 197 °C requires large energy demand and thus operational cost. Hence, vacuum evaporation is employed to evaporate MEG at a relatively lower temperature (e.g. < 150 °C) to minimise the aforementioned downsides.

Several other technologies with potential to reduce energy demand have been investigated. Among them, ion exchange for MEG desalination has gained research attention as a possible means of lower energy desalination. One of the

earliest publications on ion exchange for MEG MRU desalination is the patent developed by Phelps D. W. and Fernandez L. in 2012. This patent presented a system to remove divalent cations from rich MEG using a cation exchange resin that adsorbs the divalent cations in the rich MEG prior to its entry into a flash separator [41, 42]. In 2020, He S. et al., published their work on an electrically regenerated mixed bed ion exchange resin for MEG desalination [43]. Ion exchange for MEG desalination is claimed to be less energy intensive compared to the volatility-based desalination by heating under vacuum. Further, electrically regenerated resin consumes less chemical for resin regeneration compared to conventional chemically regenerated ion exchange resins. More so, He S. et al. proposed the use of less voltage for ion backward migration, which eliminated the need for ultra-pure water. In their work, 70wt% MEG with 47.1mmol/L NaCl rich MEG composition was used; After regeneration of the resin bed for 1 hour at a voltage lower than 73 V, 33.83% of NaCl in 5.16 bed volume (BV) simulated rich MEG liquid was removed. After 15 cycles of repeated operation, the performance of the resins remained stable. The result indicated that the electrically regenerated mixed - bed ion exchange could be a promising prospect for MEG desalination in deep-water gas field operations. In recent times, research has shown a successful application of an ion exchange technology for MEG desalination [43]. The technical challenge as of today is the development of efficient regeneration of the ion exchange resin used for the MEG desalination.

2.4 MEG Recovery Unit (MRU) – System Operation and Design

There are various MRU units around the world with different design configurations. This section discusses key MRU designs.

MRU design configurations can be largely classified into three major categories.

1) Traditional MRU designs with dewatering in a distillation column and no desalination capability (Figure 2-2)
2) Integrated MRU designs with a flash drum for desalination prior to dewatering in a distillation column (Figure 2-3 and Figure 2-4)
3) Reclamation and regeneration MRU design with a desalination unit downstream of the distillation column (Figure 2-5).

2.4.1 Traditional MRU Design

The traditional MRU design closely resembles system previously used for triethylene Glycol (TEG) regeneration in TEG dewatering applications. Some of these early MRUs were retrofitted versions of the TEG regeneration unit [7]. This MRU design is essentially a distillation column that separates water from MEG and has no desalination capabilities, as described schematically in Figure 2-2. The rich MEG skimmer in this diagram is not unique to this design configuration and is meant for the removal of carryover hydrocarbon in MEG as a pre-treatment.

The main challenge with the direct transfer of technology from TEG regeneration to MEG regeneration is that TEG was mainly used in gas dehydration units with little dissolved condensed water and salt contents. On the contrary, MEG in the MRU has a much higher salt content; the MRU is used topside of deepwater gas operations where there is possibility of formation water breakthrough from the gas reservoir. Formation water is water associated with the oilfield reservoir formation and can hold total dissolved solids generally more than 10^5 mg/L [44], with a high concentration of divalent ions (primarily calcium and magnesium salts). While this traditional MRU design is simple, compact, and easy to deploy, it is not suitable to handle the high salt content in rich MEG, as it has led to multiple reports of scaling and reboiler fouling [7]. A salt slurry may be occasionally removed by de-bottoming

the settling tank in Figure 2-2. However, it is worth mentioning that there are plenty of examples of MRU which do not handle formation water in which case, MEG had been recovered and recycled for nearly 30 years with minor top-up [45].

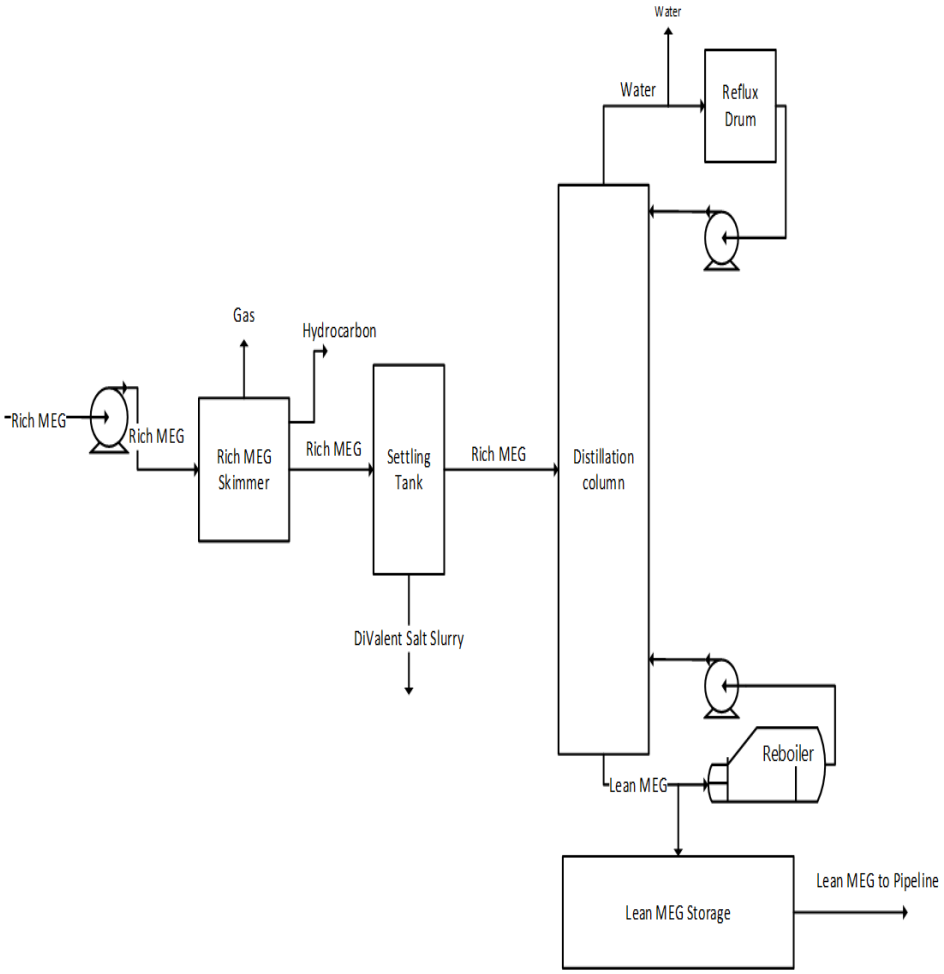

Figure 2-2: Traditional MRU design.

When salts are present, the traditional MRU system needs to be regularly replenished with fresh MEG to maintain salt content within a threshold. The replenishment process minimises the accumulation of salt content after MEG has been circulated for a period of time. However, the salt content still reportedly accumulates beyond its solubility limits in the MEG stream, especially in facilities that have formation water breakthrough. Consequently, salts precipitate at undesirable points either in the production pipeline,

topsides or even in the MEG cycle, causing blockage and process upsets. Scaling has been reported in the MRU inlet heater, column and reboiler with this traditional MRU configuration and formation water in the Statoil operated Troll (Kollsnes) gas plant [45, 46]. The scaling problem encountered with the traditional MRU design prompted a modification to improve the effectiveness of the MEG recovery process. High MEG waste and losses are also drawbacks of this MRU system, frequent replacement and top-up are required with salt accumulation and salt slurry removal within the system [45, 46].

2.4.2 Integrated MRU Design

The integrated MRU design was introduced to reduce scaling problem in the MEG regeneration distillation column by desalinating rich MEG upstream of the distillation column. Nazzer and Keogh (2007) describes this design configuration as used in New Zealand's Maui gas plant in the early 90s and the schematic of this design is shown in Figure 2-3 [47].

In this design configuration, rich MEG is desalinated in a flash separator operating under vacuum and about 100°C temperature [48]. Hayhoe (1993) did not specify vacuum pressure for operation, but Boschee (2012) reported operating the flash separator between 3 to 4 psia and about 135°C at the Independence Hub FPSO in the Gulf of Mexico [26]. As MEG with its high salt content enters the flash separator, salt free rich MEG flashes off overhead the separator leaving the salt slurry at the bottom of the separator. The salt slurry is then syphoned to a settling tank to allow salts to crystalize. Recovered MEG from the settling tank is recirculated back into the flash separator by mixing with the rich MEG post the skimmer tank. The overhead salt-free rich MEG vapour is then further concentrated in a vacuum distillation column downstream of the flash separator. The benefits of this design configuration are two-fold. It reduces the salt loading in the MEG distillation column and design eliminates the need for a reboiler in the distillation column as the rich MEG

enters the column as vapour. Hence, it is easily fractioned into distilled water and lean MEG at the overhead and bottom of the column, respectively.

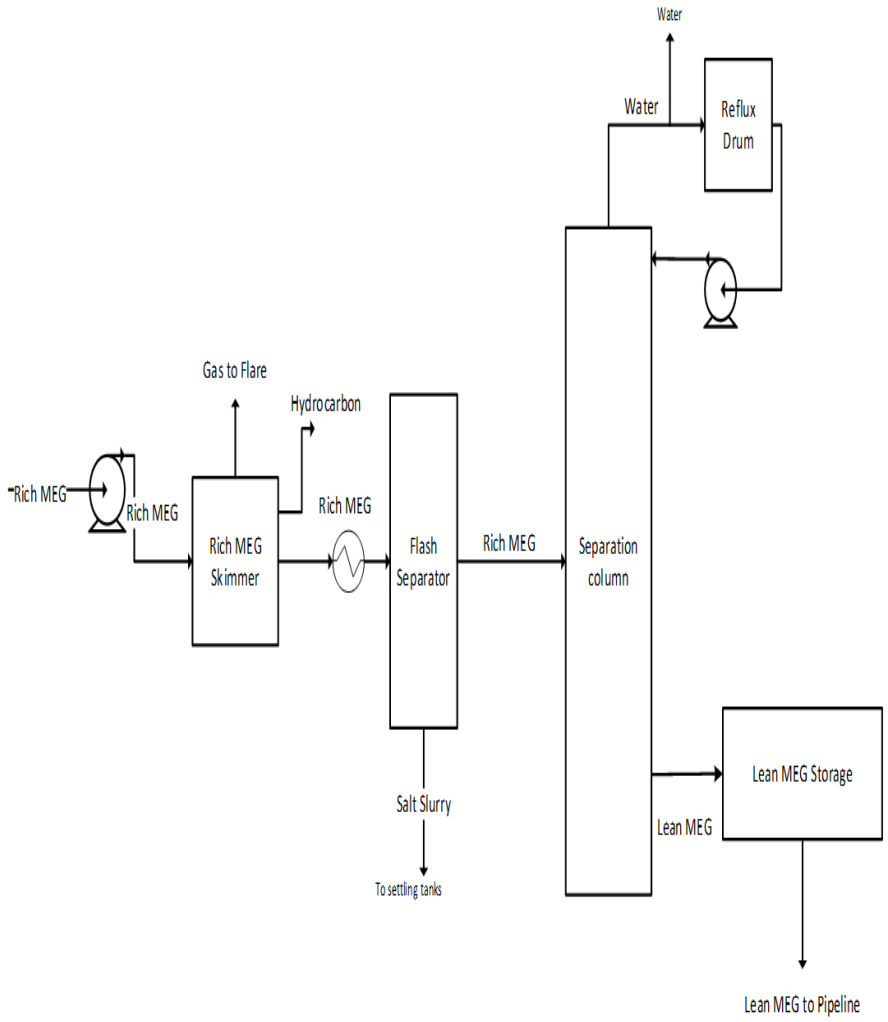

Figure 2-3: . Integrated MRU Design: extracted from Schlumberger PureMEG unit - Cameron, a Schlumberger company proprietary design [15, 51].

onetheless, Nazzer and Keogh et al. reported that the flash separator bottom recycle stream encountered a very high salt content resulting in scaling inside the recycle pump [47]. Boschee 2012, also reported that high divalent salt content, especially calcium ions, increased the viscosity of the flash separator recycles MEG stream putting more strain on the recycle pump. As a result, the viscous MEG stream had to be periodically replenished. The replenishment

increases operating cost as well as significant environmental cost to dispose used MEG [26].

A variation of the integrated MRU design was developed to minimise scaling at the recycle pump [49, 15]. In this variation, a downcomer extension is connected to the bottom part of the flash separator as shown in Figure 2-4; the recycle pump is positioned higher than the flash separator downcomer. Due to differences in density and gravity of MEG with varying salt content, the high salts concentration MEG pools to the bottom of the downcomer [49]. Therefore, the recycle pump which is positioned above the downcomer receives MEG in low salt content. This design may also include an integrated slip stream divalent ion removal system in which divalent ions can be precipitated by pH adjustment with chemical treatment.

2.4.3 Regeneration and Reclamation MRU Design

A schematic of a third MRU configuration is shown in Figure 2-5. For this MRU design configuration, divalent salts are first removed in the settling tank (pre-treatment). Subsequently, MEG is dewatered in a distillation column. Lean MEG then is desalinated under a vacuum-operated flash separation downstream of the distillation unit. MEG is evaporated in the desalination unit, thereby reducing the salt content in reclaimed MEG. Original MEG reclamation units are based on vacuum evaporation and crystallization where MEG is heated, under vacuum, to temperatures below 150 °C. MEG is flashed off, leaving salts and non-volatiles in the flash drum.

The major advantage of this configuration is that it can interchange between a full stream or slipstream reclamation. The full stream is when the entire MEG stream passes through the desalination unit, while the slipstream reclamation accommodates only a fraction of the MEG stream. A slipstream reclamation operation is suitable when salt contents are low, i.e. an early well life. As the

formation water starts to break through, the salt content rises, and the operation can be switched to the full stream reclamation. Other benefits of this design include the independence between each process. The desalination unit, whether full or slipstream, does not impact the operation of the distillation [51]. This is because the removal of water in the distillation column amounts to less volume of lean MEG requiring desalination compared to the volume of rich MEG being desalinated in design configurations 1 and 2. The small desalination unit is beneficial as it requires lower capital costs and less space requirement [51].

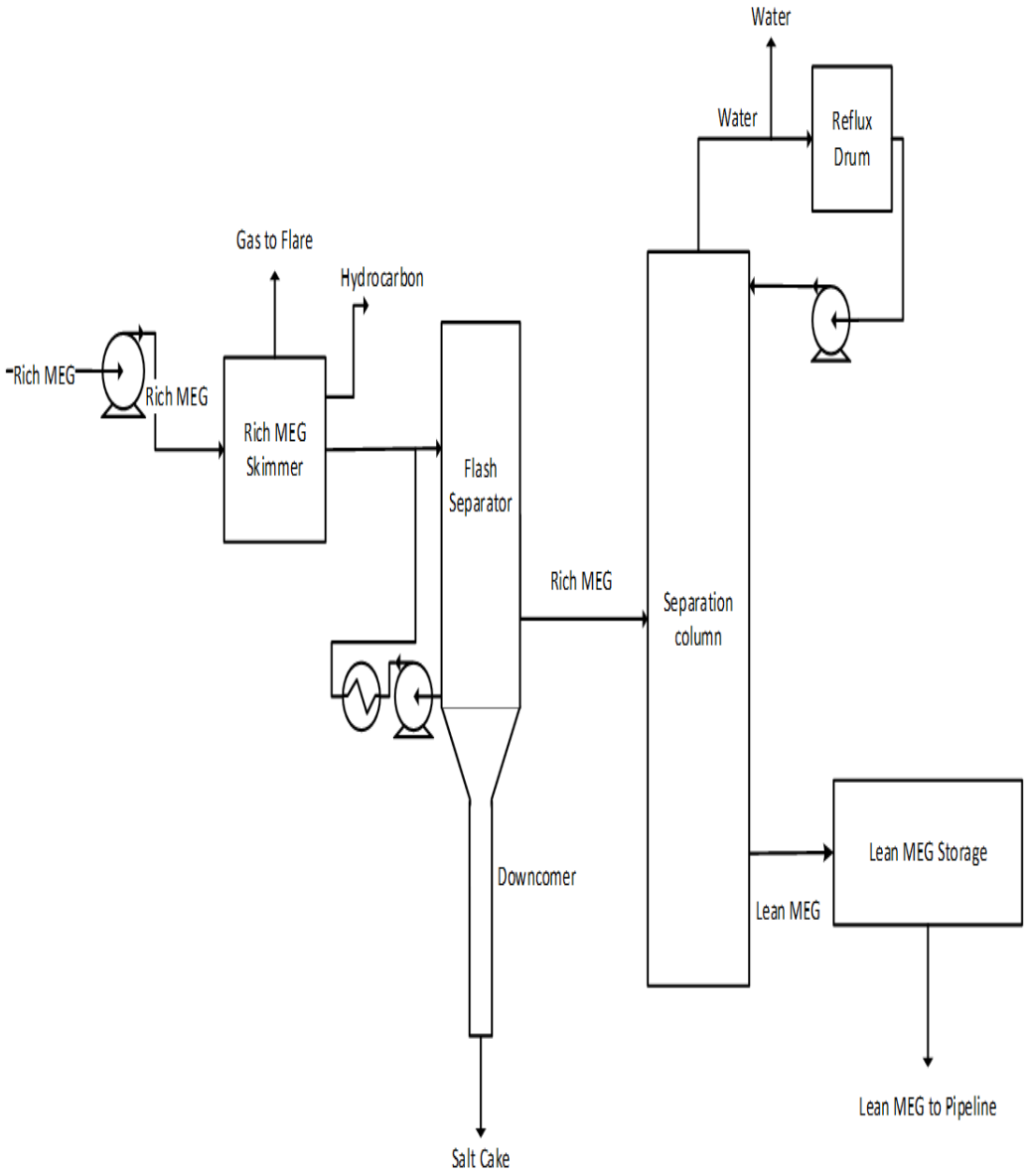

Figure 2-4: Integrated MRU design with downcomer extension to the flash separator.

MEG reclamation is an energy intense system. It was calculated that energy efficiency in an MRU drops about 1% when a slip stream reclamation unit is added to a regeneration only MRU and about 5% when a full stream reclamation is employed [52]. As a result, a slip stream reclamation system is commonly employed to minimise energy consumption and optimise overall efficiency.

2.5 MRU Factors and Efficiency

Simply put, the efficiency of a system is a measure of the system's ability to convert its inputs into the desired output. For an MRU, the desired output is the lean MEG meeting certain pre-defined specifications, whereas the input is rich MEG returning from the pipeline. Factors and efficiency discussed in this section address general operational issues that may not have been mentioned earlier in this paper but impact the efficiency and the feasibility of the entire MRU process. Key factors affecting the efficiency of the MRU are the quality of rich MEG and the specification for lean MEG. There is limited control over the quality of rich MEG returning from the gas pipeline. However, understanding the impact of pipeline flow assurance events on the quality of rich MEG and consequent effects on the MRU is crucial. The specification for lean MEG output from the MRU, on the other hand, can be defined to achieve thermodynamic hydrate inhibition, preventing scaling, corrosion and fouling inside the pipeline, and minimising cost implications for operating the MRU. Some of the essential lean MEG specifications that need to be defined are minimum MEG content, salt content, organic acid content, dissolved oxygen content, recyclable chemical additives, such as pH stabilizers, corrosion inhibitor and scale inhibitor residuals, etc. [53].

2.5.1 MEG Quality

The MEG system is a closed-loop process. Consequently, the quality of MEG in the MRU and that of MEG in the pipeline are interrelated. The performance of the MRU determines the quality of its lean MEG output while the rich MEG returning from the pipeline feeds the MRU and, in turn, influences the efficiency of the MRU to produce the required quality lean MEG for re-injection into the pipeline. The suppression of the hydrate onset temperature and delay in hydrate formation time by MEG depends on produced gas composition, MEG concentrations, and quality [54-57]. Thus, the percentage of MEG in lean

MEG output from the MRU should be high enough to suppress the hydrate onset temperature. As a general rule of thumb, the industry application of lean MEG is somewhere between 80-95wt% MEG content. A more accurate determination of the MEG-hydrocarbon vapour phase equilibria can be predicted by thermodynamic modelling [56] or simpler empirical correlations [54, 58].

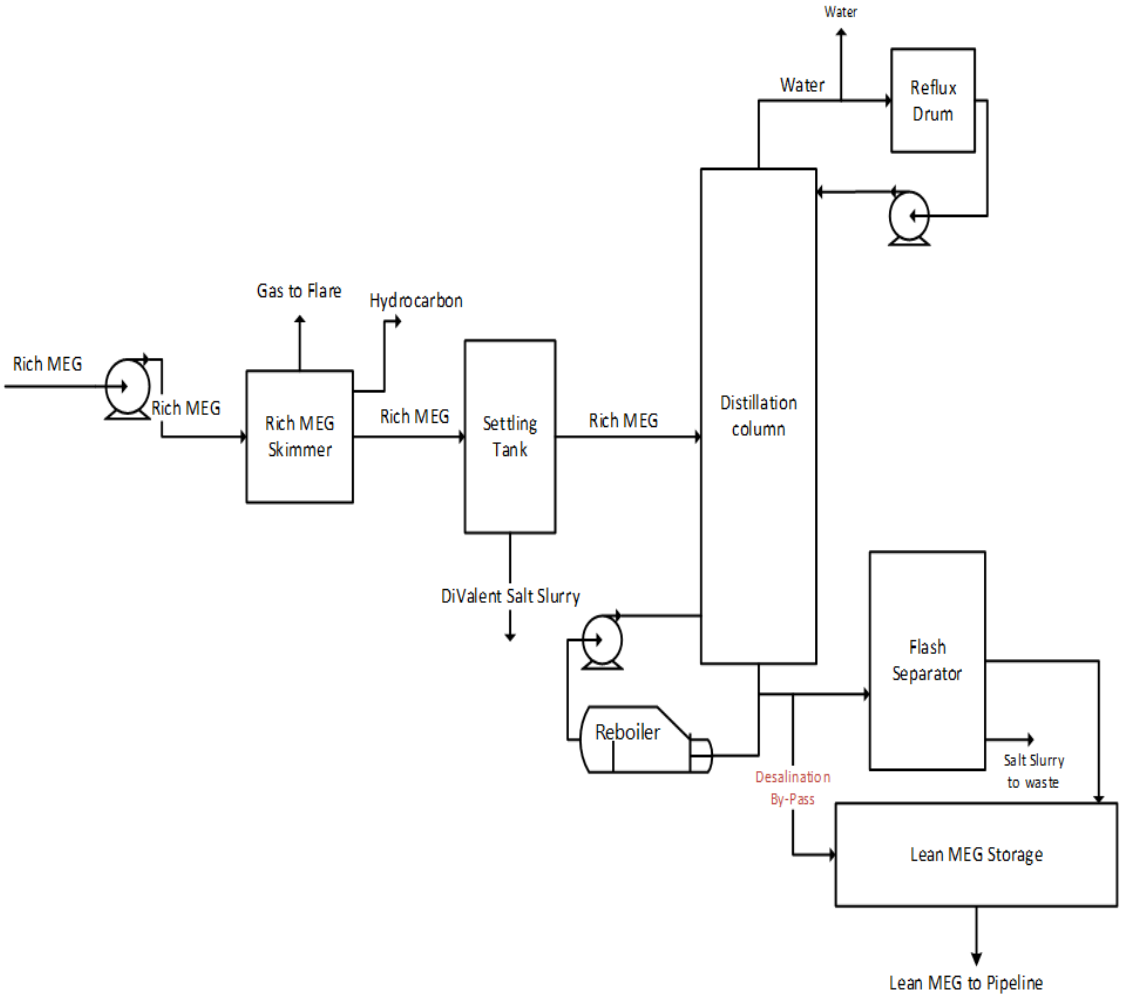

Figure 2-5: Regeneration and Reclamation MRU design. (Adapted from MRU design in Zaboon, S., et al., (2017) [31])

The salt content in the lean MEG may contribute to its hydrate inhibition effect. Lee and Kang (2011) reported that the addition of 3.5 wt.% NaCl in MEG reduced the hydrate formation temperature by 2.8-3.2 K. Masoudi et al. (2005) also showed that the presence of hydrated chloride salts in MEG increases hydrate inhibition efficiency [59]. Even though high concentrations of salts have not been experimentally tested for this synergistic effect, salts are not expected to contribute to hydrate formation in the pipeline. However, salts above their saturation point in lean MEG will deposit inside the pipeline causing a build-up of scale and fouling, which can be difficult and costly to clean up. The primary culprits contributing to scaling are carbonates of divalent cations; these salts will cause scaling and fouling in the MRU as discussed under MRU pre-treatment and scale-up inside the pipeline. Studies have shown that salts of specific divalent ions are more insoluble in the presence of MEG [53, 60]. As it is a close loop system, the divalent ions can accumulate and over-time exceed their saturation points, causing scaling of the pipelines and MRU.

Organic acids are inherently present in some hydrocarbon fields and also are products of the thermal oxidative degradation of MEG, which is accelerated at high temperature conditions such as in dewatering and desalination processes within the MRU [61, 62]. As mentioned earlier, the thermal degradation of neat MEG starts at 162 °C [40]. Moreover, salt and long-term exposure are shown to reduce the degradation onset temperature and also increase the rate of thermal degradation. Monteiro et al. (2019) used an experimental simulation of an MRU flash separator to show that MEG degrading at temperatures below 140 °C and the percentage of MEG degraded after 56 hours of long-term exposure sharply increased to 21.1% when the salt content increased to 5.52 wt.% [63].

Aside from thermal oxidative degradation of MEG, organic acids may also enter the MRU from the pipeline condensed water phase or formation water

[30]. The presence of organic acid in lean MEG poses several operational issues, including bottom-of-line and top-of-line corrosion of carbon steel pipelines and process equipment [64, 65]. The organic acid content in MEG also reduces hydrate inhibition efficiency of MEG. AlHarooni et al. (2017) reported that organic acid content in MEG as a result of thermal degradation even in neat MEG increases the hydrate onset temperature by up to 2.6 °C at 50 bar [66]. The removal of excess organic acid can be achieved during desalination and dewatering if the pH within the system is adequately controlled [26, 67].

In principle, closed-loop MRUs operate under oxygen-free conditions. However, oxygen contamination is not uncommon. The presence of oxygen in aqueous phase can accelerate thermal degradation of MEG and cause corrosion of both carbon steel and corrosion resistant alloys (CRAs). Dissolved oxygen concentration as low as 52 ppb initiated corrosion at stainless steel weldments due to the strong oxidizing effect of oxygen [68]. Ferrite dissolution and crevice corrosion were reported for duplex stainless steel with 620 ppb oxygen in salt-saturated MEG at 108 °C [69]; highlighting the detrimental impact of dissolved oxygen in MEG on pipelines and process equipment. The dissolved oxygen in MEG is thus a major cause for concern in MEG regeneration and injection into the pipelines.

2.5.2 MEG Loss in the MRU

The primary culprit for MEG losses in the MRU is the loss during hydrocarbon condensate skimming due to emulsification of MEG and condensate [70]. MEG loss also occurs during the dewatering step in the distillation column. The sudden changes in the column reflux level and accumulation of the water condensate increase boil-off liquid from the reboiler [21, 70]. Consequently, more MEG in the reboiler is vaporised and lost to the reflux drum. However, Son et al. showed that the desalination step (salt removal by centrifuge) in the MRU system with design configuration 2

led to more MEG losses than the dewatering step [32]. From desktop modelling, the desalination step accounts for up to 221 $/(kg/h) of MEG feed, whereas the dewatering step accounts for up to 25$/(kg/h), without factoring in MEG loss during dewatering due to fluctuations in the distillation column reflux rate [32]. At the cost of 1250 $ per tonne of MEG in Son et al.'s work, these losses amount to 176.8 kg MEG/h during the desalination and 20 kg MEG/h during the dewatering step. These results showed that the desalination could cause significant MEG loss from removing the precipitated salt slurry. Conversely, Kim et al. (2019) reported operational losses of 1.8 m^3 MEG/month in the reboiler [70]; assuming uninterrupted operation of 24 h in a 30-day month, which amounts to 2.5 kg/h. Kim et al. (2019) reported that MEG loss in the operating facility was reduced by up to 75.2% when freshwater was introduced into the distillation column reflux system [70]. Another significant factor contributing to MEG loss in the MRU is accumulation of highly soluble salts in the reclaimer. Examples are salts of organic acids like sodium acetate, which can accumulate to 10 wt.% [15]. or more and thereby increase the boiling temperature and the viscosity of the liquid in the reclaimer to levels that are not manageable. The only solution today, seems to be bleeding of the reclaimer slurry. This bleeding amounts to significant loss of MEG. Another process that leads to MEG loss, albeit a small quantity, is the thermal degradation of MEG.

2.5.3 Corrosion and Corrosion Mitigation in the MRU

Corrosion mitigation remains a technical challenge for maintaining the asset integrity of the MEG system. High process temperatures, high shear stress, produced or formation water, and acid gases can cause corrosion concerns with the MRU construction materials [71].

The material selection and metallurgy for use in the MRU generally takes into consideration operating conditions of the MRU, e.g., operating temperatures,

presence of acid gases in the system (if any), the salt loading and potential contaminations of the liquid phase at any point in the system, and the capital cost of the unit. Corrosion resistant alloys (CRA) are generally used in parts of the MRU where a high salt loading or low pH resulting from acid gases is expected [72]. While oil and gas pipeline metallurgy and material selection are widely published [53, 73], there are limited reports on the specific material used in MRUs. However, austenitic stainless steel (UNS S31600/03) and duplex stainless steel (UNS S32205) is relatively common, as well as Inconel® alloy 625 grade steel (UNS N06625) [72, 74-76].

For example, the overhead of the distillation unit is exposed to distilled water from the dewatering process and acid gas, especially CO_2. As such, this area is prone to acid gas corrosion, and the use of CRAs would be appropriate [67]. Latta et al. 2016 mentioned an operational example of the use of carbon steel in an MRU dewatering overhead being "severely corroded", albeit corrosion rate figures were not reported in their publication [14].

For carbon steel, such as in pipelines, corrosion mitigation uses either a film forming corrosion inhibitor (FFCI) or pH stabilization. FFCI is a surfactant that forms a thin inhibitor film on the metal surface and as a protective layer, suppressing corrosion of carbon steel. pH stabilization prevents corrosion in two ways; first, by neutralizing acidic components in the aqueous phase, eliminating the cathodic reaction and reducing the corrosion rate. Secondly, by stabilizing pH at about 8 – 9, the formation of $FeCO_3$ is facilitated. The adherent $FeCO_3$ then acts as a barrier to prevent corrosion [77]. The optimal operating pH range in MRU is where corrosion is suppressed, but the scale precipitation is not facilitated. The effects of temperature on corrosion of carbon steel components in the MRU can be complex. The consensus is that the corrosion rate of carbon steel can be effectively reduced in MEG at lower temperatures but not at elevated temperatures, such as in the reboiler condition.

Corrosion rates increase with increasing temperature when the protective corrosion product scale does not form. A 2.8 times rise in the corrosion rate of carbon steel in rich MEG solutions was reported when temperature was increased from 25 °C to 60 °C [78]. A similar trend was found when the temperature was raised from 80 °C to 120 °C in lean MEG solutions (80 wt.% MEG) saturated with CO_2 [79]. Even though the corrosion rates markedly reduced from 15.25 mm/y in MEG-free solutions to 3.18 mm/y (80 wt.% MEG) under the same condition, the resulting corrosion rate was still much greater than the accepted industry standard of 0.1 mm/y. Another study mimicked the reboiler condition with N_2 atmosphere [78]. In this case, the corrosion rate was much milder (0.43 mm/y) and was effectively mitigated with the pH stabilization method using mono-ethylamine.

However, most literature on corrosion in MEG solutions has focused on carbon steel and not on the corrosion of MEG on other construction metals, such as duplex stainless steel and other corrosion resistant alloys (CRAs), especially for corrosion in the MEG regeneration context. Joosten et al. published a work that compares the suitability of 22 Cr duplex stainless steel (UNS S31803), low alloy steel, and Alloy 625 (UNS N06625) for MEG reclamation systems [69]. However, further research is needed to fill the current gaps for other CRAs.

2.6 Summary

As MEG is widely used as a hydrate inhibitor, its regeneration and reclamation processes become vital to the overall natural gas production and processing. A review of this process is presented in this paper, which covers the use of MEG as a hydrate inhibitor and the need for regeneration and reclamation, MRU processes and the common MRU design configuration. Important factors affecting the efficiency of the MRU system were also discussed. Despite considerable research on the design and operation of the

MRU system, there seems to be significant gaps in some specific aspects of the MRU operation, as highlighted below.

Frequent fouling in the MRU remains a technical challenge with MRU operations; the cause of fouling and a credible prevention method is yet to be fully studied and understood. MRU treatment chemical additives has been suspected to contribute to fouling. However, the mechanism of this fouling is yet to be fully understood. There is also a significant knowledge gap in the mechanism of MEG degradation during MRU operation, with or without chemical additives. More work is required to explore the potential corrosive behaviour of thermally degraded MEG for MRU asset integrity.

Foaming and emulsion are also major challenges with MRU operations as it minimizes the efficiency of the MRU. The presence of foaming and stable emulsion formation in the MRU are frequently reported but no systematic study has been conducted to elucidate the causes of these incidents and prevention methods. Besides, the interaction of MEG with pipeline fluids causing foaming and stable emulsion could be further explored.

References

1. Akpabio, M. G., *Cold flow in long-distance subsea pipelines*. 2013, Institutt for petroleumsteknologi og anvendt geofysikk.
2. Hammerschmidt, E., *Formation of gas hydrates in natural gas transmission lines.* Industrial & Engineering Chemistry, 1934. 26 (8): p. 851-855.
3. Saberi, A., et al., *Experimental measurement and thermodynamic modeling of equilibrium condition for natural gas hydrate in MEG aqueous solution.* Fluid Phase Equilibria, 2018. 459: p. 110-118.
4. Liu, J., et al., *Molecular insights into the kinetic hydrate inhibition performance of Poly (N-vinyl lactam) polymers.* Journal of Natural Gas Science and Engineering, 2020. 83: p. 103504.
5. Clark, L. W., L. M. Frostman, and J. Anderson. *Low Dosage Hydrate Inhibitors (LDHI): Advances in Flow Assurance Technology for Offshore Gas Production Systems*. IPTC.
6. Lederhos, J., et al., *Effective kinetic inhibitors for natural gas hydrates.* Chemical Engineering Science, 1996. 51 (8): p. 1221-1229.
7. Brustad, S., K.-P. Løken, and J. G. Waalmann. *Hydrate Prevention using MEG instead of MeOH: Impact of experience from major Norwegian developments on technology selection for injection and recovery of MEG*. in *Offshore technology conference*. 2005. Offshore Technology Conference.
8. Dapena, J. A., et al. *Gas hydrate management strategies using anti-agglomerants: Continuous & transient large-scale flowloop studies*. in *Offshore Technology Conference*. 2017. OnePetro.
9. Tian, J., et al. *Low Dosage Hydrate Inhibitors (LDHI): Advances and Developments in Flow Assurance Technology for Offshore Oil and Gas Productions*. Offshore Technology Conference.
10. Xu, Y., M. Yang, and X. Yang, *Chitosan as green kinetic inhibitors for gas hydrate formation.* Journal of Natural Gas Chemistry, 2010. 19 (4): p. 431-435.
11. Akhfash, M., et al., *Gas Hydrate Thermodynamic Inhibition with MDEA for Reduced MEG Circulation.* Journal of Chemical & Engineering Data, 2017. 62 (9): p. 2578-2583.
12. Fan, C., et al., *Barite Nucleation and Inhibition at 0 to 200°C With and Without Thermodynamic Hydrate Inhibitors.* SPE Journal, 2010. 16 (02): p. 440-450.
13. Flaten, E. M., M. Seiersten, and J.-P. Andreassen, *Polymorphism and morphology of calcium carbonate precipitated in mixed solvents of ethylene glycol and water.* Journal of Crystal Growth, 2009. 311 (13): p. 3533-3538.
14. Latta, T. M., et al. *Design Considerations for Mitigating the Impact of Contaminants in Rich MEG on Monoethylene Glycol Recovery Unit MRU Performance*. Offshore Technology Conference.

15. *MEG Regeneration Technical Meeting*. 2009, SPE International, Victoria and Tasmania Section Schlumberger Limited: Port Campbell.
16. Babu, D., M. Hosseinzadeh, and H. Akbary, *Study links iron sulfide to MEG column burping.*
17. Babu, D. R., et al., *Carbonates precipitation in MEG loops – A comparative study of South Pars and Bass Strait gas fields.* Journal of Natural Gas Science and Engineering, 2015. 27: p. 955-966.
18. Manfield, P., et al., *Wax-On, Wax-Off: Understanding and Mitigating Wax Deposition in a Deepwater Subsea Gas/Condensate Flowline*, in *Offshore Technology Conference*. 2007, Offshore Technology Conference: Houston, Texas, U.S.A. p. 10.
19. Schümann, H., et al., *Rheology Study: Comparison of a Real Condensate-MEG System and a Model Fluid System*, in *BHR 19th International Conference on Multiphase Production Technology*. 2019, BHR Group: Cannes, France. p. 15.
20. Anthony, J., et al., *Lessons Learned from Residual Corrosion Inhibitor Measurements by LC-MS in a Mature North Sea Gas/Condensate/MEG Production System*, in *SPE International Oilfield Corrosion Conference and Exhibition*. 2018, Society of Petroleum Engineers: Aberdeen, Scotland, UK. p. 16.
21. Haque, M. E., *Ethylene glycol regeneration plan: a systematic approach to troubleshoot the common problems.* Journal of Chemical Engineering, 2012. 27: p. 21-26.
22. Soames, A., et al., *Effect of wettability on particle settlement behavior within Mono-Ethylene Glycol regeneration pre-treatment systems.* Journal of Petroleum Science and Engineering, 2019. 179: p. 831-840.
23. Ramchandran, S., *Minimize trapped components in distillation columns: here is how one plant remedied a distillation difficulty by analyzing, then counteracting, the chemistry that had led to the problem.* Chemical Engineering, 2006. 113 (3): p. 65-70.
24. Latta, T. M., et al., *Design Considerations to Minimize Hydrocarbon Entrainment in the Aqueous Phase*, in *Offshore Technology Conference*. 2018, Offshore Technology Conference: Houston, Texas, USA. p. 86.
25. Karami, H., E. Pereyra, and C. Sarica, *Effects of monoethylene glycol (MEG) on three-phase flow characteristics in near-horizontal pipes.* Journal of Petroleum Science and Engineering, 2017. 149: p. 834-843.
26. Boschee, P., *Gas Hydrate Control Using Monoethylene Glycol in the Gulf of Mexico.* Oil and Gas Facilities, 2012. 1 (03): p. 14-18.
27. Soames, A., et al., *Operation of a MEG pilot regeneration system for organic acid and alkalinity removal during MDEA to FFCI switchover.* Journal of Petroleum Science and Engineering, 2018. 169: p. 1-14.
28. Seiersten, M. and S. S. Kundu, *Scale Management in Monoethylene Glycol MEG Systems - A Review*, in *SPE International Oilfield Scale Conference and*

Exhibition. 2018, Society of Petroleum Engineers: Aberdeen, Scotland, UK. p. 10.
29. Guan, H., G. Cole, and P. J. Clark. *Inhibitor Selection for Iron Scale Control in MEG Regeneration Process*. Society of Petroleum Engineers.
30. Latta, T. M., M. E. Seiersten, and S. A. Bufton. *Flow assurance impacts on lean/rich MEG circuit chemistry and MEG regenerator/reclaimer design*. in *Offshore technology conference*. 2013. Offshore Technology Conference.
31. Zaboon, S., et al., *Recovery of mono-ethylene glycol by distillation and the impact of dissolved salts evaluated through simulation of field data.* Journal of Natural Gas Science and Engineering, 2017. 44: p. 214-232.
32. Son, H., et al., *Simulation and modeling of MEG (Monoethylene Glycol) regeneration for the estimation of energy and MEG losses.* Energy, 2018. 157: p. 10-18.
33. Braga Pires, A. P., et al., *Application of a new pilot-scale distillation system for monoethylene glycol recovery using an energy saving falling film distillation column.* Chemical Engineering Research and Design, 2020. 153: p. 263-275.
34. Ajdar, M. A., et al., *Air gap membrane distillation of MEG solution using PDMS coated polysulfone hollow fiber membrane.* Polymer Testing, 2019. 76: p. 1-9.
35. Lawson, K. W. and D. R. Lloyd, *Membrane distillation.* Journal of Membrane Science, 1997. 124 (1): p. 1-25.
36. Rincón, C., J. M. Ortiz de Zárate, and J. I. Mengual, *Separation of water and glycols by direct contact membrane distillation.* Journal of Membrane Science, 1999. 158 (1): p. 155-165.
37. Mohammadi, T. and M. Akbarabadi, *Separation of ethylene glycol solution by vacuum membrane distillation (VMD).* Desalination, 2005. 181 (1): p. 35-41.
38. Drioli, E., A. Ali, and F. Macedonio, *Membrane distillation: Recent developments and perspectives.* Desalination, 2015. 356: p. 56-84.
39. Alonso, G., E. del Valle, and J. R. Ramirez, *3 - Desalination plants*, in *Desalination in Nuclear Power Plants*, G. Alonso, E. del Valle, and J. R. Ramirez, Editors. 2020, Woodhead Publishing. p. 31-42.
40. AlHarooni, K., et al., *Inhibition effects of thermally degraded MEG on hydrate formation for gas systems.* Journal of Petroleum Science and Engineering, 2015. 135: p. 608-617.
41. Phelps, D. W. and L. E. C. Fernandez, *Divalent Cation Removal From Rich Monoethylene Glycol (MEG) Feed Streams By Ion Exchange*. 2017, Google Patents.
42. Phelps, D. W. and L. E. C. Fernandez, *Hydrocarbon and divalent cation removal from rich mono ethylene glycol (MEG) feed streams by regenerable filters*. 2015, Google Patents.

43. He, S., et al., *Low-voltage and ion-free-reverse-migration electrically regenerated mixed-bed ion exchange for MEG desalination.* Asia-Pacific Journal of Chemical Engineering, 2020. 15 (6): p. e2559.
44. Renpu, W., *Chapter 1 - Basis of Well Completion Engineering*, in *Advanced Well Completion Engineering (Third Edition)*, W. Renpu, Editor. 2011, Gulf Professional Publishing. p. 1-74.
45. Olsen, S., A. Dugstad, and O. Lunde. *pH-stabilization in the Troll gas-condensate pipelines*. in *CORROSION 99*. 1999. OnePetro.
46. BRUSTAD, S., K. LOKEN, and J. K. A. WAALMANN, *Engineering and Technology Hydrate Prevention using MEG instead of MeOH: Impact of experience from major Norwegian developments on technology selection for injection and recovery of MEG.* S. OTC, 2005. 17355.
47. Nazzer, C. A. and J. Keogh. *Advances in Glycol Reclamation Technology*. in *Offshore Technology Conference*. 2006. Houston Texas: Offshore Technology Conference.
48. Hayhoe, P., *Glycol purification-a novel approach to an old problem.* New Zealand Engineering, 1993. 48 (5): p. 12.
49. Hou, R., et al., *Operational study of a monoethylene glycol (MEG) desalination pilot plant. Part I: Development of a new method for the estimation of MEG content in the presence of NaCl solid particles.* Chemical Engineering Research and Design, 2019. 146: p. 344-351.
50. *PUREMEG Monoethylene glycol reclamation and regeneration unit*, S. Limited, Editor. 2020, Schlumberger Limited.
51. Condilis, A., J. E. Vale, and T.-E. Stranna, *Closed loop glycol systems—experience from BP's Shah Deniz gas export project and advances in technology.* The APPEA Journal, 2008. 48 (1): p. 249-260.
52. Teixeira, A. M., et al., *Exergy Analysis of Monoethylene glycol recovery processes for hydrate inhibition in offshore natural gas fields.* Journal of Natural Gas Science and Engineering, 2016. 35: p. 798-813.
53. Halvorsen, A. M. K., et al. *The Relationship Between Internal Corrosion Control Method, Scale Control and Meg Handling of a Multiphase Carbon Steel Pipeline Carrying Wet Gas with CO2 And Acetic Acid*. in *CORROSION 2007*. 2007.
54. Cha, M., et al., *Thermodynamic and kinetic hydrate inhibition performance of aqueous ethylene glycol solutions for natural gas.* Chemical Engineering Science, 2013. 99: p. 184-190.
55. Haghighi, H., et al., *Experimental and thermodynamic modelling of systems containing water and ethylene glycol: Application to flow assurance and gas processing.* Fluid Phase Equilibria, 2009. 276 (1): p. 24-30.
56. Kontogeorgis, G. M., et al., *Ten Years with the CPA (Cubic-Plus-Association) Equation of State. Part 1. Pure Compounds and Self-Associating Systems.* Industrial & Engineering Chemistry Research, 2006. 45 (14): p. 4855-4868.

57. Lee, J.-W. and S.-P. Kang, *Phase Equilibria of Natural Gas Hydrates in the Presence of Methanol, Ethylene Glycol, and NaCl Aqueous Solutions.* Industrial & Engineering Chemistry Research, 2011. 50 (14): p. 8750-8755.
58. Bahadori, A., *A simple mathematical predictive tool for estimation of hydrate inhibitor loss in hydrocarbon liquid base.*
59. Masoudi, R., et al., *Measurement and prediction of gas hydrate and hydrated salt equilibria in aqueous ethylene glycol and electrolyte solutions.* Chemical Engineering Science, 2005. 60 (15): p. 4213-4224.
60. Tomson, M. B., A. T. Kan, and G. Fu. *Inhibition Of Barite Scale In The Presence of Hydrate Inhibitors*. in *SPE International Symposium on Oilfield Scale*. 2004.
61. Psarrou, M. N., et al., *Carbon Dioxide Solubility and Monoethylene Glycol (MEG) Degradation at MEG Reclaiming/Regeneration Conditions.* Journal of Chemical & Engineering Data, 2011. 56 (12): p. 4720-4724.
62. Rossiter Jr, W. J., P. W. Brown, and M. Godette, *The determination of acidic degradation products in aqueous ethylene glycol and propylene glycol solutions using ion chromatography.* Solar Energy Materials, 1983. 9 (3): p. 267-279.
63. Monteiro, M. F., et al., *Thermal Degradation of Monoethylene Glycol in Aqueous Saline Solution: Evaluation by Thermogravimetric and Physicochemical Analyses.* Industrial & Engineering Chemistry Research, 2019. 58 (27): p. 12159-12165.
64. Ikeh, L., G. Enyi, and G. Nasr. *Inhibition Performance of Mild Steel Corrosion in the Presence of Co 2, HAc and MEG*. in *SPE International Oilfield Corrosion Conference and Exhibition*. 2016. Society of Petroleum Engineers.
65. Liu, D., Z. Chen, and X. Guo, *The effect of acetic acid and acetate on CO2 corrosion of carbon steel.* Anti-Corrosion Methods and Materials, 2008. 55 (3): p. 130-134.
66. AlHarooni, K., et al., *Influence of Regenerated Monoethylene Glycol on Natural Gas Hydrate Formation.* Energy & Fuels, 2017. 31 (11): p. 12914-12931.
67. Soames, A., A. Barifcani, and R. Gubner, *Removal of Organic Acids during Monoethylene Glycol Distillation and Reclamation To Minimize Long-Term Accumulation.* Industrial & Engineering Chemistry Research, 2019. 58 (16): p. 6730-6739.
68. Rogne, T., et al., *The influence of some environmental factors on the corrosion of stainless steel weldments exposed to simulated well flow*. Conference: Corrosion '89, New Orleans, LA (USA), 17-21 Apr 1989; Other Information: Technical Paper 89470. 1989: Houston, TX (USA); National Assoc. of Corrosion Engineers. Medium: X; Size: Pages: (12 p).
69. Joosten, M. W., et al. *Materials Considerations for MEG (Mono Ethylene Glycol) Reclamation Systems*. in *CORROSION 2007*. 2007.

70. Kim, J., et al. *Mono Ethylene Glycol Regeneration System Upgrade*. in *SPE/IATMI Asia Pacific Oil & Gas Conference and Exhibition*. 2019.
71. Bikkina, C., et al. *Development of MEG regeneration unit compatible corrosion inhibitor for wet gas systems*. in *SPE Asia Pacific oil and gas conference and exhibition*. 2012. OnePetro.
72. Kim, H., et al., *Economic evaluation of MEG injection and regeneration process for oil FPSO.* Journal of Petroleum Science and Engineering, 2018. 164: p. 417-426.
73. Hagerup, O. and S. Olsen. *Corrosion Control by pH Stabilizer, Materials and Corrosion Monitoring in 160 km Multiphase Offshore Pipeline*. in *CORROSION 2003*. 2003.
74. Moussa, A. M., S. Habib, and A. Shinaishin. *Scarab/Saffron Development Project Case study: Material Selection Criteria for the Monoethylene Glycol Recovery Package*. 2004. Egypt.
75. Malik, A. U., et al., *The influence of pH and chloride concentration on the corrosion behaviour of AISI 316L steel in aqueous solutions.* Corrosion Science, 1992. 33 (11): p. 1809-1827.
76. Olsson, J., *Stainless steels for desalination plants.* Desalination, 2005. 183 (1): p. 217-225.
77. Soames, A., et al., *Corrosion of Carbon Steel during High Temperature Regeneration of Monoethylene Glycol in the Presence of Methyldiethanolamine.* Industrial & Engineering Chemistry Research, 2019. 58 (32): p. 14814-14822.
78. Gonzalez, J. J., M. E. Alfonso, and G. Pellegrino, *Corrosion of Carbon Steels in Monoethylene Glycol*, in *CORROSION 2000*. 2000, NACE International: Orlando, Florida. p. 13.
79. Pojtanabuntoeng, T., M. Salasi, and R. Gubner, *The Influence of Mono Ethylene Glycol (MEG) on CO2 Corrosion of Carbon Steel at Elevated Temperatures (80 to 120oc)*, in *CORROSION 2014*. 2014, NACE International: San Antonio, Texas, USA. p. 13.

Chapter 3

Ion chromatography for MEG assay and application to MEG Recovery Unit

3.1 Abstract

Monoethylene glycol (MEG) is a thermodynamic hydrate inhibitor (THI) commonly used to inhibit hydrate formation in long gas tie-backs in deepwater applications. MEG can be regenerated and reused over several cycles, increasing its economic viability for use. Moreover, MEG is much more environmentally friendly and less toxic compared to other hydrate inhibitors. Nonetheless, several technical challenges are associated with regeneration of MEG in the MEG Recovery Unit (MRU), including but not limited to scaling, gunking and internal system corrosion. A robust and effective MEG quality monitoring program is crucial to the proper operation of the MEG, hence requiring effective MEG assay methods. This work focuses on developing test methods for MEG assay using the ion chromatography (IC) technique as a relatively lower cost option compared to other existing test methods like the inductively coupled plasma (ICP) and Fourier Transform Infrared (FTIR) spectroscopy. Cation and anion IC test methods were developed and validated

for accuracy and precision on MRU MEG samples. The analysis of MEG samples from a pilot scale MRU using the newly developed methods yielded satisfactory results with spikes recovery >91% and Relative standard deviation <5.25% (n = 20).

Keywords: Ion Chromatography, Monoethylene glycol, MEG Recovery Unit, cation, anion

3.2 Introduction

As the world moves towards cleaner and more environmentally friendly energy sources amidst growing global demand for energy, natural gas continues to emerge as a cleaner alternative to fossil fuels, increasingly replacing coal and oil [1]. As of 8 offshore natural gas production from deepwater wells with long tie-backs accounted for 28% of the world's natural gas supply [2]. Gas hydrate formation is a risk that continually challenges flow assurance for producing natural gas from deep waters [3]. Natural gas hydrates are solid crystalline lattices of water molecules encapsulating natural gas molecules [4], formed by the physical combination of low molecular weight natural gases (i.e. methane, ethane, propane and Carbon dioxide as well as nitrogen and hydrogen sulphide) and water under relatively high pressures (> 170 psi) and relatively low temperatures (≈4 °C) [5]. The hydrate formation curve defines the exact pressures and temperatures at which natural gas hydrate is formed [5]. If formed in the gas pipelines, natural gas hydrates can obstruct the flow of production fluid and could eventually block the pipeline causing significant losses to production [3]. Thus, robust hydrate control strategies to mitigate these losses are crucial.

MEG is a thermodynamic hydrate inhibitor (THI) commonly used for deep water production. The benefits of using MEG include low losses to the gas and condensate phases during processing and its ability to be regenerated and reclaimed [6]. However, MEG degradation, scaling and gunking are common problems plaguing the MEG recycle process in the MEG Recovery Unit (MRU), hence requiring excellent control of the quality of MEG in the system [7-8].

In general, lean MEG with low water content (< 20 wt.%) and low salt content (<1000 ppm) is injected at the wellhead. After mixing with produced water (formation or condensed water), water content increases and this is referred to

as rich MEG with water content from 40 – 50 wt. % water. The rich MEG stream is returned to topside processing and the MEG Recovery Unit (MRU) [7]. Rich MEG feed to the MRU carries along all other pipeline aqueous phase constituents, including any reservoir salts, subsea chemical additives and pipeline corrosion products [9]. The function of the MRU is to remove chemical contaminants and water from rich MEG to make it suitable for subsea re-injection as lean MEG. As the MRU is a closed loop system, contaminants can gradually accumulate. The efficiency of the MRU and entire production flow assurance is greatly determined by the quality of the MEG in (and out of) the MRU; scaling and gunking being direct consequences of poor MEG quality [9-10].

Thus, the assay of the MEG streams in the MRU is periodically analysed for concentrations of salts and contaminants, necessitating robust analytic methods for MEG assay [11]. Several analytical test methods are currently employed for MEG assay, the major ones being Karl Fischer titration, Inductively Coupled Plasma (ICP) and Fourier Transform Infrared (FTIR) spectroscopy. Though robust, these analytical methods are usually employed in synergy as no single method can provide a comprehensive MEG quality assay. The Karl Fischer titration is a well-established, accurate and precise method for determining free and bound water content in MEG samples [12-13]. The hydrate inhibition capacity of lean MEG largely depends on its water content, hence the need for accurate determination of water in MEG by the Karl Fischer titration [14]. FTIR is a cost-effective and relatively easy-to-deploy technique, offering a unique method for compositional analysis of solids, liquids and gases by infra-red spectroscopy [15-16]. While FTIR is highly sensitive and very efficiently returns qualitative and quantitative results for inorganic samples, accurate analysis in aqueous samples remains a technical challenge with the FTIR technique. FTIR is often blinded by the very strong and

broad absorbance band for water in the IR spectrum. This absorbance band is around 3200-3600 (aym and sym O-H str.) and it can cause other FTIR responsive compounds to go undetected in aqueous solutions [16-17]. Often, FTIR will identify aqueous solutions as simply water due to this overwhelming signal [16-17]. Consequently, the accurate determination of ions like sodium, potassium etc., in MRU MEG samples (which contain about 20 – 50 wt% water) by FTIR is difficult.

The ICP technique is another accurate elemental analysis method, especially for trace elements [18]. With the ICP, the test sample is atomised by an Inductively Coupled Plasma, creating atomic ions, which can be characterised by either mass spectrometry for ICP-MS [19] or optical emission spectroscopy for ICP-OES [20]. The ICP-OES is used to validate results in this study, and it proved to be very accurate and fast for determining metal and alkali metal content in MRU MEG samples. However, the ICP only detects elements as it atomises the analyte sample; consequently, it is not applicable for the measurement of organic molecules like organic acids and Methyl di-ethanolamine (MDEA) in MRU MEG samples, for which the ion chromatography methods in this study are employed. Another significant drawback of using the ICP technique is the significant capital investment in acquiring the instrument and the equally significant associated running costs. While capital costs can vary significantly with the system configuration, the cost for sample analysis by ICP-MS is approximately double of that for similar analysis by IC [21-23]. The IC methods in this study have been developed as simple, cost-effective and easy-to-deploy methods for MRU MEG assay.

Ion chromatography (IC) is a separation technique based on the selective affinity of ionic analytes in a mobile phase (eluent) onto the surface of a stationary phase (separation column) [24]. The mechanism for separation in ion chromatography can be one of three; ion-exchange with high polarizability for

ion-exchange chromatography, ion-exclusion governed by Donnan exclusion, steric exclusion and sorption processes as in ion-exclusion chromatography, or ion-adsorption onto low polarity resin as in ion-pair chromatography [25]. The ion-exchange chromatography mechanism is most applicable for solutions containing highly polarised ions, such as the salt and organic acid ions in Rich MEG [24].

Ion-Exchange chromatography is based on the affinity of oppositely charged ions in the mobile phase to the stationary phase [24]. The stationary phase carries functional groups with a fixed charge; the oppositely charged ion in the mobile phase temporarily replaces the fixed charge in the stationary phase as the mobile phase continually flows past. The retention time (i.e., the length of time an ion remains fixed to the stationary phase) of each charged ion on the stationary phase alters according to their affinities to the stationary phase. Differences in retention times mean that differently charged ions elute the stationary phase at different times resulting in separation. The ions eluting from the separation column at specified retention times are quantified by detection in a conductivity measurement cell.

In MEG samples from various parts of the MRU, typical cation constituents of rich MEG are sodium, potassium, calcium, magnesium, barium and strontium from reservoir fluids [11; 26]. The protonated MDEA is another common constituent of the MEG streams when MDEA is used as a pH stabiliser for corrosion mitigation [26]. In concentrations greater than their solubility limits in the MEG streams, these cations could precipitate as carbonates and drop out of solution resulting in scaling within the MRU and in the wet gas pipeline [27-28]. Accurate determination of these cation concentrations is a quality control mechanism that could mitigate scaling and other consequences.

On the flip side, organic acid anions can be accumulated in the MEG streams either from reservoir fluids or from the degradation of MEG in the MRU [29]. Organic acid accumulation could contribute to gunking, lack of pH control and consequently corrosion in certain parts of the MRU [10; 26]. Organic acids are also significant products of MEG degradation and could reduce the efficacy of MEG as a hydrate inhibitor [30]. Proper monitoring of the organic acid concentration in the MRU is required as significant quality control for MEG as a THI and to mitigate gunking and corrosion within the MRU. Both cation and anion chromatographic methods were applied to the MEG assay in this work. The cation analyses were used to determine significant cations in MRU MEG samples; these are cations of sodium, potassium, magnesium, calcium, strontium, barium and Methyl di-ethanolamine (MDEA). The organic acids of interest in this work are acetate, formate, glycolate, oxalate and propionate. Water content in MEG samples can be determined by Karl-fischer titration if required.

3.3 Methodology

3.3.1 Ion chromatography system configuration

The basic configuration of the IC system consists of 6 stages – eluent delivery, sample injection, separation, suppression, detection, and data analysis. A schematic of a basic IC system configuration is shown in Figure 3-1. The IC process starts with eluent delivery to the separation column through a high-pressure pump. During a test, analyte samples are injected into the mobile phase and carried into the separation column, where the separation occurs. A smaller guard column, usually made of the same material as the separation column, is installed prior to the separation column to protect the separation column and enhance separation by acting as a pre-separation column before

the analytes pass through the main separation column. Conductivity measurements detect and quantify the eluting ions from the separation column.

Two Thermo Scientific Dionex ICS-2100 Integrated Reagent-Free IC Systems were used in this work; one for cation analysis and the other for anion analysis. Both systems had very similar configurations, as shown in Figure 3-1. Both systems were equipped with the following:

i. An Eluent generator Cartridge
ii. Sample injection unit
iii. A thermostated main separation column and A thermostated guard column
iv. A Suppression unit
v. A Digital conductivity detection unit
vi. Chromeleon™ 7.2 Chromatography Data System (CDS) software
vii. A thermostated auto-sampler

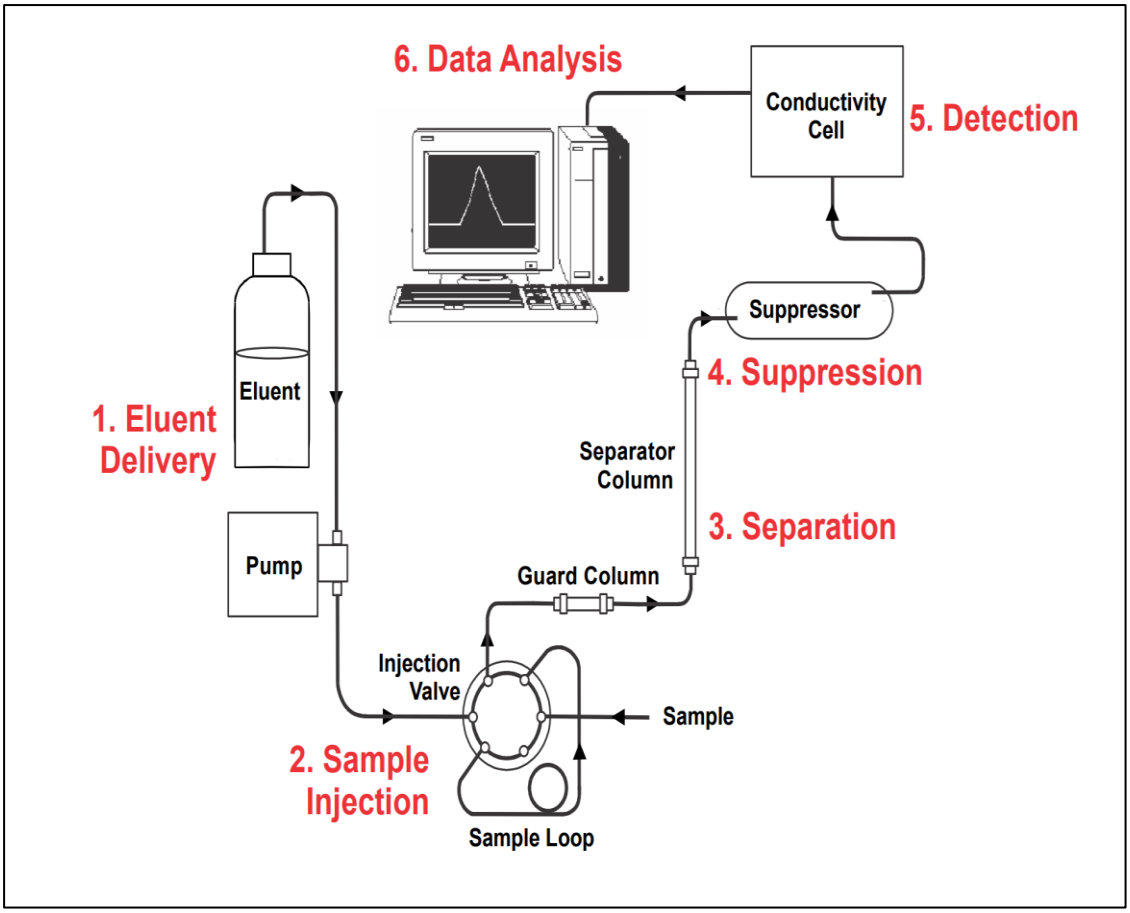

Figure 3-1: Ion Chromatography system Configuration (extracted from [31])

The configurations for the IC systems used for cation and anion analysis in MEG for this work were slightly different in the choice of eluent suppression system used for each system. Ions are detected by measuring the conductivity of the eluting solution from the separation column; this includes the conductivity of the eluting analyte ions and the conductivity of the eluent background ions. Using a suppressor between the separation column and the conductivity detection cell reduces the conductivity of the eluent background ions while increasing the sensitivity of the measuring cell to the conductivity of the analyte ion resulting in reduced background noise to analyte signal ratio and lower detection limits in measurement [25].

The electrolytic suppression mechanism was selected for the cation analysis, while the chemical suppression mechanism was selected for the anion analysis. Chemical suppression, first established in 1985, is the older of both suppression

techniques [25; 32]. Electrolytic suppression, established in 1995, has the advantages of being easy to use and not requiring the need for constant solvent make-up since it uses ultra-pure water for regeneration [25; 32]. However, electrolytic suppression has limited solvent compatibility and is not the best suited for weak organic acids. Karu's (2012) thesis on suppressed ion chromatography of organic acids reported 5 – 15% analyte losses during electrolytic suppression; analyte ions can permeate the suppressor membrane into the regenerant solution resulting in low recovery for organic acid analysis [32]. Simplicity and ease of use were significant considerations for the method development in this work, and the easier application of the electrolytic suppression made it the first choice for selection. However, the electrolytic suppression was not selected for the organic acid analyses because of these reported analyte losses and low recovery. Consequently, chemical suppression was selected for all organic acid analysis in this work, while electrolytic suppression was selected for the cation analysis. Eluent suppression selected for anion chromatography in this study is illustrated in Figure 3-2.

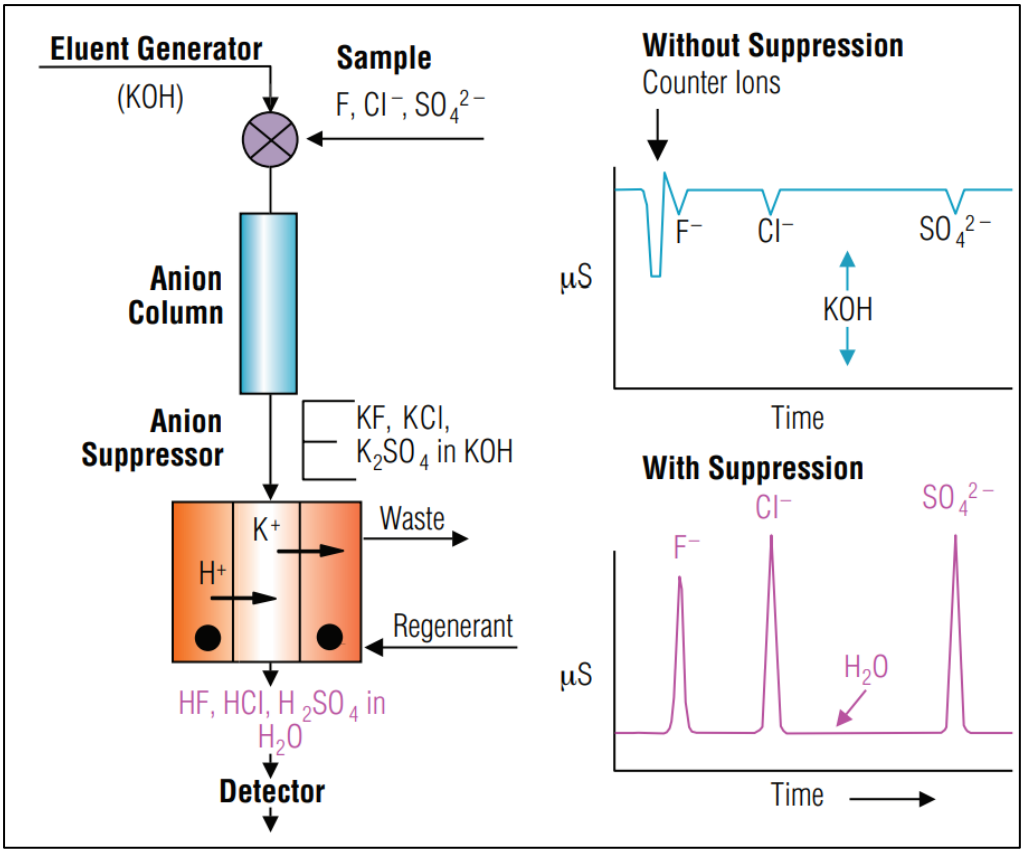

Figure 3-2: Eluent suppression schematic for anion chromatography (extracted from [33])

The electrolytic suppression mechanism applies a DC (direct current) voltage across the inbuilt cathode and anode electrodes to electrolytically split ultra-pure water into its electrolysis ions following the equation (3.1) at the anode and the equation (3.2) at the cathode [25; 32]. The applied voltage required for splitting the water molecules must be greater than the standard potential for the electrolysis of water which is approximately 1.5 V [32].

$$3H_2O \rightarrow 2H_3O^+ + \frac{1}{2}O_2 + 2e^- \quad (3.1)$$

$$2H_2O + 2e^- \rightarrow 2OH^- + H_2 \quad (3.2)$$

During cation suppression, as applied in this work, the applied current drives the migration of eluent ions through an ion exchange screen to the anode, where they combine with H_3O^+ to form acid waste with? the analyte ions [24; 34]. The same principle applies for anion electrolytic suppression except that

the eluent ions combine with the OH^- since the anion eluent base ions are cations. The electrolytic suppression process for cation suppression in MethaneSulphonic acid (MSA) eluent is summarized and illustrated in Figure 3-3 [32]. The strength of the applied current controls the extent of suppression.

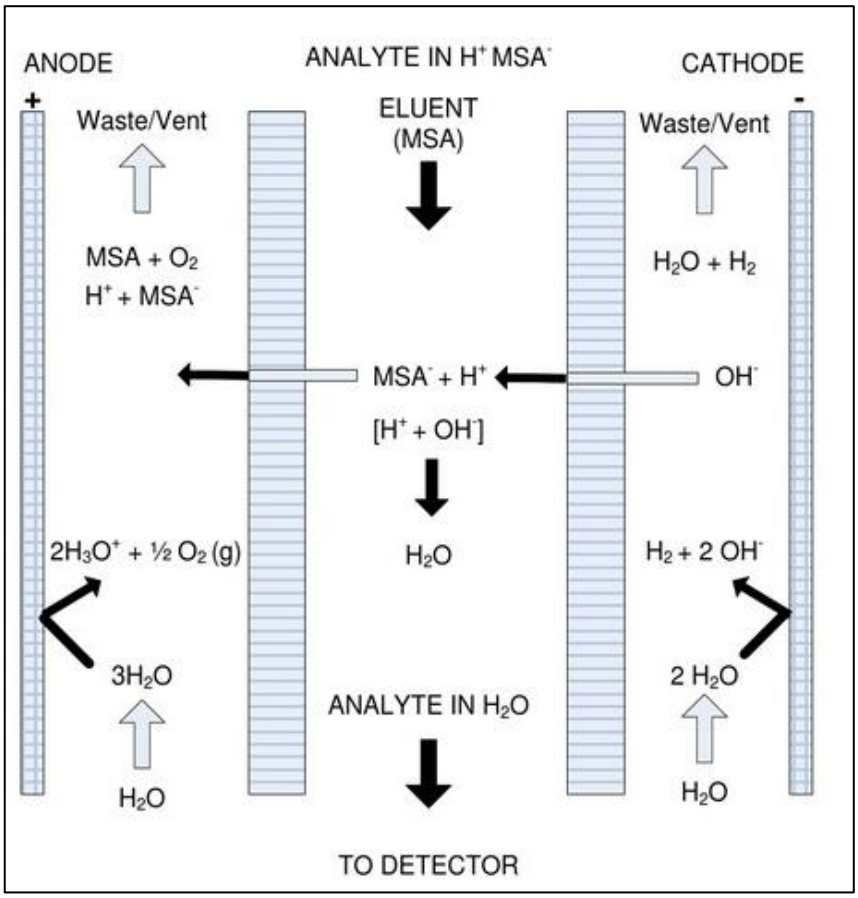

Figure 3-3: Cation electrolytic suppression with MethaneSulphonic acid (MSA) eluent (extracted from [35])

With chemical suppression, a chemical regenerate is the source of the eluent counter ion. There are no anodic and cathodic electrodes; the eluent ions migrate across ion exchange membranes where they react with the chemical regenerate, displacing the counter ion to create waste. For example, with anion suppression in a sodium hydroxide (NaOH) eluent, a strong acid regenerant like sulphuric acid (H_2SO_4) is the chemical regenerant. In this case, suppression is achieved when the sodium ions in the eluent displaces the H^+ in the regenerant to produce salt waste. The extent of suppression is controlled by the

flow rate of the chemical regenerant. This suppression mechanism is summarized and presented in Figure 4.

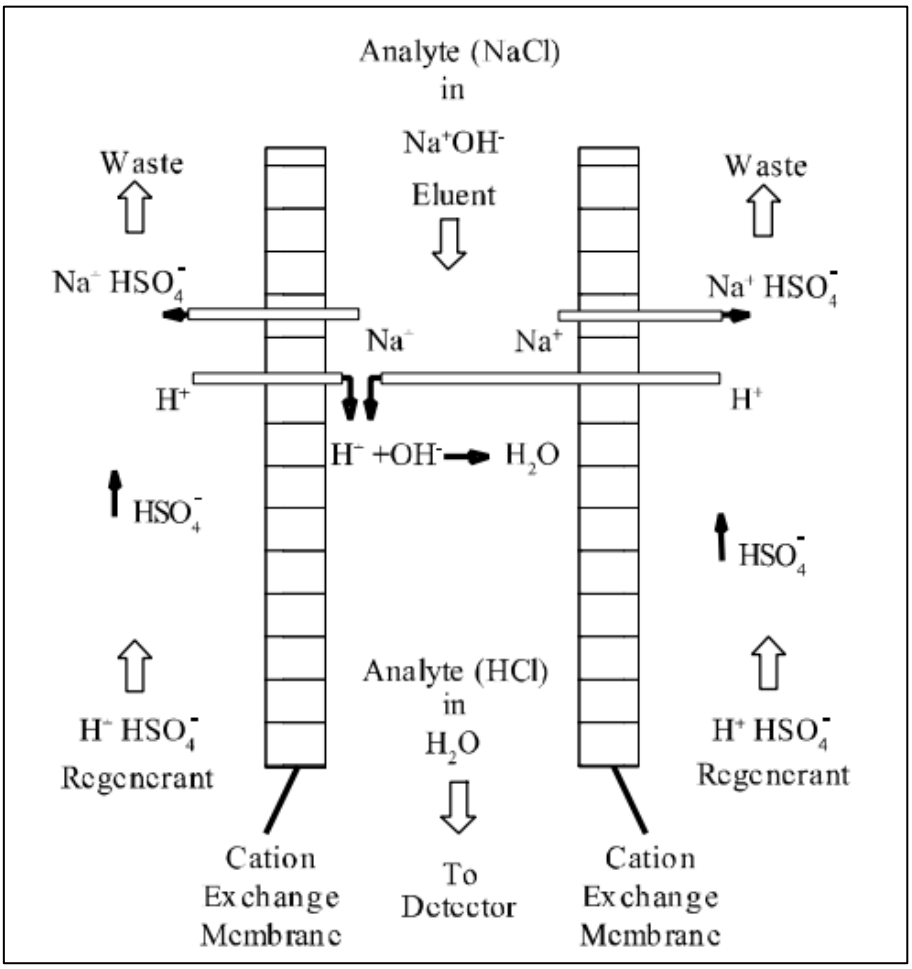

Figure 3-4: Anion chemical suppression with NaOH eluent and H_2SO_4 regenerant (extracted from [36])

The Dionex™ Eletrolytically Regenerated Suppressor 500 (CERS 500) was used for cation method development in this work, while the Dionex™ Anion Chemically Regenerated Suppressor 500 (ACRS-ICE 500) was used for the organic acid analysis. The ACRS 500 was chemically regenerated with 25 mM sulphuric acid, which was pumped through with a Dionex™ AXP pump. Specifications for these suppressor units are presented in Table 3-1.

Table 3-1: Manufacturer's specifications for Dionex™suppression units. (Extracted from [33; 35-36])

	CERS 500	ACRS-ICE 500
Regeneration requirement	Electrolytic	Chemical
Size	4mm	4mm
Suppressor capacity	110 μeq/min	-
Temperature range	15-40 °C	15-40 °C
Recommended back pressure	30 – 100 psi	40 psi
Maximum eluent flow rate	3 mL/min	3 mL/min
Maximum regenerant flow rate	5 mL/min	10 mL/min

3.3.2 Ion Chromatography Stationary Phase

Two defining properties of an ion exchange column are the base matrix and the functional ion-exchange site [37]. The base matrix is the supporting material attached to the functional ion exchange sites. The type of analyte ions determines the choice of the ion-exchange site; a cation exchange site is required for cation analyte analyses while an anion exchange site is required for anion analyte analyses. Weak cation exchange sites work best for alkaline and alkaline earth metals as well as amines like MDEA which can be present in MRU MEG samples. One major challenge with the cation analysis for MRU MEG samples is the separation of alkaline metals from MDEA as these ions are known to co-elute from most IC separation columns. Separation efficiency and resolution of the analyte peak are primarily determined by the structure and packing of the base matrix of the separation column [38].

In Ion-exchange chromatography, organic polymeric base matrices are more widely employed because they are stable across extreme pH ranges from 0 - 14. 55% cross-linked ethyl vinyl benzene (EVB)–divinyl benzene (DVB) copolymer is a common base material that is stable across the 0 – 14 pH range. Cross-linking is the formation of a covalent bond between polymer chains, and the 55% cross-linked ethyl vinyl benzene (EVB)–divinyl benzene (DVB) copolymer is a cross-link with 55% DVB in EVB [39-40]. 55% cross-linked EVB/DVB

copolymer retains its porosity and stability at extreme pH ranges [40]. The columns used for analysis in this work have the 55% EVB/DVB copolymer base matrix. The AS11 column used for anion separation in this work is a latex-bonded EVB/DVB copolymer matrix [41]. Specifications for the Dionex IonPac AS11 column used for anion analysis in this study is presented in Table 3-2.

Table 3-2: Anion Column specification [42]

	IonPac™ AS11
Substrate	Ethylvinylbenzene (EVB)–divinylbenzene (DVB) copolymer
Substrate X-linking (%)	55%
Ion exchange functional group	Alkanol quaternary ammonium
Ion exchange type	Strong Anion-exchange latex coating
Particle core	60 – 80 m^2/g
Column size (mm)	250 X 2
Column capacity	15 μeq/column
Hydrophobicity	Very low
Substrate structure	Microbeads
Particle size (μm)	13
Pore size	<10 Å
Latex diameter (μm)	85
Latex X-linking %	6

This study tested two columns for the cation analysis – the Dionex IonPac CS16 and the IonPac CS19 columns. The properties of both columns are presented in Table 3-3. The CS19 column has a 2000 Å pore size and a super-macroporous bead structure compared to the 150 Å pore size and microporous bead structure of the CS16 column. The significant differences between both columns are substrate structure and pore sizes. Smaller substrate structure and larger pore sizes results in higher porosity which in turn presents increased available exchange site and increased ion-exchange capacity manifesting in more resolved analyte peaks and better separation [20, 30, 39]. However, the smaller bead structure risks limiting diverse concentration ratios for adjacent peaks during separation [34].

Table 3-3: Cation Column specification from manufacturer [43-44]

	IonPac™ CS16	IonPac™ CS19
Substrate	ethylvinylbenzene (EVB)–divinylbenzene (DVB) copolymer	ethylvinylbenzene (EVB)–divinylbenzene (DVB) copolymer
Substrate X-linking (%)	55%	55%
Ion exchange functional group	Grafted Carboxylic acid	Grafted Carboxylic Acid
Ion exchange type	Weak cation exchange	Weak cation exchange
Particle core	60 – 80 m^2/g	60 – 80 m^2/g
Column size (mm)	250 X 3	250 X 4
Column capacity	3000 μeq/column	2410 μeq/column
Hydrophobicity	Medium	Medium
Substrate structure	Microporous bead	Super-macroporous bead
Particle diameter (μm)	5	4
Pore size	150 Å	2000 Å

3.3.3 Ion Chromatography Mobile Phase

The type of eluent used in ion chromatography depends on the detection system used and the type of stationary phase. The detection system, as mentioned earlier, could be suppressed conductivity or non-suppressed conductivity detection; suppression could be either chemical or electrolytic. It is important that the selected eluent can exhibit low background conductivity during detection with either detection system used [25; 45]. Also, the elution order for analyte ions is determined by the interaction between the analyte ions with the stationary phase ion-exchange sites, which in the case of suppressed conductivity detection, leaves the selection of eluent to its suppression characteristics with the selected stationary phase [45]. For this reason, the choice of eluent used in this work was based on the manufacturer's recommendation for the selected stationary phase (separation column). MethaneSulphonic acid (MSA) eluent was used for both CS16 and CS19 cation separation columns [43-44], and Potassium hydroxide (KOH) eluent was used for the AS11 anion separation column [42].

The MSA and KOH eluents were used with the Dionex eluent generation cartridges eliminating the need for frequent hand-made eluent preparation. The eluent generation cartridges produce online high purity contaminant free

eluent from a concentrated electrolyte reservoir and Ultra-pure water [46]. The eluent generation cartridges also make it easy to change eluent concentration [46]. Eluent concentration and temperature are two possible variations in the IC mobile phase; increased eluent concentration results in increased elution time, and increasing temperature results in increased peak resolution [47]. This study used a series of trials to select eluent concentration and temperature for optimal separation.

3.3.4 Chemicals and reagents

High purity single component ISO-certified ion chromatography standards were purchased from High-Purity Standards® USA. Methyl diethanolamine (MDEA) was purchased from Fisher Scientific®, and MEG was purchased from Sigma Aldrich®. Calibration standards were prepared daily using ultrapure water (18 MΩ or greater) from Merck Millipore water purification system. A list of all reagents used is presented in Table 3-4 below.

Table 3-4: list of chemicals and reagents

Reagent	Purity
Sodium (Na^+)	1000 µg/mL in 1% HNO_3
Potassium (K^+)	1000 µg/mL in 1% HNO_3
Calcium (Ca^{2+})	1000 µg/mL in 2% HNO_3
Magnesium (Mg^{2+})	1000 µg/mL in 2% HNO_3
Barium (Ba^{2+})	1000 µg/mL in 2% HNO_3
Strontium (Sr^{2+})	1000 µg/mL in 1% HNO_3
Acetate	1000 µg/mL in H_2O
Formate	1000 µg/mL in H_2O
Glycolate	1000 µg/mL in H2O
Oxalate	1000 µg/mL in H2O
Propionate	1000 µg/mL in H2O
Methyl diethanolamine (MDEA)	99+%
MEG	anhydrous, 99.8%

3.3.5 MRU samples preparation

Two sets of samples were used to validate and check the applicability and robustness of the IC test methods for MRU samples – one set of thirty-six samples was collected from the pilot scale MRU and the second set were 20 lab-

prepared MRU representative samples – making a total of 56 samples. The pilot scale MRU samples were obtained from different locations on the plant to represent the different matrices obtainable from the plant. Rich glycol (RG) samples were taken from the rich glycol storage tank and the MEG pre-treatment vessel, while Lean glycol (LG) samples were taken from the lean glycol storage tank, the reboiler and the glycol reclamation units.

The MRU representative samples were prepared in the lab using analyte concentrations similar to those from the MRU samples – 5 samples, each of the rich glycol and lean glycol, to represent the diverse analyte concentrations throughout the MRU. The MRU representative samples were prepared with analytical-grade chemicals with known concentrations. The design, build and operation of the pilot MRU from which samples were collected is that reported by Soames et al. (2018) [26] and Zaboon et al. (2017) [48]. This MRU configuration has a pre-treatment unit for hydrocarbon removal, a distillation unit for MEG dewatering and a vacuum evaporation unit for MEG desalting. The samples collected from this MRU mimicked actual samples from a typical regeneration plant with very high salt and particulate contents.

Also, samples from the MEG plant had significant variations between individual analyte concentrations in samples; all samples had very high concentrations of sodium ions (ca. 7000 ppm) and relatively low concentrations of other ions (less than 500 ppm). Calcium and magnesium ions contribute to scale formation [48]; during operation, their concentrations are minimised to control scale formation within the system; thus, the concentration of calcium and magnesium in samples was significantly lower than those of sodium and potassium.

MDEA concentration depends on the method of corrosion management being employed. MDEA concentration is high, up to about 14,000 ppm during the pH

stabilisation method. However the pH stabilization method for corrosion management presents significant risk of scale deposition with produced water breakthrough [26]. Produced water is water that comes out of the reservoir with the hydrocarbons and its total dissolved solids ranges upwards of 40,000 ppm [49-50]. With the breakthrough of produced water during production, corrosion management is usually switched from MDEA pH stabilization method to the use of a film forming corrosion inhibitor [26]. During switchover, the concentration of MDEA is gradually reduced and is at its minimum can be less than 200 ppm during film-forming corrosion mitigation [26]. Consequently, samples had to be diluted prior to analyses.

All samples were filtered with 45µm pore size syringe filters, with Nylon membrane and polypropylene housing, and diluted with ultra-pure water before injection into the IC unit. While the samples did not contain drilling mud, filtration was necessary to eliminate the introduction of particles into the IC unit, which could result in the blocking of the polyether ether ketone (PEEK) tubes. The first 1 mL of sample filtrate was discarded, and the remainder was used for analysis. Sample dilution and injection were done with the Dionex™ AS-AP Auto-sampler for ease of analysis and also for comparability with expected industry practice where it is expected that an auto-sampler will be used for fast analysis turnaround. All calibration samples were diluted using a 50 mL volumetric flask where necessary.

3.4 Results and Discussion

3.4.1 Cations test method

Separation of selected cations in aqueous solutions was tested on two columns, the IonPac™ CS16 and the IonPac™ CS19. Both columns were used with their corresponding guard column. Seven major cations present in MEG from the MRU were included in this test method.

The results show that potassium and MDEA peaks could not be separated with the CS16 column, while other analytes were distinguished (Figure 3-5). Potassium and MDEA cations were seen to co-elute from the column under all test conditions. Thus, it can be concluded that the CS16 column was unsuitable for analysing samples with potassium and MDEA.

Better specificity was achieved on the IonPac CS19 column; potassium and MDEA peaks could be separated at much lower eluent concentrations and shorter retention times, as shown in Figure 3-6.

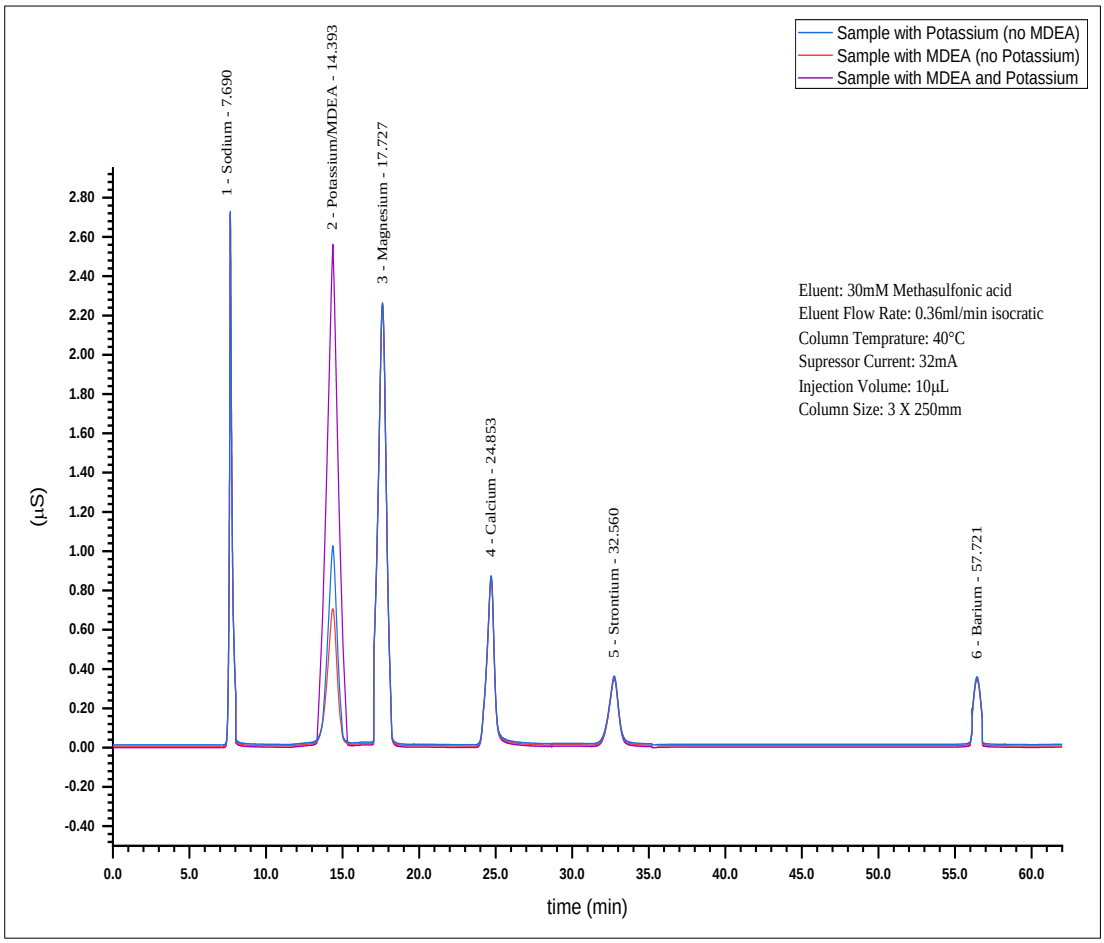

Figure 3-5: Separation of three samples in aqueous solution with CS16 column

Optimum cchromatographic detection parameters for both columns are presented in .

Table 3-5 and Table 3-6. These results show that a much lower eluent concentration achieved good separation on the CS19 column compared with the CS16 column.

Table 3-7 and Table 3-8 show peak specificity parameters for the CS16 and CS19 columns, respectively. The target for separation was to achieve good peak asymmetry, resolution and column efficiency. Peak asymmetry for good separation is between 0.9 and 1.2 [24], and peak resolution is greater than 1.5 [24]; higher peak resolution values will result in excessively long analysis time.

The results confirmed a better peak resolution for potassium and MDEA on the CS19 column operated at 30 °C compared to the CS16 column operated at 40 °C. However, at this temperature the CS19 column showed a reduced resolution of magnesium and calcium peaks, see Figure 3-6.

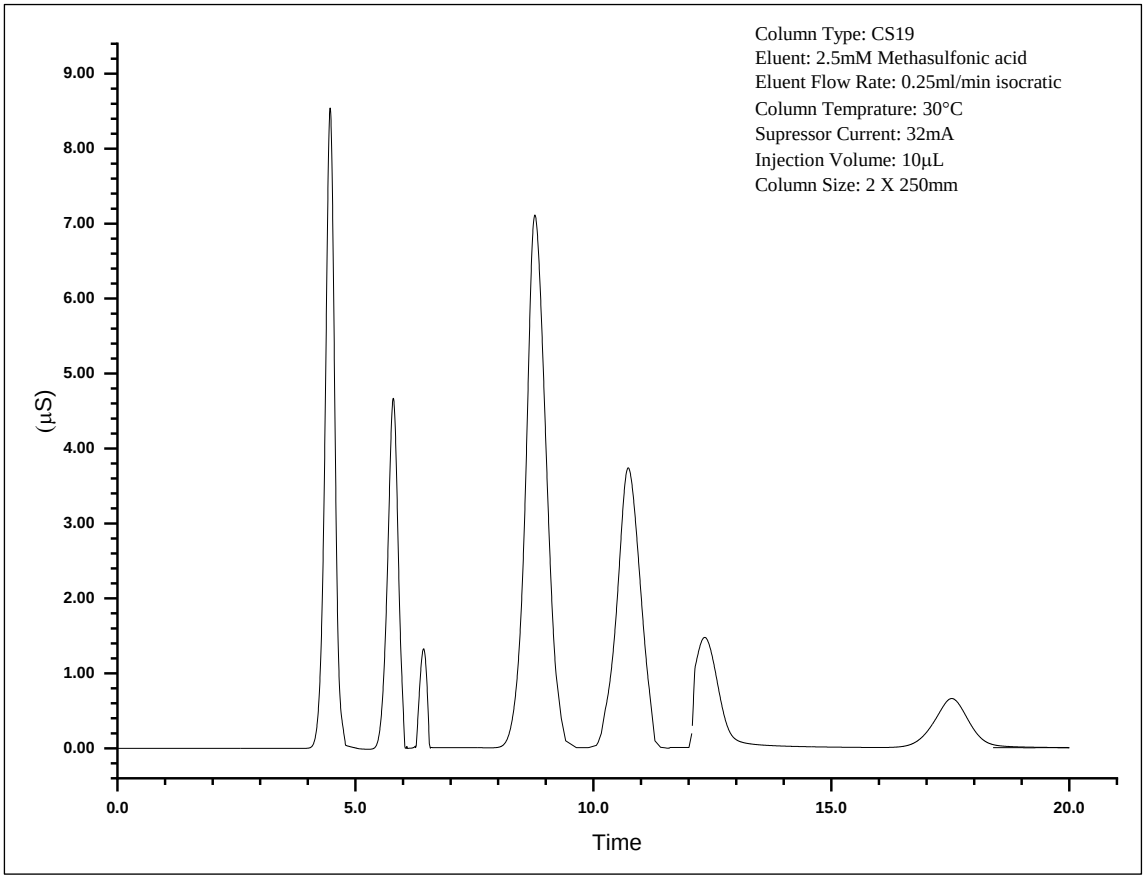

Figure 3-6: Chromatogram showing good resolution for potassium and MDEA peaks in aqueous solution with CS19 column.

Table 3-5: IC test method and parameters for CS16 column

Eluent	30mM MethaneSulphonic Acid
Eluent regime	isocratic
Eluent Flowrate	0.36 ml/min Isocratic
Suppressor current	32mA
Column temperature	40°C
Column size	3 X 250mm
Injection volume	10µL
Detection	Suppressed conductivity
Run time	60 mins

Table 3-6: IC test method and parameters for CS19 column

Eluent	8mM MethaneSulphonic Acid
Eluent regime	isocratic
Eluent Flowrate	0.25ml/min Isocratic
Suppressor current	32mA
Column temperature	30°C
Column size	2 X 250mm
Injection volume	10µL
Detection	Suppressed conductivity
Run time	20 mins

Table 3-7: CS16 column analyte peak specificity parameters

Analyte	Number of replicates	Retention time (min)	Peak Asymmetry (AIA)	Peak resolution (EP)
Na^+	14	7.674	1.15	4.05
K^+/MDEA	14	14.427	1.60	3.14
Mg^{2+}	14	17.637	1.17	6.01
Ca^{2+}	14	24.725	1.20	4.81
Sr^{2+}	14	32.766	1.24	7.72
Ba^{2+}	14	57.76	1.28	5.23

Table 3-8: CS19 column analyte peak specificity parameters

Analyte	Number of replicates	Retention time (min)	Peak Asymmetry (AIA)	Peak resolution (EP)
Na^+	14	4.467	0.89	1.80
K^+	14	5.757	0.90	1.54
MDEA	14	6.430	1.39	5.74
Mg^{2+}	14	8.767	1.25	3.69
Ca^{2+}	14	10.733	1.14	2.38
Sr^{2+}	14	12.371	1.17	3.19
Ba^{2+}	14	17.281	1.13	2.83

Calibration parameters for each analyte are also presented in Table 3-9 and Table 3-10. Linear calibration was achievable for all analytes except potassium and MDEA over the validated range of 0.1 – 200 ppm on the CS16 column. On the CS19 column, when potassium and MDEA are present, linear curve fitting was achievable up to 80 ppm potassium and 5 ppm MDEA. However, when a quadratic curve fitting function was used for MDEA, the calibration range was extended to 40 ppm on the CS19 column. While the validity range is much lower than the expected MDEA concentration in actual MRU samples, samples can be diluted to bring them inside this range.

Table 3-9: Summary of calibration parameter on CS16 column

Analyte	Number of replicates	Intercept	Slope	Curve	R^2	LOD[a] (ppm)	Rel.Std.Dev. (%)	Range (ppm)
Na^+	14	0.000	0.501	0.000	0.9999	0.28	2.753	0.05-200
K^+	14	n.a.	n.a.	n.a.	n.a.	n.a.	n.a.	n.a.
MDEA	14	n.a.	n.a.	n.a.	n.a.	n.a.	n.a.	n.a.
Mg^{2+}	14	0.000	0.891	0.000	0.9999	0.11	1.283	0.1-200
Ca^{2+}	14	0.042	0.273	0.000	0.9999	0.11	2.812	0.1-200
Sr^{2+}	14	-0.005	0.172	0.000	0.996	0.13	3.732	0.1-200
Ba^{2+}	14	-0.015	0.125	0.000	0.9970	0.41	6.131	0.1-200

[a]LOD calculated as 3 times the relative standard deviation of background noise

Table 3-10: Summary of calibration parameter on CS19 column

Analyte	Number of replicates	Intercept	Slope	Curve	R^2	LOD[a] (ppm)	Rel.Std.Dev. (%)	Range (ppm)
Na^+	14	0.010	0.896	0.000	0.9993	0.38	3.875	0.05 - 200
K^+	14	-0.004	0.913	0.000	0.9998	0.12	1.736	0.1-80
MDEA	14	-0.001	0.866	-0.002	0.9994	0.21	3.232	0.1 - 40
Mg^{2+}	14	-0.015	0.884	0.000	0.9997	0.15	2.163	0.1-200
Ca^{2+}	14	-0.003	0.816	0.000	0.9998	0.15	2.060	0.1-200
Sr^{2+}	14	-0.011	0.820	0.000	0.9994	0.23	3.387	0.1-200
Ba^{2+}	14	-0.013	0.844	0.000	0.9971	0.51	7.931	0.1-200

[a]LOD calculated as 3σ+ average noise

Accuracy of test methods was determined by measuring the percentage recovery in 20 spiked samples across 10 days. Precision was measured by the relative standard deviation of test results between the 20 quality-control

samples. Results for the accuracy and precision are presented in Table 3-11 and Table 3-12.

Table 3-11: Quality control data on CS16 column

		Na^+	K^{+*}	MDEA**	Mg^{2+}	Ca^{2+}	Sr^{2+}	Ba^{2+}
Number of replicates		20	20	20	20	20	20	20
5 ppm spike	**% Ave. recovery**	104	105	94	102	105	116	114
	% Rel. Std. Dev	1.937	2.449	2.479	2.380	2.506	2.462	2.503
50 ppm spike	**% Ave. recovery**	98	112	-	98	107	94	117
	% Rel. Std. Dev	2.387	2.412	-	2.462	2.454	2.404	2.470

*K+ data in samples with no MDEA

** MDEA data in sample with no K+

- not tested

Table 3-12: Quality control data on CS19 column

		Na^+	K^{+*}	MDEA**	Mg^{2+}	Ca^{2+}	Sr^{2+}	Ba^{2+}
Number of replicates		20	20	20	20	20	20	20
5 ppm spike	**% Ave. recovery**	99	97	91	98	99	91	92
	% Rel. Std. Dev	1.166	1.726	2.828	2.799	3.180	2.276	2.394
50 ppm spike	**% Ave. recovery**	99	103	-	100	99	96	103
	% Rel. Std. Dev	2.907	2.591	-	2.524	2.430	2.257	2.507

- not tested

All calibration standards were prepared in water, while all the quality control samples were MEG samples. It is not possible to matrix match between samples and calibration standards as MEG is non-ionic, and the percentage recovery data presented in Table 3-11 and Table 3-12 shows good recovery without the need for matrix matching. There was no noticeable difference in peak retention time or height in samples prepared in water or MEG.

3.4.2 Organic Acid test method

The parameters for the organic acid test method are presented in Table 3-13.

Table 3-13: Organic acid test method parameters

Eluent	KOH
Eluent regime	Gradient elution
Eluent gradient	0 mins 6 mM 20 mins 6 mM 35 mins 28 mM 37 mins 55 mM 39 mins 55 mM 40 mins 6 mM 55 mins 6 mM
Eluent Flowrate	0.10 ml/min
Chemical suppressor	25mM H_2SO_4
Column temperature	35°C
Column size	3 X 250mm
Injection volume	10µL
Detection	Suppressed conductivity
Run time	55 mins

The AS11 column was used for organic acid analysis in MEG with good peak asymmetry and resolutions, as shown in Table 3-14. Peak Asymmetry was between the acceptable range of 0.9 and 1.2 [1] for all analytes except Glycolate, with slight tailing and 1.62 asymmetry. Peak resolution was also good for all analytes, all greater than 1.5 and ranging from 2.38 to 4.55 for all analytes.

Table 3-14: Organic acid test method analyte peak specificity parameters

Analyte	Number of replicates	Retention time (min)	Peak Asymmetry (AIA)	Peak resolution (EP)
Glycolate	14	7.567	1.62	3.77
Acetate	14	8.113	1.15	2.38
Formate	14	8.850	0.94	4.20
Propanoate	14	11.157	1.06	4.55
Butryate	14	21.830	1.10	2.48

Calibration and quality control results for the organics acid test method are presented in Table 3-15 and Table 3-16. Coefficients of determination (R^2) for all calibrations were greater than 0.999, with Relative standard deviations between 0.290 and 0.414. Greater than 91% average recovery was achieved for all spiked samples, as shown in Table 3-16.

Table 3-15: Summary of calibration parameter on Organic acid test method

Analyte	Number of replicates	Intercept	Slope	Curve	R^2	Rel.Std.Dev. (%)
Glycolate	14	0.016	0.788	0.000	0.9997	0.290
Acetate	14	0.020	0.823	0.000	0.9991	0.325
Formate	14	0.031	0.827	0.000	0.9993	0.414
Propanoate	14	0.046	0.880	0.000	0.9991	0.229
Butryate	14	0.052	0.834	0.000	0.9997	0.308

[a]LOD calculated as 3σ+ average noise

Table 3-16: Quality control on Organic acid test method

		Glycolate	Acetate	Formate	Propanoate	Butyrate
Number of replicates		10	10	10	10	10
5 ppm spike	**% Ave. recovery**	98.85	92.47	92.85	94.82	90.57
	% Rel. Std. Dev	3.86	2.14	2.68	2.24	2.23
50 ppm spike	**% Ave. recovery**	97.38	90.51	92.40	91.13	98.91
	% Rel. Std. Dev	4.42	2.04	4.61	2.17	5.25

3.4.3 Application of test method to MRU samples

The ion chromatography test methods reported in Table 3-6 and Table 3-13 were applied to MRU actual and representative samples. Two lots of samples were used to check the applicability and robustness of the IC test methods for MRU samples. One lot of Thirty-six samples collected from the pilot scale MRU and another lot of 20 lab-prepared MRU representative samples – making a total of 56 samples. The pilot scale MRU samples were obtained from different locations on the plant to represent the different matrices obtainable from the plant. Rich glycol (RG) samples were taken from the rich glycol storage tank

and the MEG pre-treatment vessel, while lean glycol (LG) samples were taken from the lean glycol Storage tank, the reboiler and the glycol reclamation units. The MRU representative samples were prepared in the lab using analyte concentrations similar to those from the MRU samples – 5 samples, each of the rich glycol and lean glycol, to represent the diverse analyte concentrations throughout the MRU. The MRU representative samples were prepared with analytical-grade chemicals with known concentrations.

Results from the IC methods presented in Table 3-6 were compared with the inductively coupled plasma optical emission spectrometry (ICP-OES) to check for the degree of agreement between both methods. The ICP-OES is a well-established method for analysing chemical elements in any matrix [2-4]. MDEA could not be tested in the ICP because the ICP identifies atomic composition in samples and cannot be used to measure MDEA [4]. This is a significant advantage of the IC test method over the well-established ICP-OES in that complex molecules like MDEA can be measured by IC but not by ICP. Thus, MDEA is only reported in the 20 representative samples, and results are compared with the actual concentration of MDEA added to the sample during preparation.

The Bland-Altman plot was used to evaluate the degree of agreement between the new IC method and the reference ICP-OES method [5]. This evaluation's results are presented in Figure 3-7. A Bland-Altman plot has been widely used to determine the correlation between two analytical methods [6]. It shows the agreement interval within which 95% of the differences between both methods exist while factoring the biases associated with each analytical method[7]. Bland J.M. and Altman D.G (1995) defines the 95% limit of agreement as ± 1.96 times the standard deviation of the mean differences between both analytical methods [8]. Results presented in plots in Figure 3-7 show that more than 95% of the mean difference between the IC and ICP methods falls between the upper

and lower limits of agreement, indicating acceptable agreement between both methods for the analytes tested. The larger values for differences for the sodium analyte are a consequence of the higher concentration of sodium in the samples compared to the other analytes.

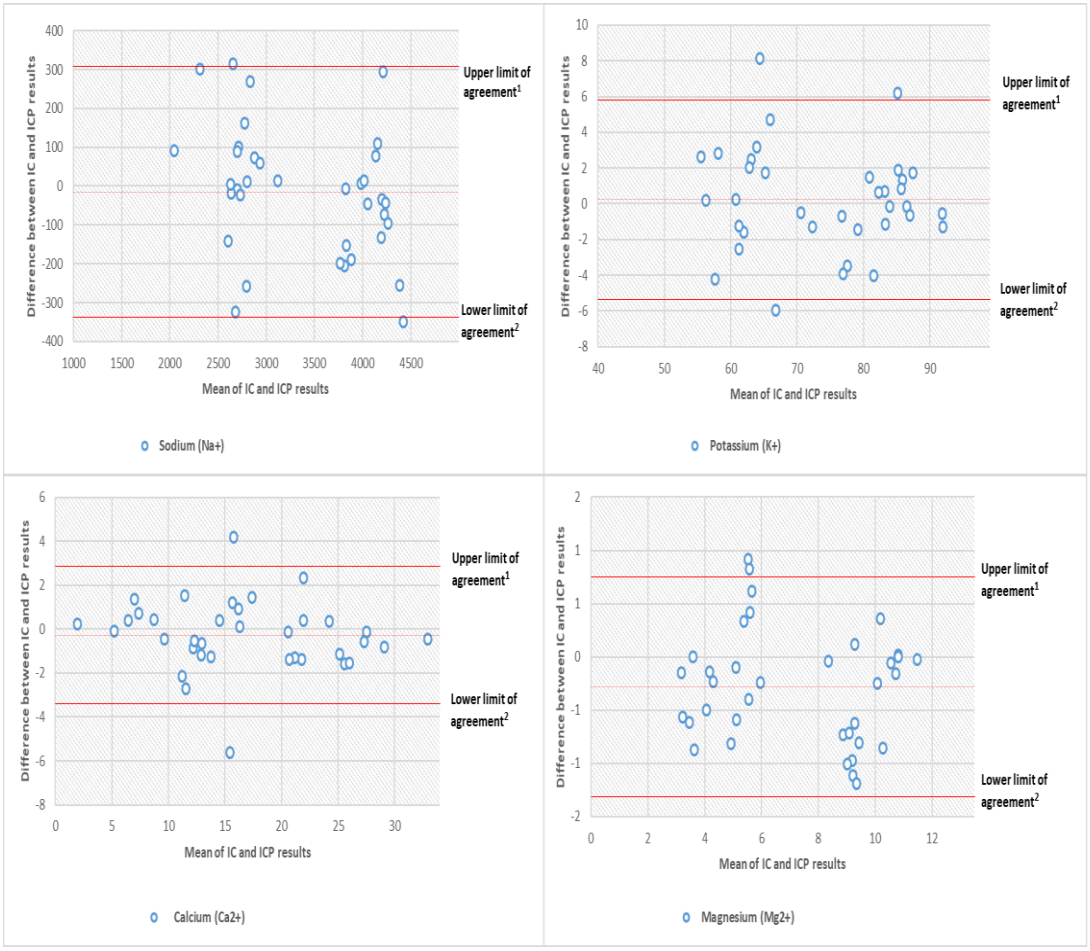

Figure 3-7: Bland-Altman plots for the new IC method and ICP-OES test results

1 - Upper limit of agreement = mean difference between IC and ICP results + 1.96 standard deviation

2 - Lower limit of agreement = mean difference between IC and ICP results - 1.96 standard deviation

Correlation plots of analyte concentration from the IC methods with makeup in MRU representative samples are presented in Figure 3-8, and the calculated correlation coefficient is presented in Table 3-17. The calculated correlation coefficients in Table 3-17 range from 0.9305 to 0.9994; while a correlation coefficient of +1 depicts perfect correlation, values greater than 0.9 are generally accepted as very high positive correlations [9]. Consequently, it can be concluded that results in Figure 3-8 and Table 3-17 show a high positive

correlation between the new IC methods reported in this study and the concentration of analytes in the MRU representative samples. It also confirms the applicability and accuracy of the new IC methods in application to MRU MEG samples.

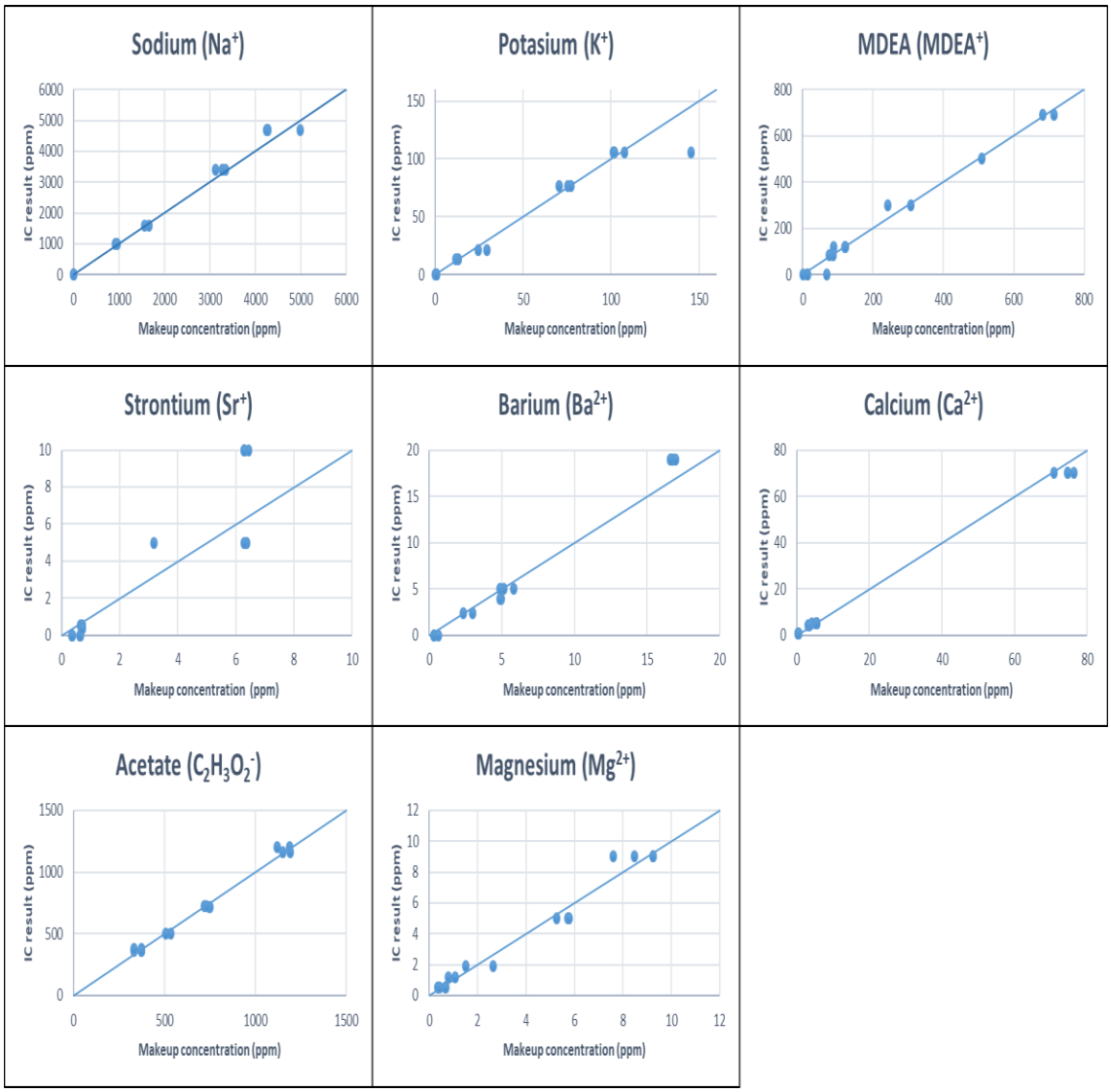

Figure 3-8: Correlation plots for IC methods and MRU solution makeup concentrations

Table 3-17: correlation coefficients for IC methods and MRU solution makeup concentrations

	Na^+	K^+	MDEA	Sr^{2+}	Ba^{2+}	Ca^{2+}	Acetate	Mg^{2+}
Correlation coefficients	0.9953	0.9759	0.9994	0.9871	0.9939	0.9305	0.9975	0.9955

3.5 Conclusion

This chapter details the development of a robust technique that cover wider range of cation and organic acid assay for MRU samples. Ion chromatography was applied to the assay of MEG samples from the MEG Recovery Unit (MRU); cation and organic acid IC methods were developed and tested for robustness and application to MRU MEG samples. Both the Dionex™ CS16 and CS19 columns were applicable for analysing significant cations found in MRU MEG samples; however, the CS16 column is only applicable when MDEA is not present for corrosion mitigation. The test method parameters for cation analysis, as applicable to MRU MEG samples, on the Dionex™ CS16 and CS19 columns and the organic acid analysis on the Dionex™ AS11 column are well defined and presented in .

Table 3-5: IC test method and parameters for CS16 column Table 3-6: IC test method and parameters for CS19 column and Table 3-13: Organic acid test method parameters. Existing methods based on the ICP is accurate but cannot be used for MDEA determination. The IC technique detailed in this chapter ensures simultaneous determination of MDEA and other cations.

References

1. (IEA), I.E.A. *Global Energy Review 2021*. Global Energy Review 2021, 2021.
2. gGmbH, m., *World Ocean Review*, in *WOR 3 Marine Resources – Opportunities and Risks | 2014*, D.S.P. Erna Lange, Dr. Lars Rüpke, Dr. Emanuel Söding, Dr. Klaus Wallmann, Editor. 2014, maribus gGmbH: Hamburg, Germany.
3. Guo, B., S. Song, and A. Ghalambor, *Chapter 1 - Introduction*, in *Offshore Pipelines (Second Edition)*, B. Guo, et al., Editors. 2014, Gulf Professional Publishing: Boston. p. 1-10.
4. Hammerschmidt, E., *Formation of gas hydrates in natural gas transmission lines.* Industrial & Engineering Chemistry, 1934. **26**(8): p. 851-855.
5. Baillie, C. and E. Wichert, *Chart gives hydrate formation temperature for natural gas.* Oil Gas J.; (United States), 1987. **85:14**: p. Medium: X; Size: Pages: 37-39 2009-12-17.
6. Seo, Y., *Hydrate Inhibitors and Their Interferences in Corrosion Inhibition*, in *Corrosion Inhibitors in the Oil and Gas Industry*. 2020. p. 407-419.
7. Odeigah, E.A. and T. Pojtanabuntoeng, *Regeneration and Reclamation of Mono-Ethylene Glycol (MEG) Used as a Hydrate Inhibitor: A Review.* American Journal of Chemical Engineering, 2022. **10**(2): p. 32-45.
8. Baraka-Lokmane, S., et al., *Technical challenges and solutions in a closed loop MEG regeneration system for gas field offshore, UK.* WIT Transactions on Engineering Sciences, 2013. **79**: p. 511-522.
9. Latta, T.M., M.E. Seiersten, and S.A. Bufton. *Flow assurance impacts on lean/rich MEG circuit chemistry and MEG regenerator/reclaimer design*. in *Offshore technology conference*. 2013. Offshore Technology Conference.
10. SPE International, V.a.T.S. *MEG Regeneration Technical Meeting*. 2009.
11. Latta, T.M., et al. *Design Considerations for Mitigating the Impact of Contaminants in Rich MEG on Monoethylene Glycol Recovery Unit MRU Performance*. in *Offshore Technology Conference Asia*. 2016. OnePetro.
12. MacLeod, S.K., *Moisture determination using Karl Fischer titrations.* Analytical chemistry, 1991. **63**(10): p. 557A-566A.
13. Bruttel, P. and R. Schlink, *Water determination by Karl Fischer titration.* Metrohm monograph, 2003. **8**(5003): p. 2003-2009.
14. Haque, M.E., *Ethylene Glycol Regeneration Plan: A Systematic Approach to Troubleshoot the Common Problems.* Journal of Chemical Engineering, 2013. **27**(1): p. 21-26.
15. Carron, K. and R. Cox, *Qualitative analysis and the answer box: a perspective on portable Raman spectroscopy*. 2010, ACS Publications.
16. Larkin, P., *Infrared and Raman spectroscopy: principles and spectral interpretation*. 2017: Elsevier.

17. Gasdia-Cochrane, M. *How Water Affects Raman and FTIR Identification of Unknown Substances*. 2018 09/11/2018 [cited 2022 20/1/2022]; Available from: https://www.thermofisher.com/blog/identifying-threats/how-water-affects-raman-and-ftir-identification-of-unknown-substances/.
18. Thompson, M., *Handbook of inductively coupled plasma spectrometry*. 2012: Springer Science & Business Media.
19. Beauchemin, D., *Inductively coupled plasma mass spectrometry.* Analytical chemistry, 2008. **80**(12): p. 4455-4486.
20. Soltanpour, P.N., et al., *Inductively coupled plasma emission spectrometry and inductively coupled plasma-mass spectrometry.* Methods of Soil Analysis: Part 3 Chemical Methods, 1996. **5**: p. 91-139.
21. Wilschefski, S.C. and M.R. Baxter, *Inductively coupled plasma mass spectrometry: introduction to analytical aspects.* The Clinical Biochemist Reviews, 2019. **40**(3): p. 115.
22. *ICP-MS Analysis charges*. 2022 [cited 2022 20/22/2022]; Available from: https://wordpress.nmsu.edu/mchidest/ion-chromatography-system/ion-chromatography/.
23. *Ion chromatography analysis charges*. 2022 [cited 2022 20/11/2022]; Available from: https://wordpress.nmsu.edu/mchidest/ion-chromatography-system/ion-chromatography/.
24. Weiss, J., *Handbook of Ion Chromatography, 3 Volume Set*. Vol. 1. 2016: John Wiley & Sons.
25. Weiß, J., *Ion chromatography—A review of recent developments.* Fresenius' Zeitschrift für analytische Chemie, 1987. **327**(5): p. 451-455.
26. Soames, A., et al., *Operation of a MEG pilot regeneration system for organic acid and alkalinity removal during MDEA to FFCI switchover.* Journal of Petroleum Science and Engineering, 2018. **169**: p. 1-14.
27. Babu, D.R., et al., *Carbonates precipitation in MEG loops – A comparative study of South Pars and Bass Strait gas fields.* Journal of Natural Gas Science and Engineering, 2015. **27**: p. 955-966.
28. Natsi, P.D., S.G. Rokidi, and P.G. Koutsoukos, *Calcium Carbonate Scale Formation in Water- Mono Ethylene Glycol (MEG)*, in *CORROSION 2019*. 2019, NACE International: Nashville, Tennessee, USA. p. 14.
29. Rossiter, W.J., et al., *An investigation of the degradation of aqueous ethylene glycol and propylene glycol solutions using ion chromatography.* Solar Energy Materials, 1985. **11**(5): p. 455-467.
30. AlHarooni, K., et al., *Inhibition effects of thermally degraded MEG on hydrate formation for gas systems.* Journal of Petroleum Science and Engineering, 2015. **135**: p. 608-617.
31. Inc., T.F.S., *Dionex Aquion Ion Chromatography System; Operator's Manual (Document 22179-97003)*, in *Thermo Fisher Scientific Inc*. 2016, Thermo Fisher Scientific Inc: Sunnyvale, CA, USA.

32. Karu, N., *Suppressed ion chromatography of organic acids with universal detection*. 2012, University of Tasmania.
33. Inc., T.F.S., *Thermo Scientific Dionex eluent suppressors for ion chromatography - Product specifications (Document PS70690-EN 0317S)*, T.F.S. Inc., Editor. 2017, Thermo Fisher Scientific Inc.: Sunnyvale, CA, USA.
34. Haddad, P.R., *Ion chromatography.* Analytical and bioanalytical chemistry, 2004. **379**(3): p. 341-343.
35. Inc., T.F.S., *Dionex ERS 500 Suppressor Product manual (Document 031956-11)*, T.F.S. Inc., Editor. 2017, Thermo Fisher Scientific Inc: Sunnyvale, CA, USA.
36. Inc., T.F.S., *Dionex CRS 500 Product Manual (Document 031727-07)*, T.F.S. Inc., Editor. 2015, Thermo Fisher Scientific Inc.: Sunnyvale, CA, USA.
37. Jungbauer, A. and R. Hahn, *Ion-exchange chromatography.* Methods in enzymology, 2009. **463**: p. 349-371.
38. Janson, J.-C., *Protein purification: principles, high resolution methods, and applications*. 2012: John Wiley & Sons.
39. Jun, Y., X. Rongnan, and Y. Juntan, *Swelling of porous ethylvinylbenzene–divinylbenzene copolymers and the stability of the pore structure.* Journal of applied polymer science, 1989. **38**(1): p. 45-54.
40. Okay, O., *Heterogeneous styrene–divinylbenzene copolymers. Stability conditions of the porous structures.* Journal of applied polymer science, 1986. **32**(6): p. 5533-5542.
41. Smith, R.E. and R.A. MacQuarrie, *Organic anion chromatography on new latex-bonded pellicular anion exchangers.* Journal of chromatographic science, 1991. **29**(6): p. 232-236.
42. Corporation, D., *product manual for IonPac AG11 IonPAc AS11* 2008, Dionex Corporation Sunnyvale CA, USA.
43. Inc., T.F.S., *IonPac CS16 Cation-Exchange Colum*. 2010, Thermo Fisher Scientific Inc. : Sunnyvale CA, USA.
44. Inc., T.F.S., *Dionex IonPac CS19 Cation-Exchange Column*. 2014, Thermo Fisher Scientific Inc. : Sunyvale CA, USA.
45. Pohl, C.A., J.R. Stillian, and P.E. Jackson, *Factors controlling ion-exchange selectivity in suppressed ion chromatography.* Journal of Chromatography A, 1997. **789**(1-2): p. 29-41.
46. Scientific, T., *Product Manual for Dionex Eluent Generator Cartridges*. 2020, Thermo Scientific: Sunnyvale CA, USA. p. 94.
47. Kopaciewicz, W. and F.E. Regnier, *Mobile phase selection for the high-performance ion-exchange chromatography of proteins.* Analytical Biochemistry, 1983. **133**(1): p. 251-259.
48. Zaboon, S., et al., *Recovery of mono-ethylene glycol by distillation and the impact of dissolved salts evaluated through simulation of field data.* Journal of Natural Gas Science and Engineering, 2017. **44**: p. 214-232.

49. Igunnu, E.T. and G.Z. Chen, *Produced water treatment technologies.* International journal of low-carbon technologies, 2014. **9**(3): p. 157-177.
50. Nasiri, M. and I. Jafari, *Produced water from oil-gas plants: A short review on challenges and opportunities.* Periodica Polytechnica Chemical Engineering, 2017. **61**(2): p. 73-81.
51. Olesik, J.W., *Elemental analysis using icp-oes and icp/ms.* Analytical Chemistry, 1991. **63**(1): p. 12A-21A.
52. Olesik, J.W., *Peer reviewed: Fundamental research in ICP-OES and ICPMS.* Analytical Chemistry, 1996. **68**(15): p. 469A-474A.
53. Boumans, P., *Inductively coupled plasma-atomic emission spectroscopy: its present and future position in analytical chemistry.* Fresenius' Zeitschrift für Analytische Chemie, 1979. **299**(5): p. 337-361.
54. Canepari, S., et al., *Determination of soluble ions and elements in ambient air suspended particulate matter: inter-technique comparison of XRF, IC and ICP for sample-by-sample quality control.* Talanta, 2009. **77**(5): p. 1821-1829.
55. Bunce, C., *Correlation, agreement, and Bland–Altman analysis: statistical analysis of method comparison studies.* American journal of ophthalmology, 2009. **148**(1): p. 4-6.
56. Giavarina, D., *Understanding bland altman analysis.* Biochemia medica, 2015. **25**(2): p. 141-151.
57. Bland, J.M. and D.G. Altman, *Comparing methods of measurement: why plotting difference against standard method is misleading.* The lancet, 1995. **346**(8982): p. 1085-1087.
58. Hinkle, D.E., W. Wiersma, and S.G. Jurs, *Applied statistics for the behavioral sciences*. Vol. 663. 2003: Houghton Mifflin College Division.

Chapter 4

The effect of Monoethylene Glycol on Calcium carbonate solubility at high temperatures

Published in Industrial & Engineering Chemistry Research

*Edith A. Odeigah**[a], *Thunyaluk Pojtanabuntoeng*[a], *Franca Jones*[b] *and Rolf Gubner*[a]

[a] WA School of Mines: Minerals, Energy and Chemical Engineering, Curtin University, Bentley, Western Australia 6102, Australia.

[b] School of Molecular and Life Sciences, Curtin University, Bentley, Western Australia 6102, Australia.

4.1 Abstract

This study presents the solubility of calcium carbonate in monoethylene glycol (MEG)/water solution at high temperatures and high MEG concentrations. The conditions simulate the water removal process During MEG regeneration. Solubility was measured by dissolution at equilibrium and the thermodynamic of dissolution process of calcium carbonate was also explored. The solubility of calcium carbonate decreased with increasing temperature up to 120 °C and showed a slight increase above 120 °C. The presence of MEG increased the activity coefficient of calcium carbonate and calcium ions with respect to temperature. The effect of MEG degradation on the solubility of calcium carbonate was also studied. At all temperatures studied (90 °C to 145 °C), MEG degraded in the presence of residual dissolved oxygen to produce acetate ions which complexed with calcium ions resulting in an increase in calcium solubility.

Keywords: Monoethylene glycol, Calcium, Carboxylic acids, thermal oxidative degradation, Solvent effects

4.2 Introduction

Monoethylene glycol (MEG) is commonly used as a hydrate inhibitor in gas pipelines; the ability to recycle it makes it financially viable.[1] As a hydrate inhibitor, MEG is injected into the gas pipeline to prevent hydrate formation. As a result, MEG downstream of the gas pipeline is usually at a lower concentration and loaded with salts that were present in the produced water. The MEG regeneration and reclamation process ensures that used MEG is restored to a form suitable for reuse as a hydrate inhibitor.[2] These processes include the removal of salts and the distillation of rich MEG (ca. 60 % MEG) to lean MEG (ca. 90 % MEG). Analysis on a reboiler system by Zaboon et.al (2017)[3] finds that lean MEG purification to above 80 wt.% is achievable above 135 °C.

One major technical challenge for the regeneration of MEG is the scaling and fouling of the reboiler where MEG is exposed to high temperatures.[4] Scaling and fouling in the MEG reboiler occurs when various substances precipitate and deposit on the reboiler tubes and walls. Among other salts, calcium carbonate is a major component of the scale formed. To reduce the potential of calcium carbonate precipitation in the reboiler, its precipitation is encouraged in a pre-treatment tank upstream of the reboiler. Thermodynamic data on the solubility behavior of calcium carbonate in the reboiler are necessary to understand how the salt is being dissolved or precipitated in solution inside the reboiler.

Calcium carbonate precipitation is complex. Among various forms, calcite is the most stable form of precipitated calcium carbonate in water.[5] Aragonite has been observed at high temperature in water but it eventually converts to calcite after 1300 minutes.[6] Little is known about the transformation mechanism of calcium carbonate in the NaCl/MEG/H_2O system.

Previous literature has shown that the solubility of calcium carbonate decreases with increasing temperature[7] and increasing MEG content.[8] All available studies on calcium carbonate solubility in MEG have been done at lower temperatures (< 90 ^{0}C) and in a CO_2 saturated environment.[8-9] Solubility data for many salts in MEG-water solutions at temperatures below 100 ^{0}C have been published but, at the time of writing this paper, there are no published data for the solubility of calcium carbonate at reboiler conditions: high temperatures (ca. 120-145 °C), high MEG % (ca. 80-90 %), low CO_2 partial pressure (0.5 to 5 mol%) and high pH (ca. pH 9 to 12). Another challenge associated with MEG regeneration and reclamation process is the thermal cycling which can lead to oxidative degradation that produce organic acids.[8; 10] Aged MEG is reported to enhance corrosivity[11] and reduce hydrate inhibition efficiency.[12]

The aim of this study is to determine solubility data and understand the solubility behavior of calcium carbonate at conditions close to those in the reboiler to extend existing knowledge in this area. In addition, the effect of degradation on the solubility of calcium carbonate in the NaCl/MEG/H_2O system is investigated. In this study, the concentration of calcium carbonate that dissolved in lean MEG (90 v/v% MEG/H_2O) in the presence of NaCl and under CO_2 free and saturated conditions was determined. The results are compared with existing models published by Lu. Kan and Tomson (2010)[9] and Sandengen (2006)[8] that are being used to predict calcium carbonate solubility in MEG/water solutions

4.3 Materials and Methods

The calcium carbonate solubility in MEG water solution at temperatures between 120 ^{0}C and 145 ^{0}C was measured by the dissolution method in an airtight 1 L glass cell setup. A known excess amount of calcium carbonate (2 g) was added to 700 ml NaCl-MEG-water solution. The solution was heated to 10

^{0}C above the desired temperature and subsequently maintained at the desired temperature for the period of experiments. The solution was stirred continuously using a magnetic stirrer set to 300 rpm. Samples were drawn through a 22 μm filter connected to a syringe. For experiments in a CO_2-free environment, the cell was continuously sparged with high purity N_2 (99.99 %, BOC Australia). A CO_2 saturated environment on the other hand was achieved by continuously sparging the cell with CO_2 (99.99 %, BOC Australia). All reagents were analytical grade and used without any further purification. Heating and temperature control was done using IKA® RCT basic heater equipped with the IKA® PT 1000.60 stainless steel temperature sensor in a glass sleeve and accuracy of temperature measurement was ±1 °C.

Sandengen (2006)[8] found that higher temperature significantly increased the dissolution rate and at temperatures higher than 80 ^{0}C equilibrium was achieved in 2 days. For most of the experiments conducted in this study, Samples were taken hourly after the 2 days mark and experiments were completed when there was no change in the calcium concentration measured in three consecutive samples. The experimental setup was validated by measuring the solubility of calcium carbonate in CO_2 saturated 90 % MEG/H_2O solution at 80 ^{0}C and comparing the results with data from existing literature. Each experiment was conducted at least 3 repeats.

Samples were analyzed for calcium contents by ion chromatography on a Dionex™ ICS-2100 Integrated Reagent-Free IC System equipped with a Dionex™ electrolytically regenerated suppression system, accuracy for measurement was ± 0.5 ppm. Organic acid degradation products of MEG were also measured by ion chromatography on a Dionex™ ICS-2100 Integrated Reagent-Free IC System equipped with a Dionex™ chemically regenerated suppressor system. Samples for calcium measurement were collected in plastic containers and immediately acidified with a few drops of nitric acid to prevent

recrystallization or precipitation, accuracy for measurement was ± 0.5 ppm. Samples for organic acid measurement were quenched by dipping in cold water and tested immediately. To measure the pH, samples were cooled to 25 ^{0}C in an airtight water-jacketed glassware with a nitrogen blanket over the sample to prevent air ingress. The pH probe was calibrated following the method published by Sandengen (2007).[13]

Two sets of experiments were conducted, one set in which the MEG was allowed to undergo degradation and another in which there was no degradation. MEG oxidative degradation can produce organic acid[10] which can in turn affect the amount of calcium dissolved in the system. The organic acid content were used to identify samples that had degraded at the end of the experiment; samples with no degradation had no organic acid.

4.3.1 Thermodynamic calculation

The solubility product for calcium carbonate K_{SP} is calculated from the product of the activities of calcium ($\alpha_{Ca^{2+}}$) and carbonate ions ($\alpha_{CO_3^{2-}}$) as shown in equation Eqn.[1]. Individual ion activities, however, equals the molality (m) of each ion multiplied by their individual activity coefficients (γ) seen in equation Eqn.[2].

$$K_{SP} = \alpha_{Ca^{2+}} \times \alpha_{CO_3^{2-}} \quad \text{Eqn.[1]}$$

$$K_{SP} = m_{Ca^{2+}}\gamma_{Ca^{2+}} \times m_{CO_3^{2-}}\ \gamma_{CO_3^{2-}} \quad \text{Eqn.[2]}$$

In a salt/MEG/H_2O system, the influence of salt and MEG on individual ion activity coefficients.[14] Thus K_{SP} can be calculated as:

$$K_{SP} = m_{Ca^{2+}} \times {\gamma^S}_{Ca^{2+}} \times {\gamma^N}_{Ca^{2+}} \times m_{CO_3^{2-}} \times {\gamma^S}_{CO_3^{2-}} \times {\gamma^N}_{CO_3^{2-}} \quad \text{Eqn.[3]}$$

Where m and γ represent molality and molal activity coefficient of the subscripted species. γ^S represents the activity coefficients due to the salt effect and γ^N represents the activity coefficients due to the MEG effect. Rearranging equation Eqn.[3] gives:

$$K_{SP} = m_{Ca^{2+}} \times {\gamma^S}_{Ca^{2+}} \times m_{CO_3^{2-}} \times {\gamma^S}_{CO_3^{2-}} \times [{\gamma^N}_{Ca^{2+}} \times {\gamma^N}_{CO_3^{2-}}] \quad \text{Eqn.[4]}$$

The molality of calcium $m_{Ca^{2+}}$ was measured experimentally and was equal to the molarity of carbonate $m_{CO_3^{2-}}$ as there was no other source of carbonate in the CO_2-free system. The salt components of individual ion activities were calculated using the Pitzer model.[15] The term $[{\gamma^N}_{Ca^{2+}} \times {\gamma^N}_{CO_3^{2-}}]$ which refers to the effects of MEG in the $CaCO_3$ solubility can be calculated by comparing K_{SP} obtained from the salt/MEG/H_2O system to the K^*_{SP} from the salt/H_2O system. K^*_{SP} values for calcite were used in this study and were calculated using the Plummer and Busenberg (1982) model.[7]

In the absence of MEG, the solubility product of $CaCO_3$ in a salt/H_2O system is represented with K^*_{SP} as shown in equation 5.

$$K^*_{SP} = m_{Ca^{2+}} \times {\gamma^S}_{Ca^{2+}} \times m_{CO_3^{2-}} \times {\gamma^S}_{CO_3^{2-}} \quad \text{Eqn.[5]}$$

Substitute equation into equation Eqn.[4] gives

$$K_{SP} = K^*_{SP} \ [{\gamma^N}_{Ca^{2+}} \times {\gamma^N}_{CO_3^{2-}}] \quad \text{Eqn.[6]}$$

And

$$\left[{\gamma^N}_{Ca^{2+}} \times {\gamma^N}_{CO_3^{2-}}\right] = \frac{K_{SP}}{K^*_{SP}} \quad \text{Eqn.[7]}$$

Therefore, K_{SP} divided by K^*_{SP} gives the MEG effect on $CaCO_3$ solubility. Individual co-solvent activity coefficients for calcium and carbonate were calculated from using the expression in equation 8:[16]

$$\ln \gamma_i = \frac{\mathcal{V}.\mathcal{Z}_i^2}{\mathcal{V} + \mathcal{Z}_+^2 + \mathcal{V}_-\mathcal{Z}_-^2} \ln \gamma_{M_{\mathcal{V}+}X_{\mathcal{V}-}} \qquad \text{Eqn.[8]}$$

Where γ_i is the activity coefficient for ion $_i$ and $\gamma_{M_{\mathcal{V}+}X_{\mathcal{V}-}}$ is the activity coefficient for electrolyte *MX* (*M* represents the cation and *X* represents the anion). $\mathcal{V}$, $\mathcal{V}_-$ and $\mathcal{V}_+$ are the total number of ion, number of anions and number of cations respectively while $\mathcal{Z}_i$, $\mathcal{Z}_+$ and $\mathcal{Z}_-$ are charge on ion $_i$, total charge on cations and total charge on anions respectively. Substituting for values in equation 8, $\ln \gamma^N{}_{Ca^{2+}}$ can be calculated using equation 9.

$$\ln \gamma^N{}_{Ca^{2+}} = \frac{8}{10} \ln \gamma^N{}_{Ca^{2+}} \times \gamma^N{}_{CO_3^{2-}} \qquad \text{Eqn.[9]}$$

4.4 Results and Discussion

4.4.1 Calcium solubility in NaCl/MEG/H_2O solution

Solubility data presented in this section are measurements from experiments in which the MEG did not undergo degradation. The effect of degradation on solubility data is discussed in a latter section.

4.4.1.1 MEG effect on total calcium concentration

Total calcium concentration from experiments in a CO_2 saturated environment and temperatures below 100 °C were in concordance with extrapolated values from Sandengen (2006)[8] as shown in Figure 4-1. Experiments in this work in the CO_2-saturated environment were not extended beyond 100 °C as the focus in this study is on the CO_2 free environment in the reboiler. Solubility values

for samples in the CO_2 free environment (i.e. samples that were sparged with N_2) were much lower than those in the CO_2 saturated environment.

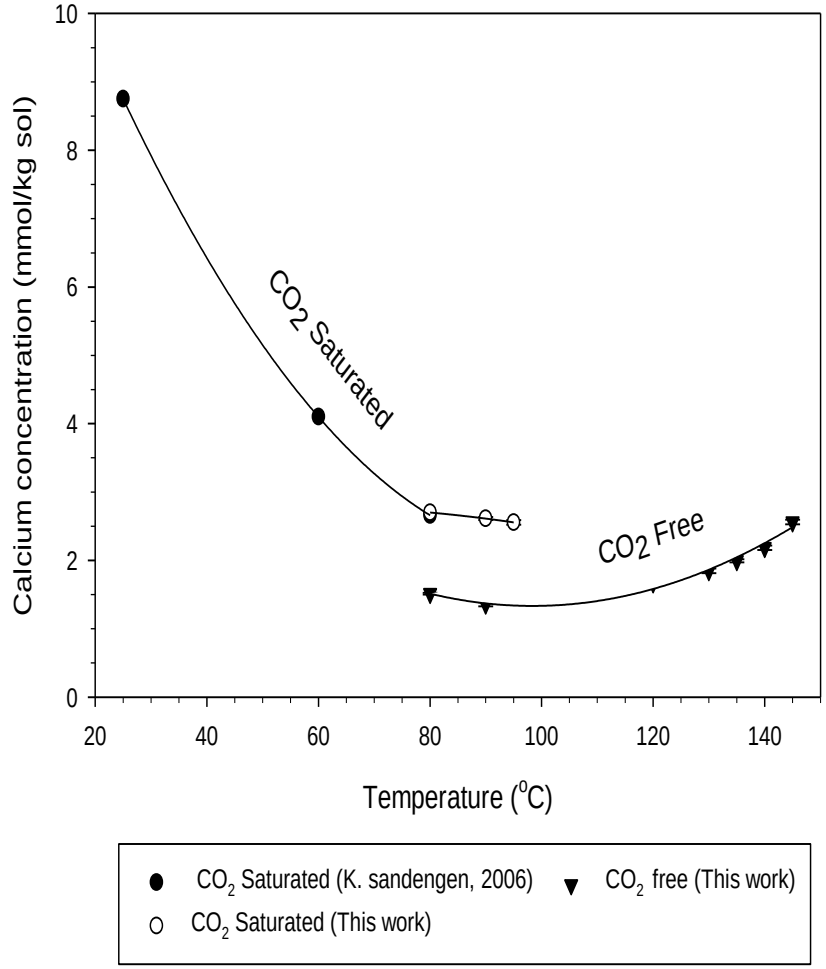

Figure 4-1: Calcium carbonate solubility with temperature (a comparison with existing literature)

In general, calcium carbonate dissolution in an aqueous solution is influenced by pH and the presence of CO_2; the dissolution process involves three reactions (equations Eqn.[10]-Eqn.[12]) occurring simultaneously. A low pH condition and the presence of CO_2 promotes the reactions in equations Eqn.[10] and Eqn.[11] while a pH value above 8 promotes reaction in equation Eqn.[12].[17] Samples in the CO_2 free environment had starting pH of about 8.76 and pH increases to above 10 depending on how much of the calcium carbonate was dissolved. This pH in a CO_2 free environment meant that only reaction in equation Eqn.[12] was plausible and thus lower solubility values.

$$CaCO_3 + H^+ \Leftrightarrow Ca^{2+} + HCO_3^- \quad \text{Eqn.[10]}$$

$$CaCO_3 + H_2CO_3 \Leftrightarrow Ca^{2+} + 2HCO_3^- \quad \text{Eqn.[11]}$$

$$CaCO_3 + H_2O \Leftrightarrow Ca^{2+} + HCO_3^- + OH^- \quad \text{Eqn.[12]}$$

Values for calcium carbonate solubility in 0.5 M NaCl 90 v/v% MEG/H_2O in a CO_2-free environment are presented in table 1 and illustrated in figure 2. Results from this work show that, in a CO_2 free environment calcium solubility reached a minimum between 90 °C and 120 °C and then started to increase slightly (Figure 2). Previous work that have reported calcium carbonate solubility in MEG have been conducted in a CO_2 environment.

The values for activity coefficients presented in table 1 are very low and far from infinity depicting a significant influence on solubility. Reason for these low values is because reference is being made between solubility in 90 v/v% MEG and pure water. The terms $\gamma^N{}_{Ca^{2+}}$ and $\gamma^N{}_{CO_3^{2-}}$ as explained in the previous section under 'Thermodynamic calculation' are the MEG effects on solubility with reference to solubility in pure water.

Table 4-1: Ca^{2+} concentration in 90 v/v% MEG/H2O with 0.5 M NaCl

No.	Temp (°C) ±1 °C	Average Ca^{2+} concentration		$[\gamma^N{}_{Ca^{2+}} \times \gamma^N{}_{CO_3^{2-}}]$ (x10^{-3})	$\gamma^N{}_{Ca^{2+}}$ (x10^{-3})
		(mmol/kg sol.) ± 0.01 mmol/kg	Standard deviation		
1	80	1.514	0.0151	0.87	0.36
2	90	1.358	0.0368	0.80	0.33
3	120	1.669	0.0399	1.88	6.60
4	130	1.847	0.0423	2.67	8.73
5	135	1.994	0.0266	3.40	10.59
6	140	2.185	0.0378	4.46	13.16
7	145	2.561	0.0393	6.72	18.27

Note: Activity coefficients were calculated from equations 7 and 9

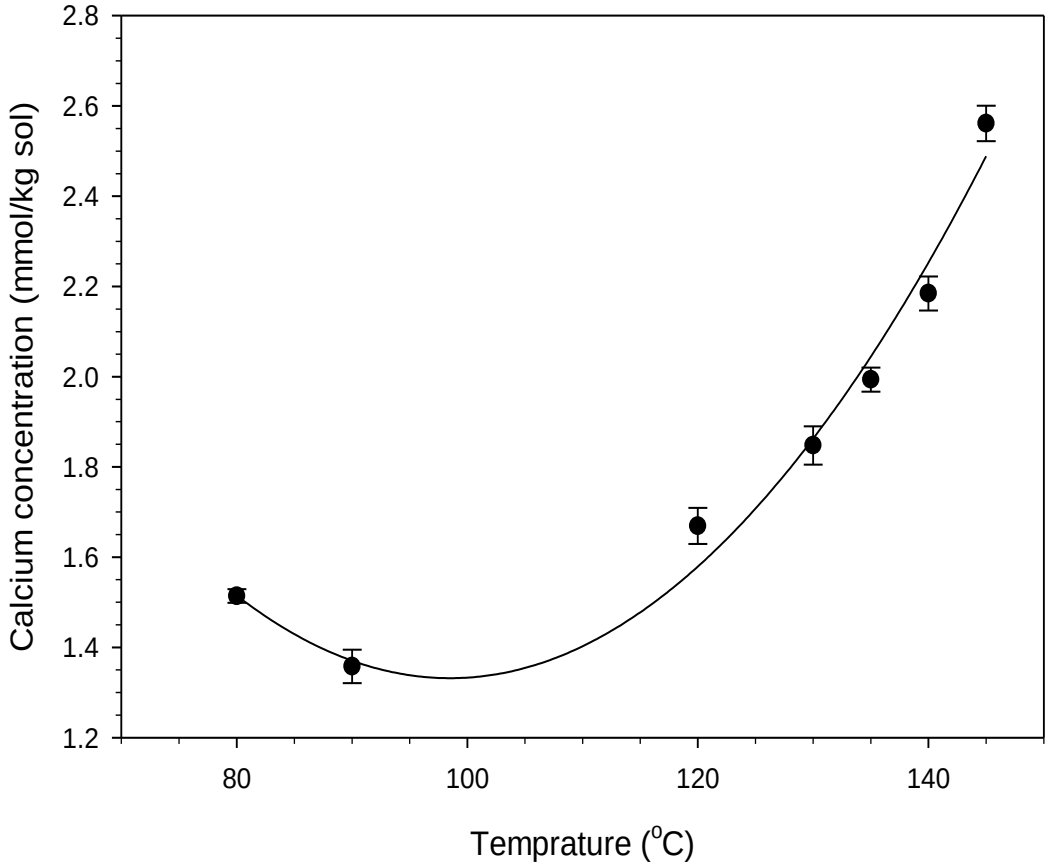

Figure 4-2: Calcium carbonate solubility in NaCl/MEG/H_2O solution with temperature

4.4.1.2 MEG effect on ion activity coefficients

Sandengen (2006) presented two models that can be used to estimate MEG effect on activity coefficients of both carbonate and calcium ions $\Upsilon^{N}_{C03^{2-}}$ and $\Upsilon^{N}_{Ca^{2+}}$ respectively[8]; these models are from experimental data up to 80 °C and do not show any temperature or ionic strength dependence for either parameters at these temperatures. Sandengen's model however does show a temperature dependence for the bicarbonate activity coefficient $\Upsilon^{N}_{HC03^{-}}$. The model presented by Lu, Kan, and Tomson (2010)[18] in the CO_2 environment shows a temperature and ionic strength dependence for $\Upsilon^{N}_{Ca^{2+}}$ but uses the bicarbonate activity coefficient $\Upsilon^{N}_{HC03^{-}}$ instead of that of the carbonate $\Upsilon^{N}_{C03^{2-}}$. A comparison with both existing models is difficult since experiments in this work are in a CO_2 free environment and we have calculated $\Upsilon^{N}_{C03^{2-}}$ as expected

from equation Eqn.[12] above. However the calculated values of $\Upsilon^{N}_{Ca^{2+}}$ and $(\Upsilon^{N}_{Ca^{2+}} \times \Upsilon^{N}_{C03^{2-}})$ from experiments in this work show that these parameters have a slight dependence on temperature as seen in figure 4-3 and figure 4-4. In comparison with existing models, it is apparent that MEG effect on calcium carbonate is much lower in a CO_2-free environment.

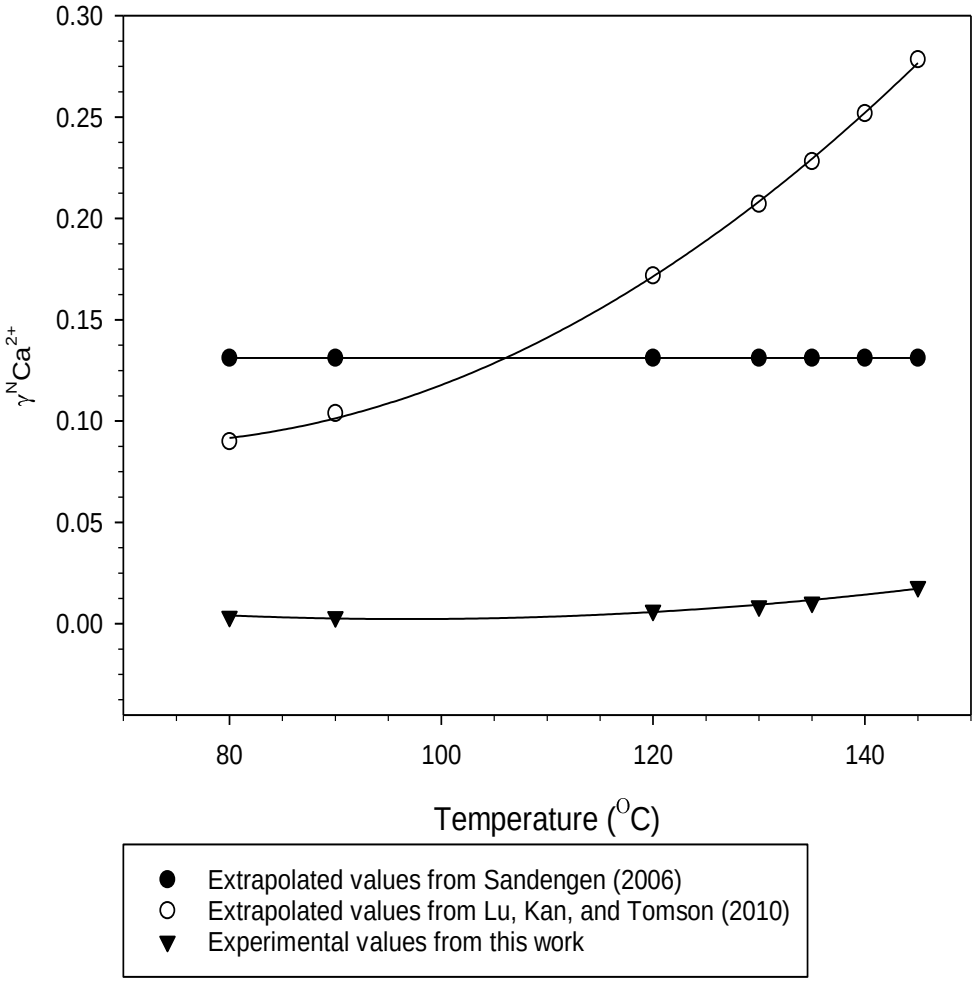

Figure 4-3: MEG effect on calcium ion activity coefficient

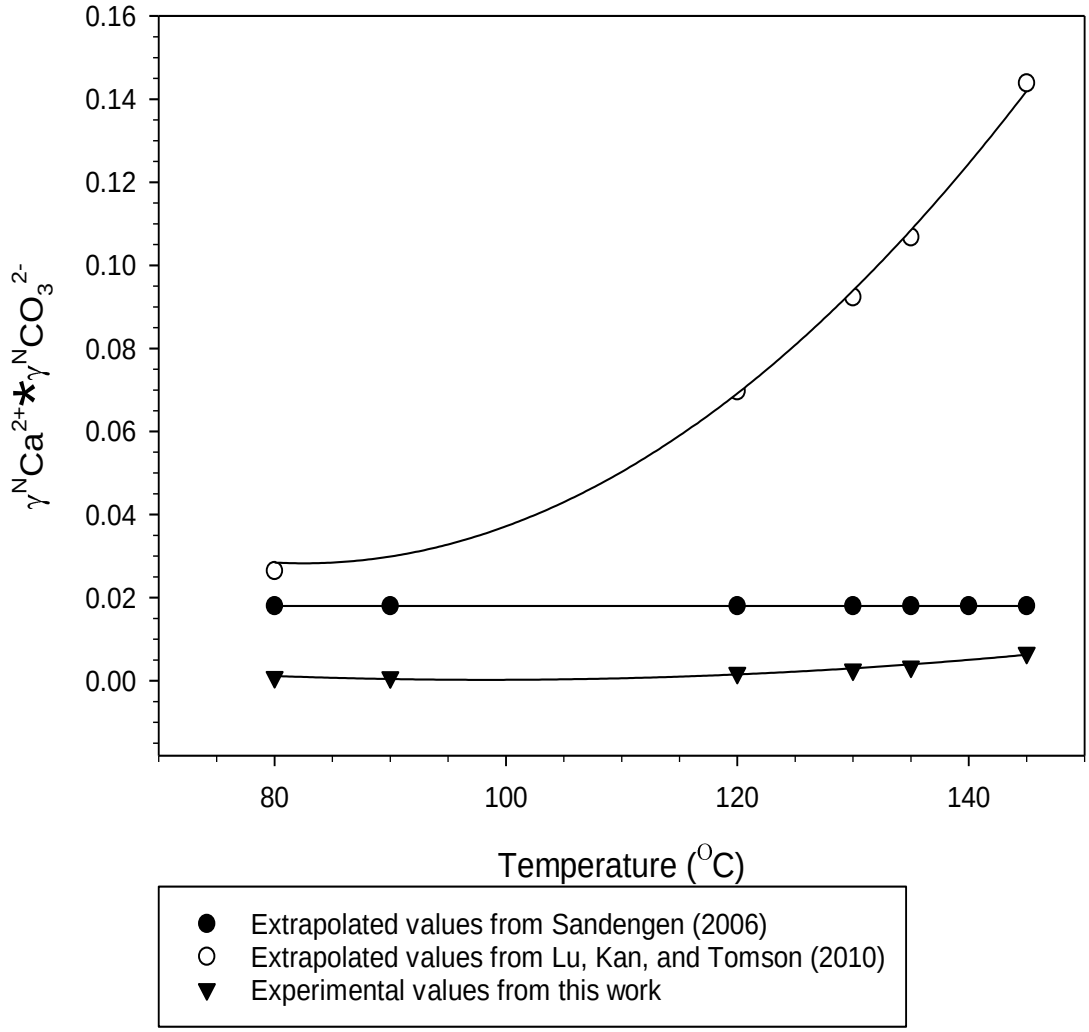

Figure 4-4: Combined MEG effect on calcium ion and carbonate ion activity coefficient

4.4.2 Effect of degradation on calcium solubility in MEG/Water solution

The original aim of this work was to produce the solubility data for calcium carbonate in lean MEG in a CO_2-free environment. To create the CO_2-free environment, the glass cell set-up was continuously sparged with high purity N_2 gas to eliminate CO_2 and O_2 and, hence, to prevent thermal oxidative degradation of the MEG. However, in some of the experiments, the MEG solutions had significantly changed color at the end of experiment as shown in figure 5. The solution remained cloudy though because of the undissolved

excess calcium carbonate and the color change was observed to be more intense at higher temperatures. A change in color has been reported to be a result of the thermal oxidative degradation of MEG.[19] Thus samples with color change were tested for organic acid content and analyzed for the effect of degradation on the calcium carbonate solubility.

Figure 4-5: Experimental solution at start of experiment (left) and after 2 days with MEG degradation at 90 °C (middle) and 135 °C (right).

Thermal oxidative degradation of MEG occurs when MEG is converted to organic acids at high temperature in the presence of oxygen.[10] Degradation in our samples indicates the presence of oxygen in the MEG solutions. There are only two ways that oxygen may be present in the experimental set-up; from air/oxygen ingress into the glass cell or from residual dissolved oxygen in the sample solution. According to Henry's law, the absorption of a gas is directly proportional to its partial pressure. Since the test solution was continuously sparged with high purity N_2 and the system maintained a positive pressure, air/oxygen ingress during experiments should be minimized. This suggested that there was residual dissolved oxygen prior to heating that caused thermal oxidation as the solution temperature was increased. There is very limited literature on the degradation pathway and outcome of NaCl/MEG/H_2O solution at high temperature, and even less information on the solubility of oxygen in MEG/H_2O and NaCl/MEG/H_2O solution. Nonetheless, it has been

reported that oxygen solubility in pure MEG reduces with increasing temperature.[20]

The produced organic acid content was used to measure the extent of the MEG degradation [10; 19; 21] and concentrations of these organic acids are presented in figure 6. Rossiter et al (1985) reported less than 50 ppm of degradation products in oxygen free pure MEG at 101 °C whereas results from this work are as much as 255 ppm at 90 °C. Rossiter et al (1985) did not report any values for dissolved oxygen in their experiment and they used pure MEG samples not NaCl/MEG/H_2O samples. In this study, we have found that acetate was the main degradation product as presented in figure 6. A plot of total organic acid concentration against temperature from solubility experiments in this work shows that after two hours of heating, the amounts of organic acid produced was higher for experiments at higher temperatures (figure 6); this is not unexpected as MEG degradation increases with increasing temperature.[10]

The amount of dissolved calcium carbonate in the degraded MEG samples also increased with temperature in a similar manner with the acetate (figure 7). Organic acid concentration can increase the concentration of dissolved calcium by either dissociation to produce more hydrogen ion H^+ which in turn reduces the pH of the solution and favors the dissolution of calcium following equation Eqn.[10][17] or by forming soluble $CaOAc^-$ complex with calcium ions.[22]

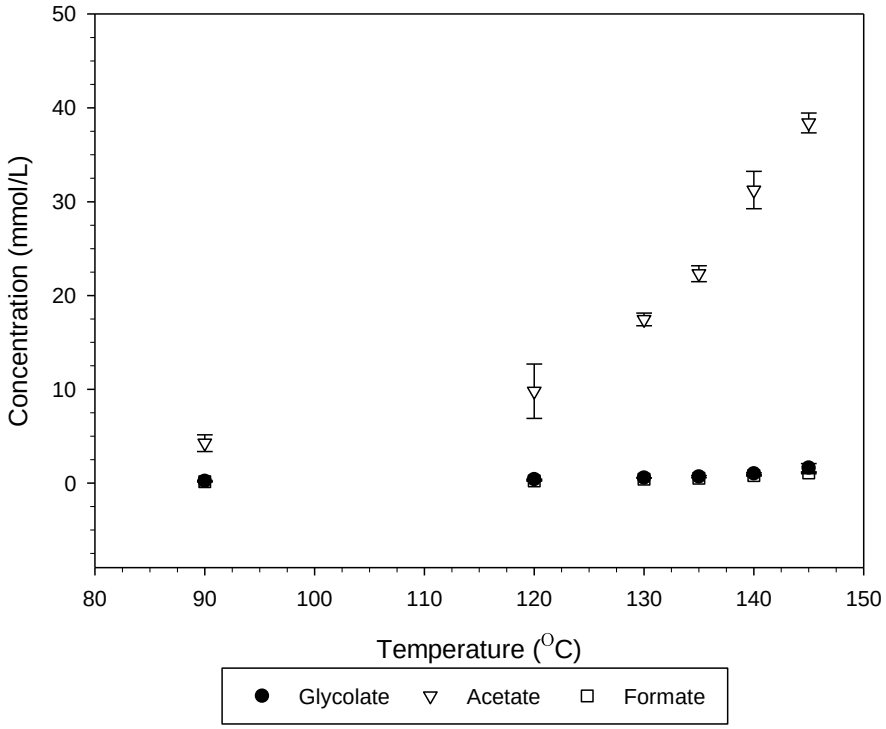

Figure 4-6: Organic acid concentrations in degraded NaCl/MEG/H2O solutions after 48 hours

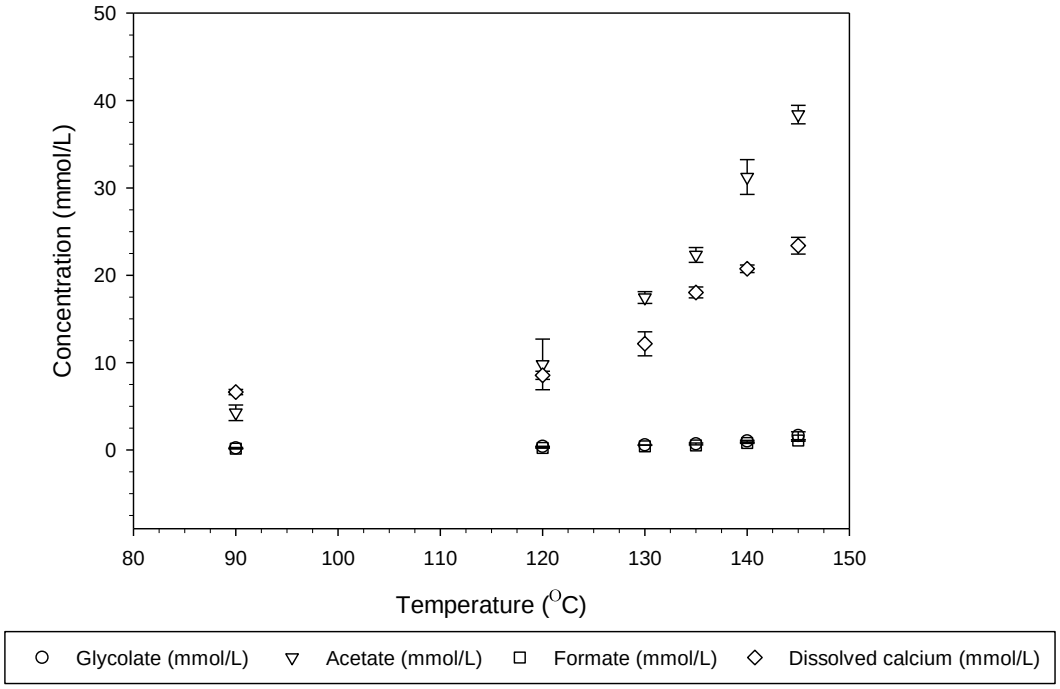

Figure 4-7: Concentration of organic acids and calcium in degraded Lean MEG

The acid dissociation constant (pKa) is a measure of how much an acid would dissociate in solution to produce hydrogen ion H^+; a low pKa indicates greater dissociation potential, which means more H^+ is produced and a bigger negative change on the pH of the solution. In other words, a lower pKa causes bigger reduction in the pH of the solution and vice versa. A. Soames et. al. (2019) reported an increase in acid dissociation constant (pKa) of acetic acid in MEG/H_2O solution with increasing MEG weight fraction, increasing temperature and decreasing ionic strength of the solution. On analysis of their data, the pKa value of acetic acid can be predicted as a function of MEG weight percentage (x), temperature (T) in Celsius and ionic strength (μ) in the expression in equation Eqn.[13]:

$$pKa = 4.264 + 1.971x + 0.002T - 0.044\mu \qquad \text{Eqn.[13]}$$

R^2 value for this model is 0.974 and the standard error of estimate is 0.069. From equation Eqn.[13], calculated values pKa of acetic acid in sample solutions in this work was 6.22 at 90 °C and 6.32 at 145 °C. These high pKa values indicate that the dissociation of any produced acetic acid is very small thus any change in pH of the experimental solution as a result of produced acetic acid is rather minimal.

Acetate in solution has been reported to increase the solubility of Ca^{2+} by the formation of the $CaOAc^-$ complex.[22] As seen in figure 7, there is a proportional increase in the amount of calcium ion dissolved in the degraded MEG and the amount of acetic acid produced. Fein (1991) reported that at the highest acetate concentration, the solubility of Ca^{2+} increased by approximately 60 % in $Ca(OH)_2$/NaOAc/H_2O system.[22] This acetate complex formation effect in Ca/NaOAC/MEG/H_2O however is yet to be fully understood. Even though direct comparison cannot be made with results from Fein (1991)[22] due to differences in temperatures and ionic strengths; we see some resemblance in

the 'acetate to calcium ratio' vs 'dissolved calcium concentration' trends in experiments in this work with results published by Fein (1991).[22] (Figure 8) These Similarities in the acetate-dissolved calcium trends point to the fact that the calcium acetate complex may be accounting for higher calcium solubility in MEG.

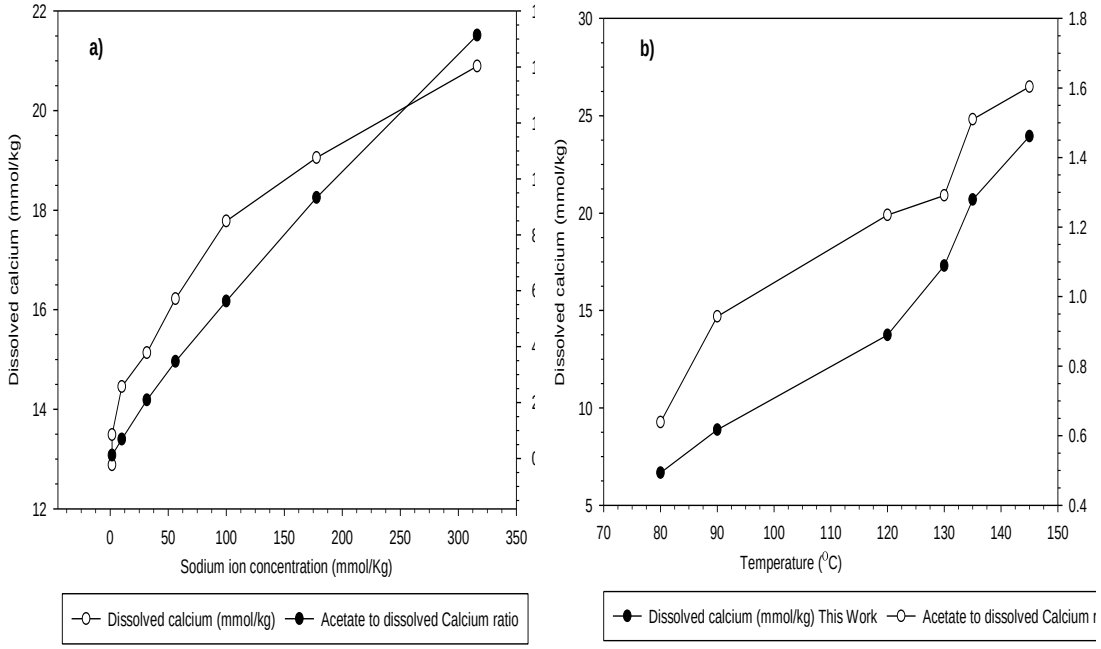

Figure 4-8: Acetate to calcium ratio vs dissolved calcium concentration; a) Fein (1991) on the left and b) experimental values from this work on the right.

Nb: Correlation between calcium and acetate ion concentration a) in aqueous solution derived from Fein (1991) at 80 C and varying ionic strength and b) in MEG-water solutions data from this work at 0.5 M ionic strength and varying temperature.

The increase in solubility of calcium carbonate in degraded MEG indicates that degradation, especially acetate concentration, is a major factor to be considered when modelling the solubility of calcium carbonate in the reboiler. As it is seen that the solubility of pure calcium carbonate increased slightly in MEG at high temperatures, it is possible that its deposition of calcium carbonate in the reboiler is probably due to influences of other substances present in the reboiler.

To resolve the undesired MEG degradation in this study, N_2 flow rate was increased from 100 ml/min to 200 ml/min and the pre-heating sparging time was increased from 60 hours to 72 hours. This was shown to be sufficient to displace dissolved oxygen to levels where degradation did not occur, thus confirming that the residual dissolved oxygen was the contributing factor in the MEG degradation. Results from this work indicate that MEG is able to degrade at a much faster rate with lower oxygen concentration than expected at 0.5 M ionic strength and high temperature. More work is being carried out to understand the degradation of high ionic strength MEG/H_2O solution at high temperatures.

4.5 Conclusion

The solubility of calcium carbonate in NaCl/MEG/H_2O at temperature from 80°C to 145°C and the effect of MEG degradation on these solubility were investigated. It has been concluded that calcium carbonate solubility decreases with temperature and reaches the minimum values at 90°C. Increasing temperature beyond 90°C promotes the dissolution of $CaCO_3$. The degradation of MEG leads to organic acids formation and increased calcium carbonate solubility. There is a correlation between acetate ions (dominant degradation product) concentration and calcium concentration.

The outcomes of this study improve our understanding about calcium carbonate precipitation during MEG regeneration. However, to determine the best practice to avoid carbonate scaling requires considerations of parameters that are out of scope of this study. For instance, the presence of small amounts of iron has been reported to affect calcium carbonate precipitation[23] and the effect of other components in the MEG regeneration system on the precipitation

of calcium carbonate are yet to be fully explored. However, this study is a very useful addition to knowledge in this field and should be considered in any software/model that seeks to predict carbonate scaling within the MEG system.

References

1. Kim, H., Yoo, W., Lim, Y., & Seo, Y. (2018). Economic evaluation of MEG injection and regeneration process for oil FPSO. *Journal of Petroleum Science and Engineering, 164*, 417-426. doi:https://doi.org/10.1016/j.petrol.2018.01.071
2. Nazzer, C. A., & Keogh, J. (2006). *Advances in Glycol Reclamation Technology*. Paper presented at the Offshore Technology Conference, Houston Texas. https://dx.doi.org/10.4043/18010-ms
3. Zaboon, S., Soames, A., Ghodkay, V., Gubner, R., & Barifcani, A. (2017). Recovery of mono-ethylene glycol by distillation and the impact of dissolved salts evaluated through simulation of field data. *Journal of Natural Gas Science and Engineering, 44*, 214-232. doi:https://doi.org/10.1016/j.jngse.2017.04.007
4. Baraka-Lokmane, S., Hurtevent, C., Seiersten, M., Flaten, E., Farrell, M., Bradshaw, O., et al. (2013). Technical challenges and solutions in a closed loop MEG regeneration system for gas field offshore, UK. *WIT Transactions on Engineering Sciences, 79*, 511-522. doi:10.2495/mpf130421
5. Lippmann, F. (1973). The Polymorphism Calcite-Aragonite. In *Sedimentary Carbonate Minerals* (pp. 97-147). Berlin, Heidelberg: Springer Berlin Heidelberg.
6. Ogino, T., Suzuki, T., & Sawada, K. (1987). The formation and transformation mechanism of calcium carbonate in water. *Geochimica et Cosmochimica Acta, 51*(10), 2757-2767. doi:https://doi.org/10.1016/0016-7037(87)90155-4
7. Plummer, L. N., & Busenberg, E. (1982). The solubilities of calcite, aragonite and vaterite in CO2-H2O solutions between 0 and 90 C, and an evaluation of the aqueous model for the system CaCO3-CO2-H2O. *Geochimica et Cosmochimica Acta, 46*(6), 1011-1040.
8. Sandengen, K. (2006). *Prediction of mineral scale formation in wet gas condensate pipelines and in MEG (mono ethylene glycol) regeneration plants.* Norwegian University of Science and Technology,
9. Lu, H., Kan, A. T., & Tomson, M. B. (2010). Effects of monoethylene glycol on carbonate equilibrium and calcite solubility in gas/monoethylene glycol/NaCl/water mixed systems. *Spe Journal, 15*(03), 714-725.
10. Rossiter, W. J., Brown, P. W., & Godette, M. (1983). The determination of acidic degradation products in aqueous ethylene glycol and propylene glycol solutions using ion chromatography. *Solar Energy Materials, 9*(3), 267-279. doi:Doi 10.1016/0165-1633(83)90049-7

11. Santambrogio, M., Perrucci, G., Trueba, M., Trasatti, S., & Casaletto, M. (2016). Effect of major degradation products of ethylene glycol aqueous solutions on steel corrosion. *Electrochimica Acta, 203*, 439-450.
12. AlHarooni, K., Barifcani, A., Pack, D., Gubner, R., & Ghodkay, V. (2015). Inhibition effects of thermally degraded MEG on hydrate formation for gas systems. *Journal of Petroleum Science and Engineering, 135*, 608-617. doi:https://doi.org/10.1016/j.petrol.2015.10.001
13. Sandengen, K., Kaasa, B., & Østvold, T. (2007). pH Measurements in Monoethylene Glycol (MEG) + Water Solutions. *Industrial & Engineering Chemistry Research, 46*(14), 4734-4739. doi:10.1021/ie061305a
14. Bromley, L. A. (1973). Thermodynamic properties of strong electrolytes in aqueous solutions. *AIChE Journal, 19*(2), 313-320. doi:10.1002/aic.690190216
15. Pitzer, K., & Brewer, L. (1961). Lewis and Randall, Thermodynamics. *McGraw Hill Book Co., Inc., New York, NY*.
16. Bates, R. G., & Vijh, A. K. (1973). Determination of pH: theory and practice. *Journal of The Electrochemical Society, 120*(8), 263C-263C.
17. Plummer, L. N., Parkhurst, D. L., & Wigley, T. M. L. (1979). Critical Review of the Kinetics of Calcite Dissolution and Precipitation. In *Chemical Modeling in Aqueous Systems* (Vol. 93, pp. 537-573): AMERICAN CHEMICAL SOCIETY.
18. Kan, A. T., Lu, H., & Tomson, M. B. (2010). Effects of Monoethylene Glycol on Carbon Dioxide Partitioning in Gas/Monoethylene Glycol/Water/Salt Mixed Systems. *Industrial & Engineering Chemistry Research, 49*(12), 5884-5890.
19. Madera, M., Höflinger, W., & Kadnar, R. (2003). Ion chromatographic identification and quantification of glycol degradation products. *Journal of Chromatography A, 997*(1), 279-284. doi:https://doi.org/10.1016/S0021-9673(03)00060-8
20. Joosten, M. W., Tier, B., Seiersten, M., & Wintermark, C. (2007). *Materials Considerations for MEG (Mono Ethylene Glycol) Reclamation Systems*. Paper presented at the CORROSION 2007, Nashville, Tennessee.
21. Rossiter, W. J., Godette, M., Brown, P. W., & Galuk, K. G. (1985). An investigation of the degradation of aqueous ethylene glycol and propylene glycol solutions using ion chromatography. *Solar Energy Materials, 11*(5), 455-467. doi:https://doi.org/10.1016/0165-1633(85)90016-4
22. Fein, J. B. (1991). Experimental study of aluminum-, calcium-, and magnesium-acetate complexing at 80 C. *Geochimica et Cosmochimica Acta, 55*(4), 955-964.
23. Flaten, E. M., Watterud, G., Andreassen, J.-P., & Seiersten, M. E. (2008). *Precipitation Of Iron And Calcium Carbonate In Pipelines At Varying Meg Contents*. Paper presented at the SPE International Oilfield Scale

Conference, Aberdeen, UK. https://www.onepetro.org:443/download/conference-paper/SPE-114089-MS?id=conference-paper%2FSPE-114089-MS

Chapter 5

Thermal-oxidative stability of Monoethylene Glycol during regeneration

5.1 Abstract

This study explores the oxidative stability of monoethylene glycol (MEG) under regeneration conditions in the MEG Recovery Unit (MRU). The MRU application relates to the recycle of MEG for use as a gas hydrate inhibitor. This study explores the effect of MEG concentration, oxygen content and ionic strength on MEG degradation/stability. The impact of these parameters on the type and concentration of organic acids produced during said degradation and effects on the pH of the degraded MEG solution is also investigated. Results from this study show that the distribution of produced organic acid varies slightly with differences in MEG concentration, oxygen content and ionic species in the degrading MEG solution at 140 °C.

Keywords: Monoethylene glycol, MEG regeneration Unit, Hydrate Inhibitor

5.2 Introduction

Modern oil and gas production has seen a significant increase in long deep-water tieback, for which hydrate prevention remains a significant technical challenge [1]. MEG, a thermodynamic hydrate inhibitor (THI), is used to prevent the formation of hydrocarbon gas hydrates in wet gas transportation pipelines. Gas hydrates are clathrate compounds in which gas molecules are trapped in a crystalline lattice structure of water, forming a solid similar to ice [1].

Hydrates are a prevalent cause of blockages in production pipelines [2], making hydrate formation an undesirable event in gas production. Thus, hydrate prevention is critical to pipeline operations [3]. In addition to MEG generally having low toxicity to the environment [4], the feasibility of the regeneration and reclamation of MEG through onsite production facilities is an advantage, making MEG an economically viable choice for hydrate prevention [5]. However, the regeneration and reclamation process can suffer fouling and gunking problems, possibly caused and/or exacerbated by the degradation of MEG during regeneration at elevated temperatures [6].

A critical step during MEG regeneration is the dewatering stage, during which the water content in rich MEG (40 – 60 wt.% water content) is reduced to produce lean MEG (10 - 20 wt.% water content) before the MEG is returned to the pipeline for hydrate prevention. To dewater, MEG is heated to temperatures of 120 °C - 140 °C in a slightly pressurized deoxygenated vessel and the water distilled off [7]. MEG has been reported to degrade into organic acids at similar temperatures [8-9]; however, there is insufficient data to define the kinetics and specific products of MEG thermal oxidative degradation under regeneration conditions.

Studies and literature into the catalytic oxidation and electro-oxidation of MEG are well established, and the possible routes and mechanisms are very well defined. Nonetheless, existing research into the thermal oxidative stability and thermal degradation of MEG is varied in scope and scattered in literature [8-15]. In the 1980s, W.J. Rossiter and his research group conducted studies into the degradation of MEG and identified glycolic, formic and oxalic acids as degradation products [8; 16]; however, their studies were focused on the degradation of MEG in the context of MEG for heat transfer; with no consideration of the effect of ionic strength. Indeed, most of all published literature on this topic are studies conducted at temperatures less than 120 °C and no salt content [8-9; 12; 16-17]. A closely related work published on the thermal degradation of MEG explores the degradation at 140 °C [11] but not the effect of oxygen concentration on this degradation and only up to 9 molar MEG solution (about 50 wt.% MEG). The thermal oxidative stability of MEG during regeneration as applied in gas pipeline hydrate prevention is less understood.

It is common practice to keep the entire MEG cycle, especially the regeneration and reclamation unit deaerated, as oxygen is known to promote degradation, corrosion and scale formation within the process vessels. Hence the MRU is operated under a gas blanket to keep it oxygen-free [18]. Ideally, the oxygen-free environment is kept that way by using a continuous stream of ultra-high purity nitrogen (>99.99% N_2). However, due to cost implications, there are cases where operators use membrane-generated nitrogen gas in the reactor vessels [19]. Albeit economically viable, membrane-generated nitrogen can sometimes hold up to 5% air (or 1.05% oxygen) as impurity [20], resulting in significant oxygen ingress into the MEG system; primarily for pressurized systems as is commonly the case for MEG regeneration and reclamation[18]. The influence

of these small amounts of oxygen on the degradation of MEG has not yet been investigated.

Another frequently reported challenge with the closed-loop MEG recycle system is the accumulation of salt and scale deposition [19; 21]. The continuous recycling of MEG in the MEG loop, as illustrated in Figure 1-2, shows that the MEG stream is reused over several cycles.

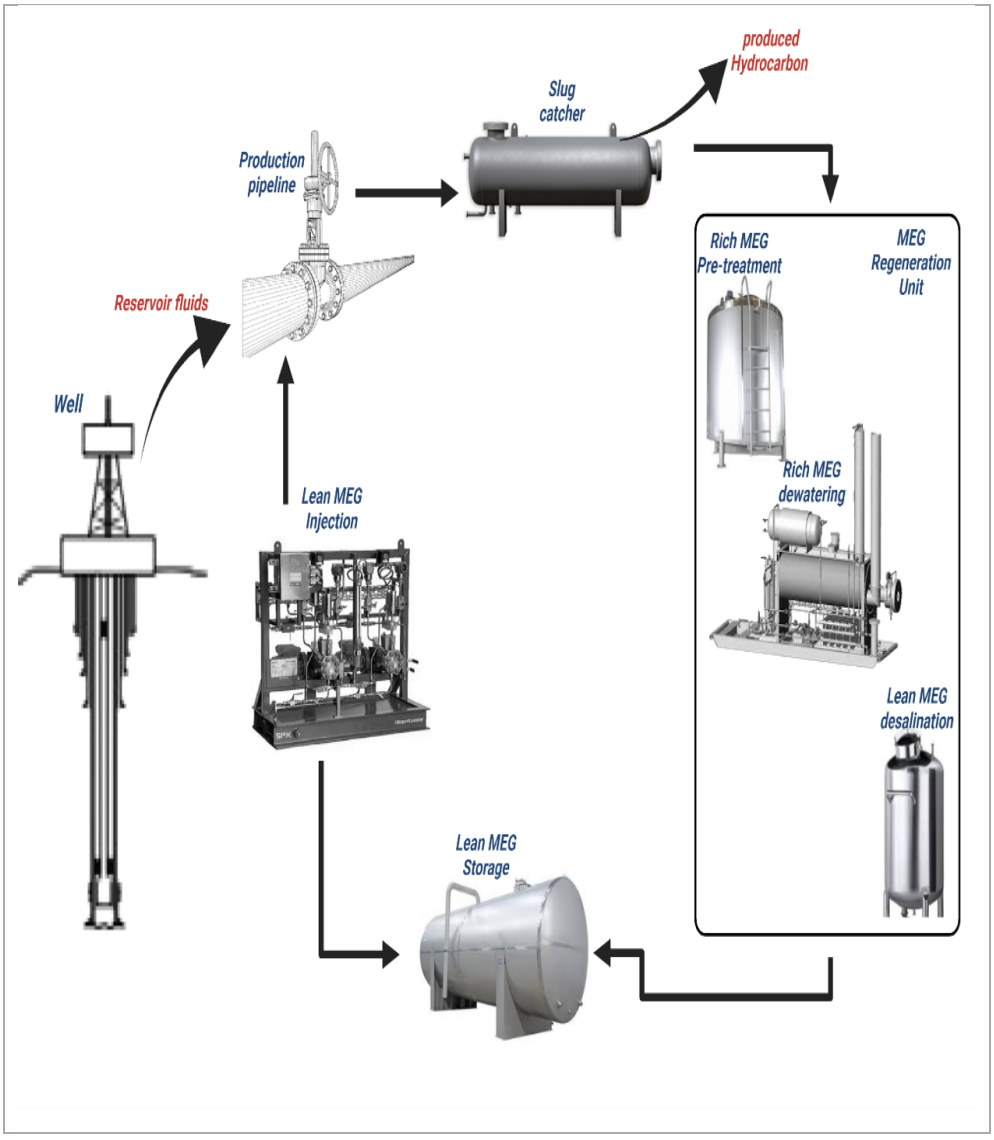

Figure 5-1: A simplified representation of the MEG stream loop for hydrate inhibition and recycle. ⟶ shows the flow for MEG containing streams ⟶ shows stream with no MEG.

The salt and ionic content of reservoir fluids partition with water into the MEG stream, thereby causing an increase in the ionic content of the MEG stream. Depending on the chemistry of the reservoir fluid and the MRU design, the accumulation of salt could be significant [22], with a possible effect on the degradation of MEG [23]. Salts of monovalent cations like sodium and potassium have very high solubility in MEG and tend to accumulate even more readily in the MEG stream. On the other hand, carbonate and sulphate salts of divalent cations are less soluble and more readily deposited within the MEG stream; calcium carbonate is the most often reported culprit [24-26]. In this work, the effect of calcium carbonate salt on the degradation of MEG is, therefore, considered.

5.3 Methodology

This work focuses on the degradation of lean MEG under regeneration and reclamation conditions, characterized by high MEG content, high ionic strength, low oxygen content and high temperature. A first set of experiments were conducted on two strengths of MEG solutions; 12.5 mol/kg sol. and 14.1 mol/kg sol. MEG. This set of experiments aimed to evaluate how a change in the MEG content affects degradation in the MEG MRU. To achieve this aim, ionic strength was kept constant at 0.5 mol/kg sol. sodium chloride, and degradation was conducted at 140 °C in the absence of oxygen. While it has been reported that the degradation of MEG is a thermally oxidative one [8; 11], the direct effect of varying oxygen content on the degradation products of MEG is investigated in this study. Thus, the second set of experiments was conducted with oxygen as the independent variable, the aim being to evaluate the influence of oxygen concentration on MEG degradation. This second set of experiments was conducted at three oxygen concentration levels – oxygen free

MEG, low-oxygen MEG and air-saturated MEG. A third and last set of experiments were conducted to evaluate the effect of salt content on degradation; for these experiments, sodium chloride and calcium carbonate were added to 14.1 mol/kg sol. MEG solutions for anaerobic (oxygen-free) degradation. Degradation products for all three sets of experiments were measured and are presented here.

5.3.1 Materials

The MEG solutions used in this study were prepared using 99.99% analytical grade MEG from Rheochem Australia, analytical grade sodium chloride and calcium carbonate from ROWE Scientific Australia and ultra-pure deionized water. The MEG solutions used in this study were prepared as per compositions presented in Table 5-1. These represent typical lean MEG compositions in an MRU [18]. For experiments with calcium carbonate, 2g of calcium carbonate was added per L of solution as per Table 5-1. The change in MEG concentration, on addition of calcium carbonate, was assumed to be negligible as the calcium carbonate made up only a 0.001 mole fraction of the solution.

Table 5-1: Composition of MEG used for degradation study

	12.5 mol/kg sol. MEG (0.5 mol/kg sol. ionic strength)	**14.1 mol/kg sol. MEG (0.5 mol/kg sol. ionic strength)**	**14.1 mol/kg sol. MEG (1 mol/kg sol. ionic strength)**
MEG (wt.%)	77.6	87.3	87.3
Deionized water (wt.%)	19.5	9.8	6.9
Sodium chloride (wt.%)	2.9	2.9	5.8

5.3.2 Experimental setup

The degradation process was the same across all samples tested; the MEG solution was prepared in the test cell, heated to 140 °C while stirring and held at 140 °C for up to four weeks. All experiments were conducted in a glass cell setup, as shown in Figure 1-3, which consisted of a 2 L glass cell on an IKA® RET Basic hot plate with thermocouples to maintain the temperature of test MEG solution between ± 1 of 140 °C. The glass cell was fitted with a glass lid, rubber gasket and clamp for an air-tight seal. The glass lid had four neck openings, one each for gas inlet into the cell, gas outlet from the cell, sample collection from the cell and temperature probe insertion into the cell. The gas inlet port was a glass tube used to introduce gas into the MEG solution, and the gas outlet port was also a condenser used to balance the pressure inside the cell. The sampling port was a glass tube connected to a short Masterflex® PTFE tube fitted with a screw compressor tubing clamp for an air-tight seal between sampling.

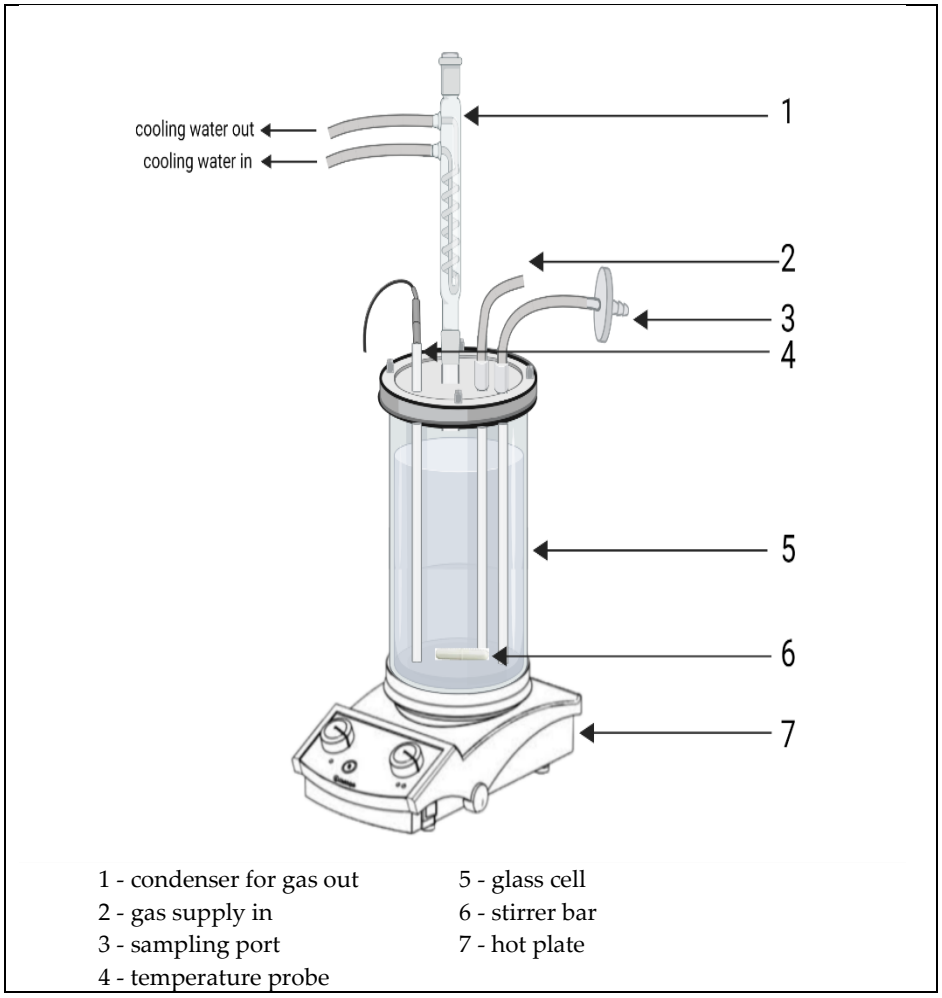

Figure 5-2: Schematic of degradation experimental setup

A primary consideration for this experiment was the control of dissolved oxygen at the start of the experiments and eliminating significant deviations in starting dissolved oxygen levels between experiments for each scenario mentioned above. To mitigate this, the test solution was initially sparged at room temperature with selected gas for at least 60 hours before the heating was started. Once the solution was heated to the desired temperature (140 °C), a gas blanket was used to maintain supply gas and a positive pressure over the solution in the heating vessel. The same gas used for sparging was used for the gas blanket during heating. This gas blanket was also necessary to minimize water loss from solution. Three gas environments were carried out: oxygen-free, low oxygen, and air-saturated tests. The oxygen-free tests were achieved

using 99.999% N_2. The low oxygen tests, which could be experienced in operations where low-quality nitrogen blanket gas is used, were achieved with 0.6% O_2 in 99.999% N_2. Lastly, the lean MEG was fully saturated with air to mimic cases where the blanketing gas is absent. The experiments that were conducted with a nitrogen blanket have been referred to as anaerobic in this thesis. While all efforts have been made to keep the experiment oxygen-free, it is acknowledged that there may be a possibility of minimal oxygen ingress. For easy reading, these experiments have been referred to as anaerobic, however it cannot be ascertained that the experiments where a zero-oxygen environment.

Another consideration in these experiments was maintaining a steady gas flow level with minimal water loss from the MEG solution. Initially, the test cell was sparged with selected gas and completely sealed off before heating commenced. However, with this approach, it was observed that degradation progressed until all the oxygen in the reactor was ultimately used up, and then degradation stopped. This method meant that the MEG–water concentration was kept constant, but degradation could not be monitored over the desired length of time. Another approach applied in this study was to use a gas blanket with minimal constant flow. The test solution did not boil at atmospheric pressure, but evaporation was significant, so a slight positive pressure was applied with a gas blanket to minimize evaporation. A similar practice of having a small pressure head is applied by Zaboon S. et al. in their design of a MEG regeneration unit and is widely applied for the regeneration and reclamation of MEG. [7] Blanket gas flow was controlled using an M-Gas Mass Flow Meter supplied by Alicat scientific, and flow was controlled at 22 SCCM to maintain a 20 psi pressure. An outlet valve from the test cell was maintained slightly open to maintain the flow rate. This approach minimized the water evaporation from the experimental solution, and the MEG–water concentration

remained constant while maintaining a constant gas supply into the vessel. The condenser gas outlet port in the test cell was also used to minimize water loss from the test solution.

5.3.3 Degradation monitoring

Samples were periodically drawn from the test cell to measure pH and degradation. Samples were collected in 25 mL vials and immediately dipped into cold water to reduce the temperature to 25 °C. pH was measured at room temperature (ca. 25 °C) with a metro GMH 5550 pH meter and 100 BNC Standard 3 molar KCL refillable glass pH electrode. The measured pH for MEG solutions varies significantly between pH electrodes [27-29], and calibration is required for every pH electrode to minimize variation and ensure accurate measurement.

The pH electrode was calibrated for MEG pH measurements according to the method proposed by Sandengen et. al.[30]. The calibration curve for the pH electrode used in this study is presented in Figure 5-3. $pH_{measured}$ is the measured pH of 0.05 M potassium hydrogen phthalate (KHPh) solutions of varying MEG concentrations, pH_{RVS} is the calculated reference value for the KHPh buffer solutions, and ΔpH_{MEG} is the correction factor for the measured value used to calculate actual pH for test MEG solutions as per (5.1) . All MEG solution pH values reported in this study are actual pH values calculated as per equation(5.1) , and ΔpH_{MEG} values used are presented in Table 5-2.

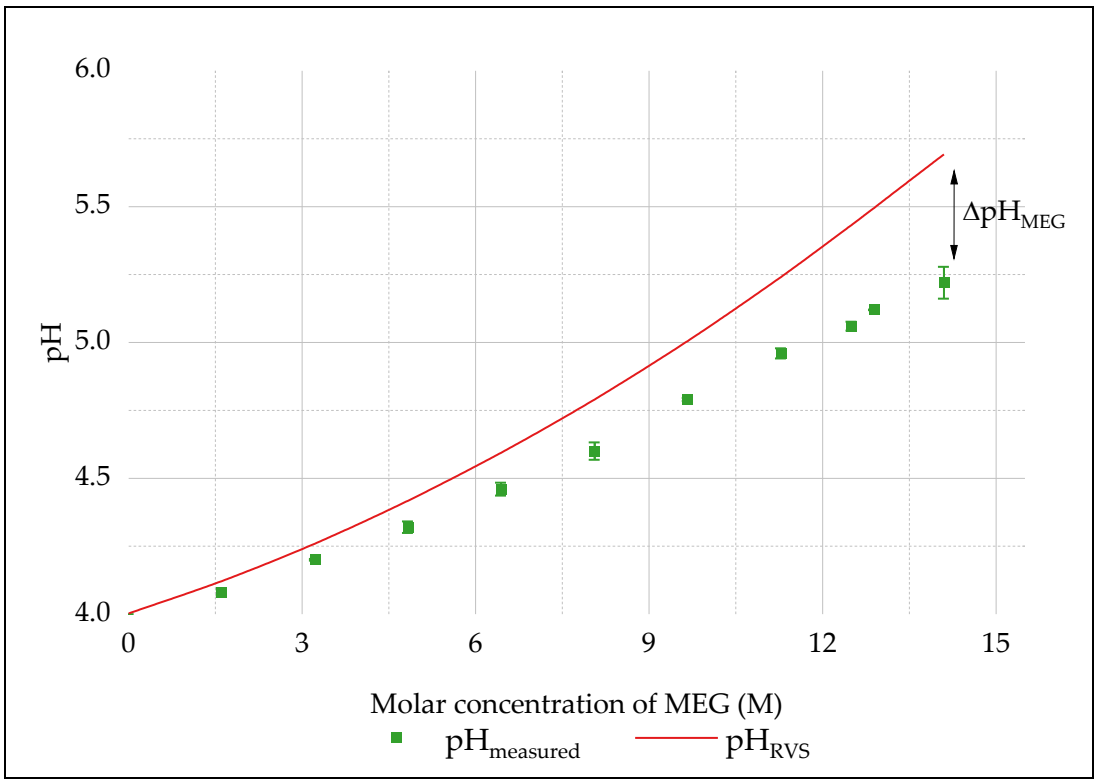

Figure 5-3: Calibration for MEG pH measurement

$$pH = pH_{measured} + \Delta pH_{MEG} \tag{4.1}$$

Table 5-2: ΔpH_{MEG} for pH electrode calibration

	12.5 mol/kg sol. MEG	14.1 mol/kg sol. MEG
ΔpH_{MEG}	0.372	0.472

Degradation products were measured by ion chromatography according to the method described in Chapter 3 "*Ion Chromatography for MEG assay and application to the MRU*". The experimental setup for degradation was repeated twice per set of conditions. pH measurement and ion chromatography analysis were conducted at least 3 times per sample. Measurements were considered reproduceable when there was no more than 10% variance between repeat measurements. Results presented in this work are an average of 3 repeats from the 2 experimental repeats. Error bars reported show the lowest and highest measurements for each test signifying the estimated error in measurement.

5.4 Results

5.4.1 Degradation and MEG concentration

Figure 5-4 and Figure 5-5 show the pH and total organic acids for anaerobic (oxygen-free) degradation of aqueous MEG solution at 140 °C; ionic strength for solutions reported here is 0.5 mol/kg sol. sodium chloride. These results show a steady accumulation of organic acid in these MEG solutions with a corresponding decline in solution pH. The rate of organic acid production of the organic acid curves in Figure 5, is 2.27×10^{-4} mM/hr for 12.5 mol/kg sol. MEG solution and 5.76×10^{-4} mM/Hr for 14.1 mol/kg sol. MEG solution. Organic acids are known to be glycol degradation products [8, 9, 32] and results in Figure 5 supports similar findings by Rossiter et al. (1985) [8] that the degradation of MEG is thermally induced and progresses even in the absence of dissolved oxygen albeit a very slow rate.

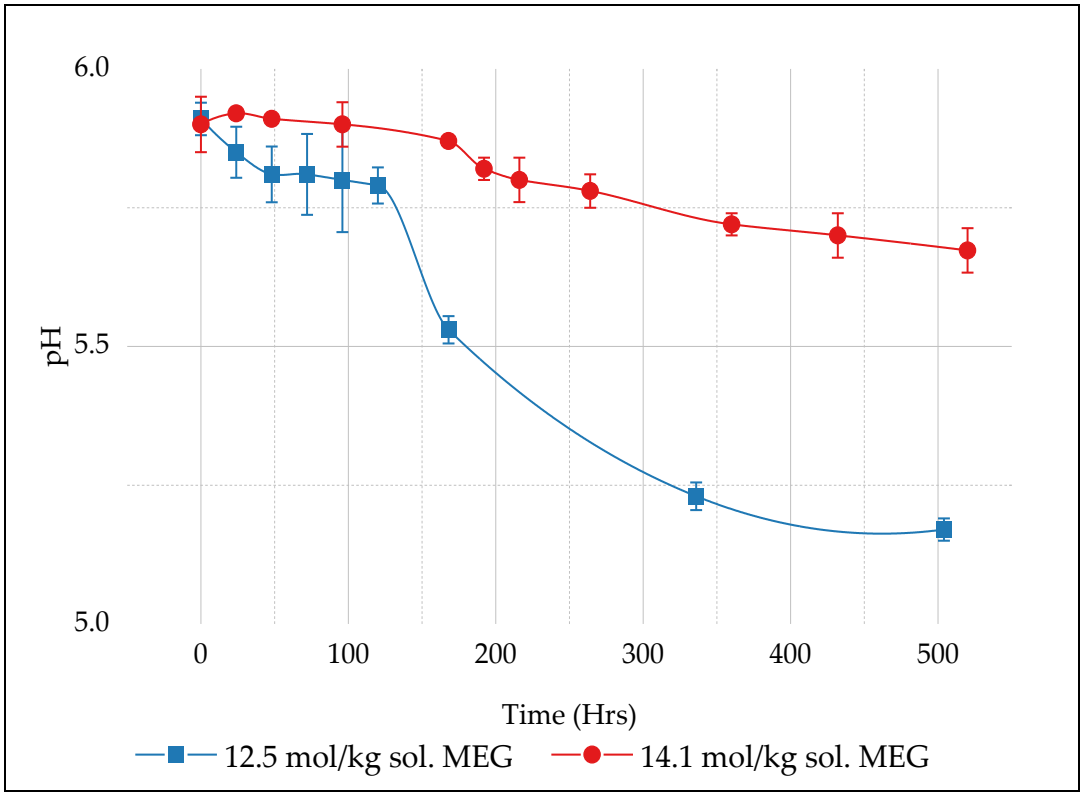

Figure 5-4: pH for anaerobic degradation of aqueous MEG solutions at 140 °C

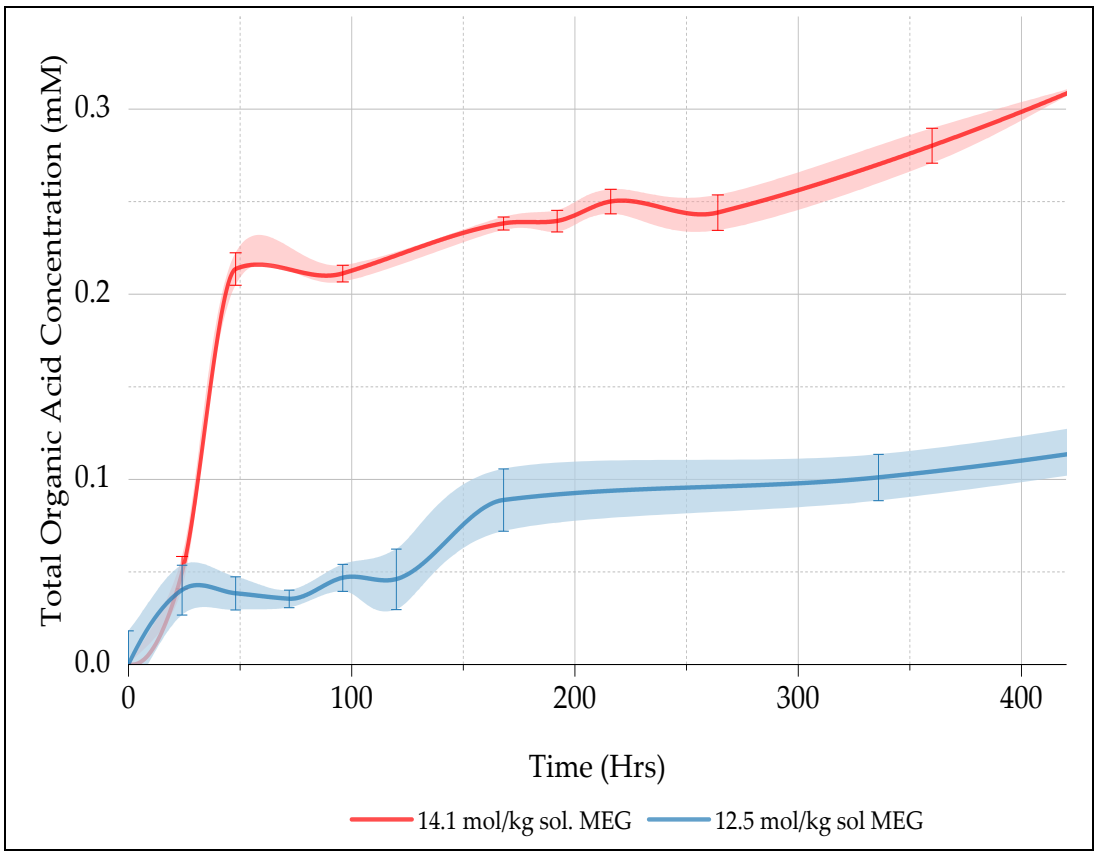

Figure 5-5: Total organic acid for anaerobic degradation of aqueous MEG solutions at 140 °C.

The pH of the degrading solution is also seen to decline at a steady state in correlation with the organic acid accumulation. However, it is observed that the rate of change in pH was higher for the less concentrated MEG solution. The acid dissociation constants (pKa) for these organic acids have been reported to increase with increasing MEG mole fraction solution [31]. pKa denotes the pH value at which a chemical species will accept or donate a proton, and pH increases with an increasing acid dissociation constant [32]. After 500 hours of anaerobic degradation, the measured pH was 5.7 (ΔpH = 0.1) for 14.1 mol/kg sol. MEG solution and 5.17 (ΔpH = 0.76) for 12.5 mol/kg sol. MEG solution.

Results from this study show glycolic and formic acids were dominant degradation products for the anaerobic degradation of MEG at 140 °C, as

shown in Figure 5-6 and Figure 5-7. Previous work described that glycolic, oxalic, and formic acids are direct oxidation products of MEG [10; 12; 33-34]. Glycolic and oxalic acid are the two most commonly reported degradation products of MEG at temperatures lower than the 140 °C investigated in this study [10; 33]. Figure 5-6 and Figure 5-7 show that any oxalic acid produced during the degradation of MEG in solution is quickly decomposed to formic acid at the test temperature. This finding is in line with existing literature which reports that oxalic acid thermally decomposes to formic acid at temperatures above 120 °C [35-36]. Acetic acid was also identified as a degradation product in the anaerobic degradation of the more concentrated 14.1 mol/kg sol. aqueous MEG solution. This result suggests the possibility of a pinacol-type rearrangement of MEG to acetaldehyde by dehydration and subsequent oxidation of the acetaldehyde to acetic acid. Similar reaction products have been reported for 10 wt.% MEG solutions over a metal catalyst [37].

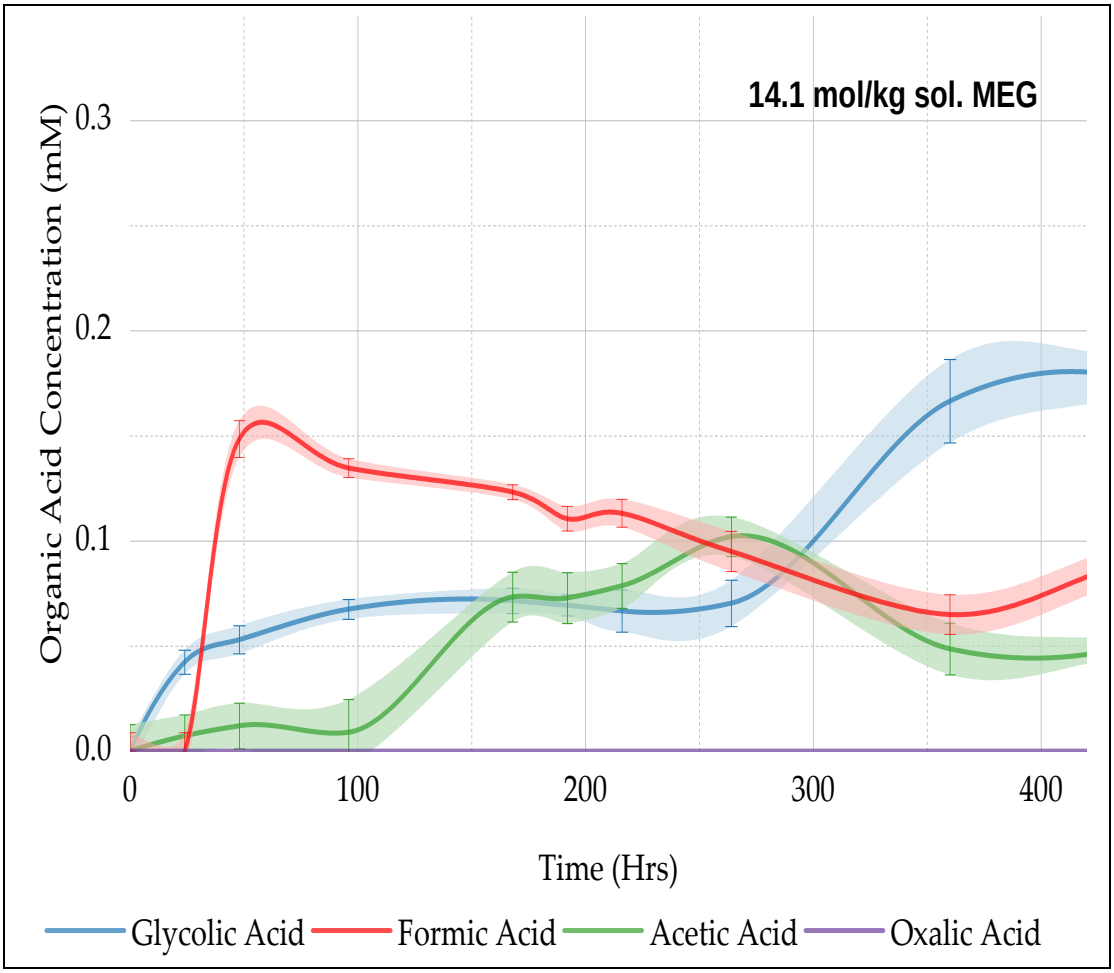

Figure 5-6: Organic acid distribution for anaerobic degradation of 14.1 mol/kg sol. MEG at 140 °C

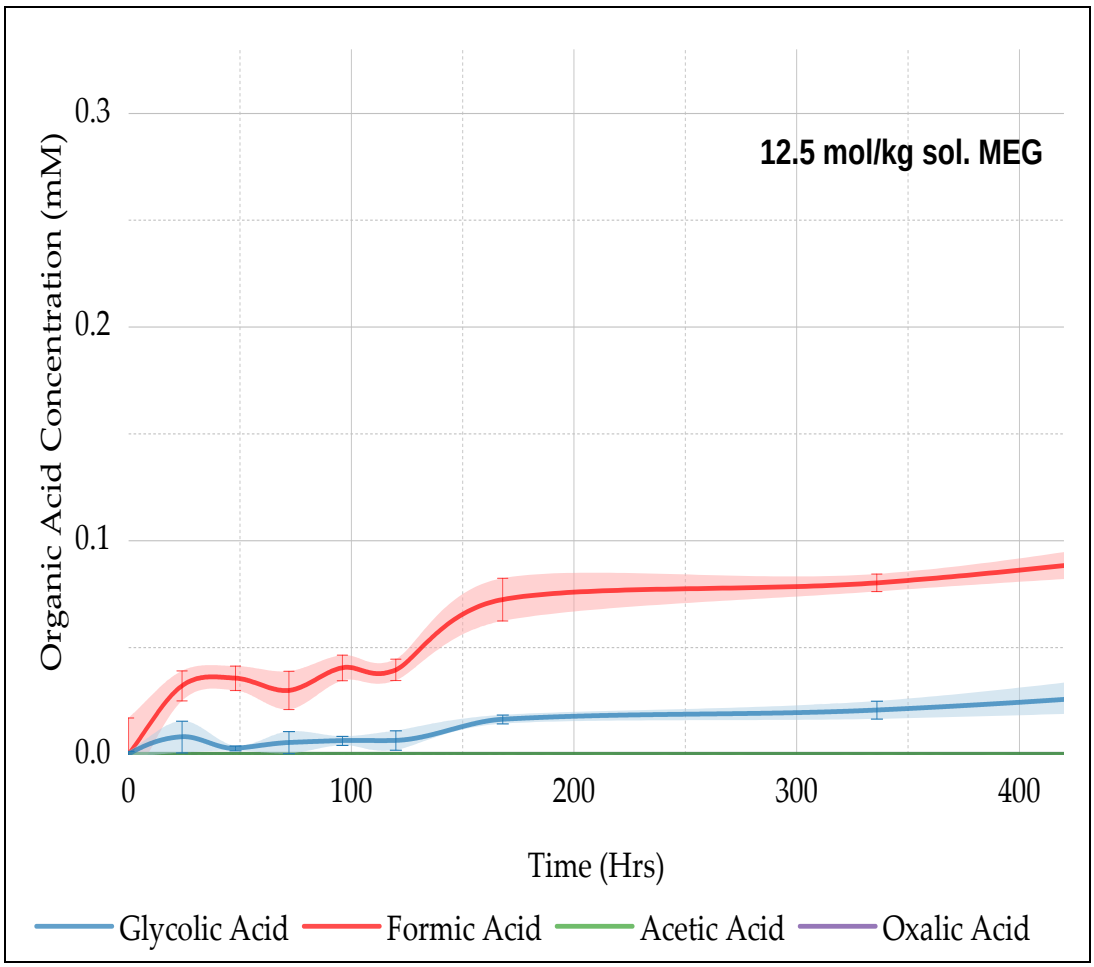

Figure 5-7: Organic acid distribution for anaerobic degradation of 12.5 mol/kg sol. MEG at 140 °C

5.4.2 Degradation and Oxygen level

The stoichiometric ratio for the degradation of MEG is 1 for glycolic, oxalic and acetic acid and 2 for formic acid, as shown in equations (5.2) - (5.5). Since the final stable degradation products of MEG are these organic acids, then the rate of degradation of MEG can be estimated using equation(5.6). Where $[CH_2OHCOOH]$, $[(COOH)_2]$, $[CH_3COOH]$ and $[COOH]$ are the molar concentrations of glycolic, Oxalic, acetic acid and formic respectively.

$$(CH_2OH)_2 + O_2 \rightleftharpoons CH_2OHCOOH + H_2O \quad (4.2)$$

$$(CH_2OH)_2 + 2O_2 \rightleftharpoons (COOH)_2 + 2H_2O \quad (4.3)$$

$$(CH_2OH)_2 + \frac{1}{2}O_2 \rightleftarrows CH_3COOH + H_2O \quad (4.4)$$

$$(CH_2OH)_2 + O_2 \rightleftarrows 2COOH + 2H_2 \quad (4.5)$$

$$\Delta[(CH_2OH)_2] = \Delta[CH_2OHCOOH] + \Delta[(COOH)_2] + \frac{\Delta[COOH]}{2} + \Delta[CH_3COOH] \quad (4.6)$$

Based on calculations from equation(4.6), the rate at which MEG degraded increased 6-fold with the increase of MEG concentration from 12.5 mol/kg sol. to 14.1 mol/kg sol. The increase in oxygen content in the aqueous MEG solutions had a more significant effect on the degradation rate. When the sparging gas changed from oxygen-free nitrogen to 0.6% oxygen in nitrogen, the rate of degradation in 14.1 mol/kg sol. MEG solution increased 27-fold according to equation (5.6). Whilst the rate of degradation was 131 times more in the air-saturated aqueous solution of 14.1 mol/kg sol. MEG compared to anaerobic degradation in the same solution. These results are presented with the total organic acid content of thermally degraded MEG solution shown in Figure 5-8. The ionic strength for solutions reported here is 0.5 mol/kg sol. sodium chloride. The increase in rate of MEG degradation between 12.5 mol/kg sol. and 14.1 mol/kg sol. MEG solutions remained the same even in air-saturated solutions. 14.1 mol/kg sol. air-saturated MEG solution degraded 6 times faster than air saturated 12.5 mol/kg sol. solution; this same difference was seen in anaerobically degraded solutions. The total organic acid content in air-saturated solutions of 14.1 mol/kg sol. and 12.5 mol/kg sol. MEG are presented in Figure 5-9.

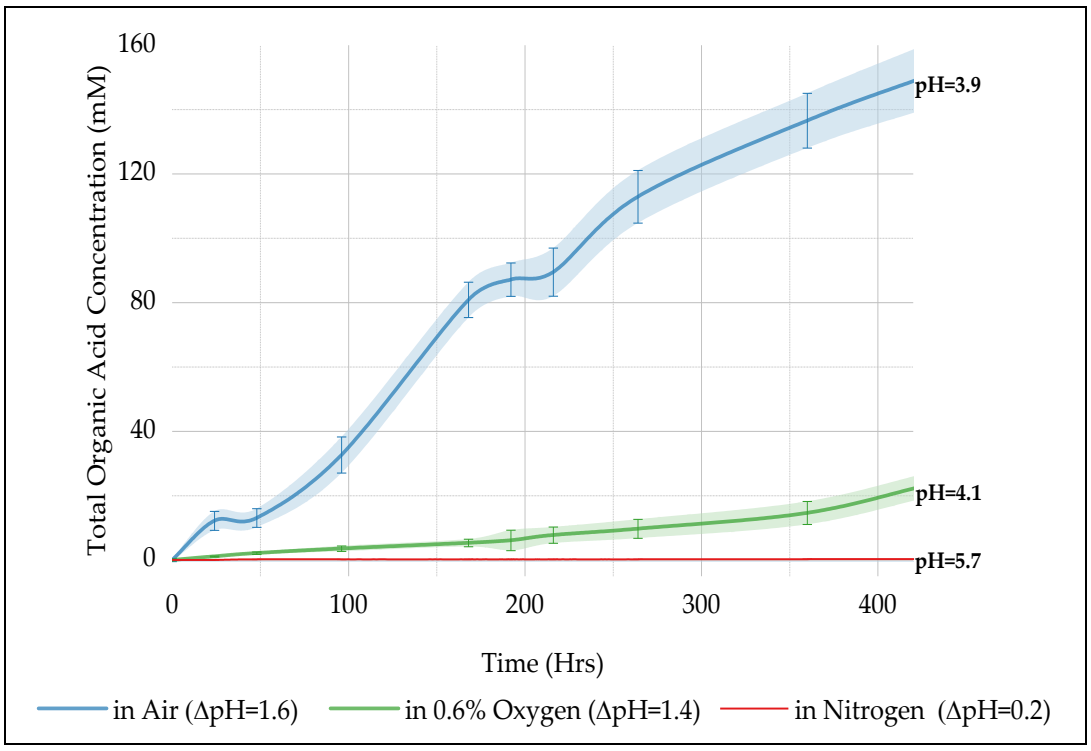

Figure 5-8: degradation in 14.1 mol/kg sol. aqueous MEG solution at varying oxygen content

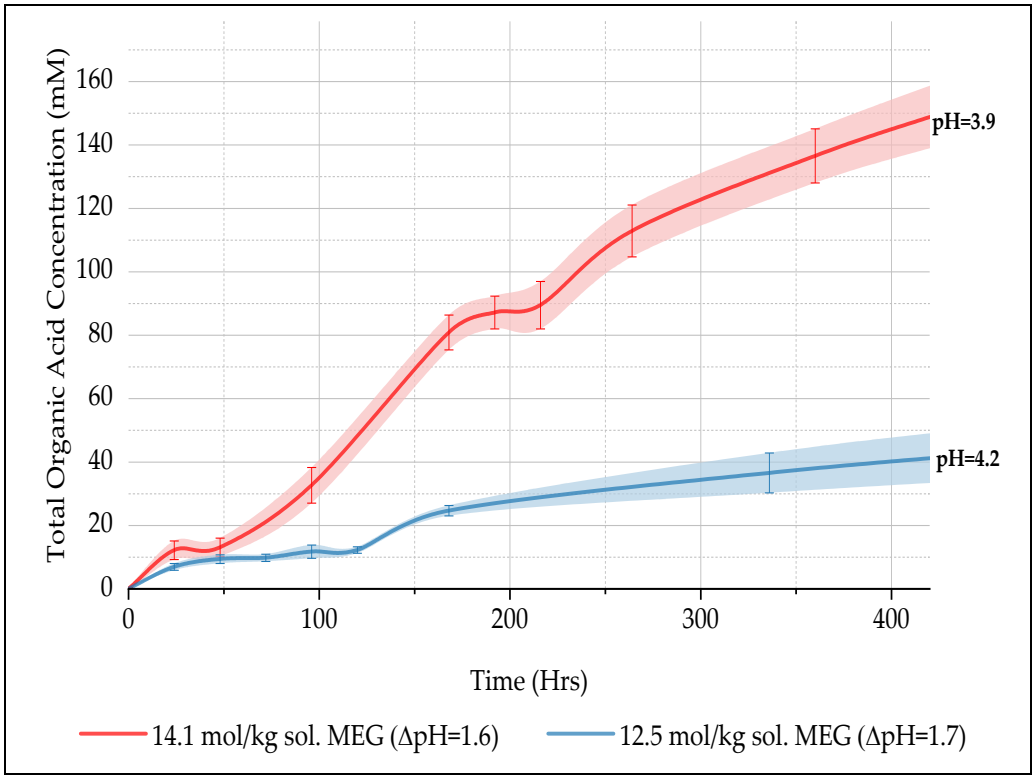

Figure 5-9: Total organic acid content in degraded air-saturated MEG solutions

Whilst acetic acid was measured during anaerobic degradation, it was not detected in aerobic thermally degraded solution, as shown in Figure 10. The distribution of organic concentration was slightly different in the aerobic thermally degraded solution compared to the anaerobic thermal degradation. The primary organic acids produced during the aerobic thermal oxidation of 14.1 mol/kg sol. aqueous MEG solution at 140 °C are glycolic and formic, as shown in Figure 5-10.

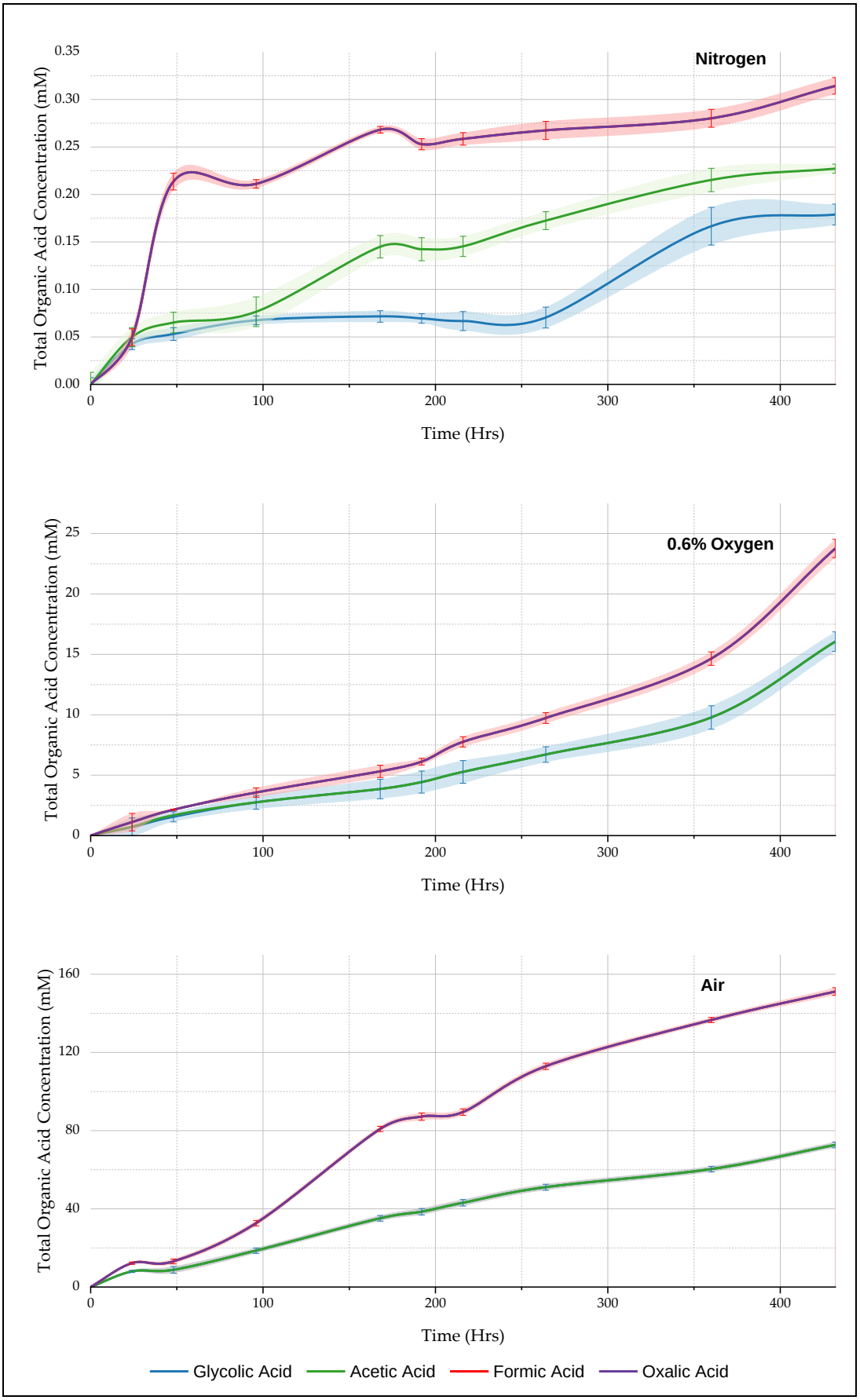

Figure 5-10: organic acid distribution for thermal degradation of 14.1 mol/kg sol. MEG at varying oxygen content. Note: oxalic acid content is negligible

5.4.3 Degradation and salt content

The organic acid distribution after 48 hours of thermal degradation of MEG with varying salt content is presented in Figure 5-11. The results show that the addition of calcium carbonate ($CaCO_3$) influenced the amount and type of organic acid produced. In experiments where calcium carbonate was added to the MEG solution, degradation of the MEG solution was significantly faster. The total organic acid concentration produced was 30 times more than in experiments without calcium carbonate. Moreover, acetic acid was the primary organic acid produced with calcium carbonate in the solution, as presented in Figure 5-11. For these experiments, 2 g (0.02 M) $CaCO_3$ was added per litre of MEG solution. While the solubility of calcium carbonate in MEG at 140 °C is much lower than 0.02 M[23], all of the added calcium carbonate was dissolved in the solution after the 48 hours test time leading to a corresponding increase in ionic strength of the solution. More work is required to determine the causative effect of calcium carbonate; it is unclear at this point if it is the calcium ion causing the increase in degradation or the carbonate ion, as the exact mechanism of the reaction remains unknown. However, various metal ions have been used to catalyse the degradation of MEG to selective products. For instance, the pinacol-type dehydration of MEG to acetaldehyde is a well-known reaction [13-15], suggesting that the calcium ion in the solution could act as a catalyst to increase the degradation of MEG into acetic acid.

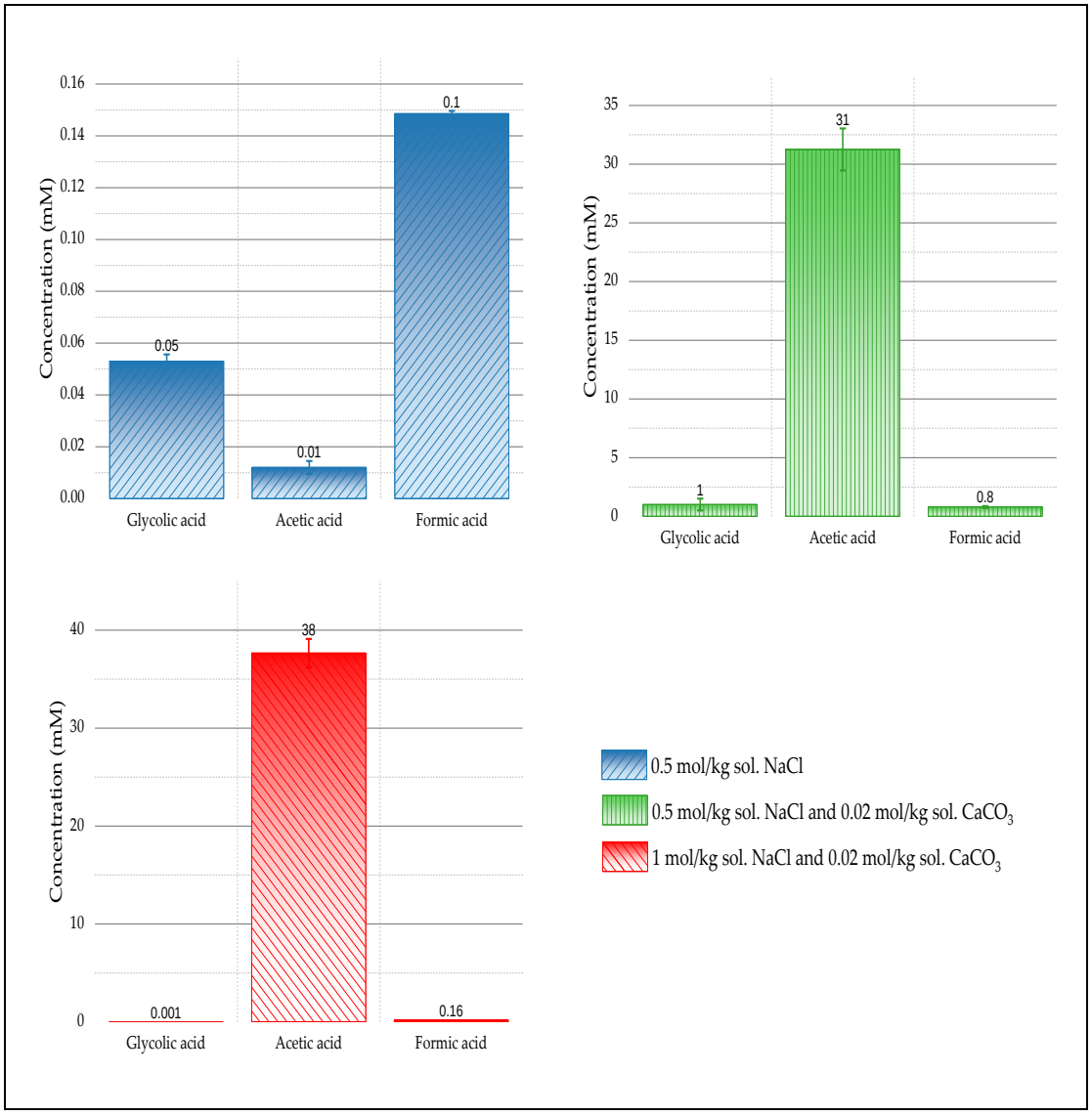

Figure 5-11: Organic acid distribution for degradation of 14.1 mol/kg sol. MEG in the presence of salts and 0.6% oxygen.

5.4.4 Further Discussion

The pH trend for the degradation of MEG at the two concentrations tested followed the expected trends. It was observed that there was a gradual decline in pH corresponding to the production of organic acids. The distribution of organic acid products of degradation was rather interesting. Glycolic and oxalic acid are commonly reported as thermal oxidative degradation products of MEG [10; 12; 33-34]. However, the studies where oxalic acid is reported were conducted at temperatures lower than current study, i.e., 140 °C. This work

shows that at 140 °C, formic and glycolic acids are the primary organic acids produced from the oxidative thermal degradation of MEG. A summary of possible routes for the production of these organic acids is presented in Figure 5-12. From this summary, it can be seen that oxalic acid is further decomposed to formic acid, which was reported to be initiated at 120 °C [35-36].

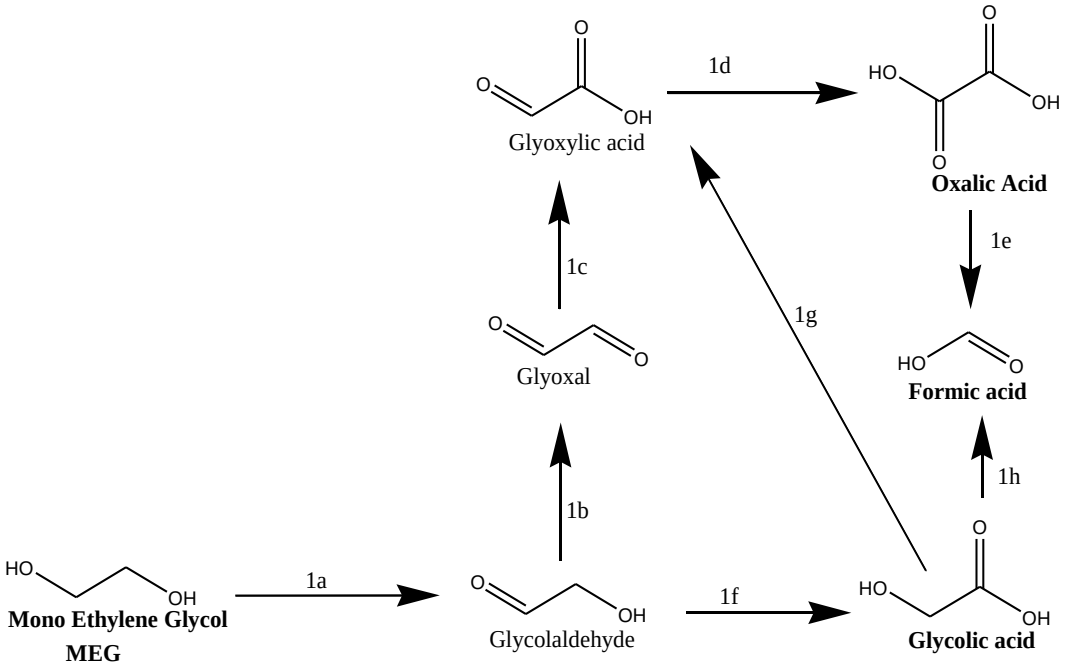

(1a) Oxidation of MEG to glycolaldehyde [38]
(1b) Oxidation of glycolaldehyde to glyoxal [38]
(1c) Oxidation of Glyoxal to Glyoxylic acid [38]
(1d) Oxidation of Glyoxylic acid to Oxalic Acid [38]
(1e) Decomposition of oxalic acid to formic acid [36]
(1f) Oxidation of glycolaldehyde to glycolic acid [38]
(1g) Oxidation of Glycolic acid to glyoxylic acid [38]
(1h) Oxidation of glycolaldehyde to formic acid [38]

Figure 5-12: Summary of MEG possible oxidation mechanism.

Acetic acid was produced when the MEG concentration increased in the oxygen-free environment. Increasing the concentration of MEG was seen to not only increase the rate of MEG degradation; but increasing in MEG concentration also changed the organic acid distribution for the anaerobic thermal degradation of MEG. It is suggested that acetic acid production during this anaerobic degradation is initiated by the pinacol-type dehydration of MEG, as presented in Figure 5-13. Results from this work suggest that this reaction

route presented in Figure 5-13 is plausible for anaerobic thermal degradation but not favoured for thermal degradation in the presence of oxygen.

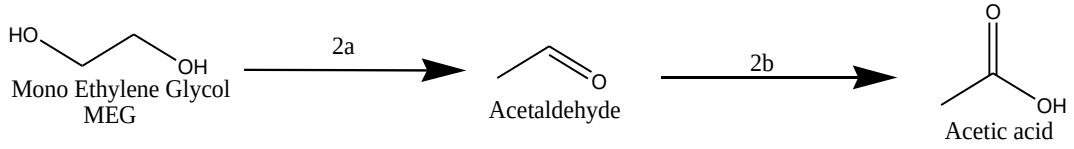

(2a) Pinacol-type dehydration of MEG [39-40]
(2b) Oxidation of Acetaldehyde to Acetic acid [38]

Figure 5-13: A suggested mechanism for the production of acetic acid from anaerobic thermal degradation of MEG.

5.5 Conclusion

This study investigated and reported the thermal oxidative degradation of MEG at 140 °C. The pH of the degrading solution is seen to decline at a steady state in correlation with the organic acid accumulation. However, it is observed that the rate of change in pH was higher for the less concentrated MEG solution, concurrent with the increase in acid dissociation constants (pKa) for these organic acids with increasing MEG mole fraction solution reported by Soammes et. al (2008) [31]. At the test temperature of 140 °C, very little oxalic was observed, glycolic acid and formic acid being the two primary organic acids produced during the degradation of MEG. The anaerobic degradation of MEG was seen to favour acetic acid production at the test temperature, especially with the more concentrated MEG solution and the presence of calcium salt.

Short chain organic acids are known content of formation water from oil and gas reservoirs; acetic and propionic acids being the most commonly reported organic acids [41-42]. Without clearly mapping the organic acid products for MEG degradation during regeneration, it is easy to misconstrue the accumulation of acetic acid for MEG degradation. While results reported in this

show that acetic acid are produced during anaerobic MEG degradation, there is also clear indication that accumulation of glycolate and/or formate ions are better indications of degradation of MEG. Both glycolic and formic acids are not major constituents of reservoir formation waters. On the other hand, for production where reservoir organic acid can be ruled out, accumulation of acetate ions in the MRU may be a sign of degradation as a result of accumulated calcium ion or oxygen ingress into the MRU. While literature reports oxalic acid as a degradation product of MEG, this works show that oxalic acid is not a reliable indicator for MEG degradation in the MRU due its high temperature decomposition to formic acid.

References

1. Wilcox, W. I., Carson, D., & Katz, D. (1941). Natural gas hydrates. *Industrial & Engineering Chemistry, 33*(5), 662-665.
2. Creek, J. (2012). Efficient hydrate plug prevention. *Energy & Fuels, 26*(7), 4112-4116.
3. Hammerschmidt, E. (1934). Formation of gas hydrates in natural gas transmission lines. *Industrial & Engineering Chemistry, 26*(8), 851-855.
4. Dobson, S. (2000). *Ethylene glycol: environmental aspects* (IPCS - 2000-22). Retrieved from Geneve Switzerland:
5. Kim, H., Yoo, W., Lim, Y., & Seo, Y. (2018). Economic evaluation of MEG injection and regeneration process for oil FPSO. *Journal of Petroleum Science and Engineering, 164*, 417-426. doi:https://doi.org/10.1016/j.petrol.2018.01.071
6. Brustad, S., Løken, K.-P., & Waalmann, J. G. (2005). *Hydrate Prevention using MEG instead of MeOH: Impact of experience from major Norwegian developments on technology selection for injection and recovery of MEG.* Paper presented at the Offshore technology conference.
7. Zaboon, S., Soames, A., Ghodkay, V., Gubner, R., & Barifcani, A. (2017). Recovery of mono-ethylene glycol by distillation and the impact of dissolved salts evaluated through simulation of field data. *Journal of Natural Gas Science and Engineering, 44*, 214-232. doi:https://doi.org/10.1016/j.jngse.2017.04.007
8. Rossiter, W. J., Godette, M., Brown, P. W., & Galuk, K. G. (1985). An investigation of the degradation of aqueous ethylene glycol and propylene glycol solutions using ion chromatography. *Solar Energy Materials, 11*(5), 455-467. doi:https://doi.org/10.1016/0165-1633(85)90016-4
9. Rossiter Jr, W. J., Brown, P. W., & Godette, M. (1983). The determination of acidic degradation products in aqueous ethylene glycol and propylene glycol solutions using ion chromatography. *Solar Energy Materials, 9*(3), 267-279.
10. Badi, D., Al Helal, A., Lagat, C., Phan, C., & Barifcani, A. (2021). Evaluation of reboiler temperature retention time on MEG degradation products at varying MEG concentrations. *Journal of Petroleum Science and Engineering, 196*, 107735. doi:https://doi.org/10.1016/j.petrol.2020.107735
11. Monteiro, M. F., Moura-Neto, M. H., Macedo, G. M., Silva, G. V., Silva, D. J., Pereira, L. S., et al. (2019). Thermal Degradation of Monoethylene Glycol in Aqueous Saline Solution: Evaluation by Thermogravimetric and Physicochemical Analyses. *Industrial & Engineering Chemistry Research, 58*(27), 12159-12165. doi:10.1021/acs.iecr.9b01914

12. Psarrou, M. N., Jøsang, L. O., Sandengen, K., & Østvold, T. (2011). Carbon dioxide solubility and monoethylene glycol (MEG) degradation at MEG reclaiming/regeneration conditions. *Journal of Chemical & Engineering Data, 56*(12), 4720-4724.
13. Yue, H., Zhao, Y., Ma, X., & Gong, J. (2012). Ethylene glycol: properties, synthesis, and applications. *Chemical Society Reviews, 41*(11), 4218-4244.
14. McGinnis, B. D., Adams, V. D., & Middlebrooks, E. J. (2001). Degradation of ethylene glycol using Fenton's reagent and UV. *Chemosphere, 45*(1), 101-108.
15. McGinnis, B. D., Adams, V. D., & Middlebrooks, E. J. (2000). Degradation of ethylene glycol in photo Fenton systems. *Water Research, 34*(8), 2346-2354.
16. Rossiter, W. J., Brown, P. W., & Godette, M. (1983). The determination of acidic degradation products in aqueous ethylene glycol and propylene glycol solutions using ion chromatography. *Solar Energy Materials, 9*(3), 267-279. doi:Doi 10.1016/0165-1633(83)90049-7
17. Madera, M., Höflinger, W., & Kadnar, R. (2003). Ion chromatographic identification and quantification of glycol degradation products. *Journal of Chromatography A, 997*(1), 279-284. doi:https://doi.org/10.1016/S0021-9673(03)00060-8
18. Zaboon, S. M. Z. (2019). *Monoethylene Glycol Distillation System Design Validation, Operation and Effluent Treatment.* Curtin University,
19. MEG Regeneration Technical Meeting. (2009). In. Port Campbell, Australia: Society of Petroleum Engineers.
20. Chong, K., Lai, S., Thiam, H., Teoh, H., & Heng, S. (2016). Recent progress of oxygen/nitrogen separation using membrane technology. *J. Eng. Sci. Technol, 11*(7), 1016-1030.
21. Baraka-Lokmane, S., Hurtevent, C., Seiersten, M., Flaten, E., Farrell, M., Bradshaw, O., et al. (2013). Technical challenges and solutions in a closed loop MEG regeneration system for gas field offshore, UK. *WIT Transactions on Engineering Sciences, 79*, 511-522. doi:10.2495/mpf130421
22. Odeigah, E. A., & Pojtanabuntoeng, T. (2022). Regeneration and Reclamation of Mono-Ethylene Glycol (MEG) Used as a Hydrate Inhibitor: A Review. *American Journal of Chemical Engineering, 10*(2), 32-45.
23. Odeigah, E. A., Pojtanabuntoeng, T., Jones, F., & Gubner, R. (2018). The Effect of Monoethylene Glycol on Calcium Carbonate Solubility at High Temperatures. *Industrial & Engineering Chemistry Research, 57*(46), 15909-15915.
24. Natsi, P. D., Rokidi, S. G., & Koutsoukos, P. G. (2019). *Calcium Carbonate Scale Formation in Water- Mono Ethylene Glycol (MEG)*. Paper presented at the CORROSION 2019, Nashville, Tennessee, USA. https://doi.org/

25. Flaten, E. M., Seiersten, M., & Andreassen, J.-P. (2010). Induction time studies of calcium carbonate in ethylene glycol and water. *Chemical Engineering Research and Design, 88*(12), 1659-1668. doi:http://dx.doi.org/10.1016/j.cherd.2010.01.028
26. Hyllestad, K. (2013). Scaling of Calcium Carbonate on a Heated Surface in a Flow Through System with Mono Ethylene Glycol.
27. Mussini, P., Mussini, T., & Rondinini, S. (1991). Thermodynamics of hydrochloric acid and recommendations for the standard emf. of the cell hydrogen/silver chloride in ethylene glycol/water mixtures from-40 to+ 50° C.
28. Mussini, P., Marcolungo, I., Rondinini, S., & Longhi, P. (1991). Acid-base equilibria and acidity scales in ethylene glycol/water solvent mixtures: recommended reference-value pH-metric standards and ionization constants for o-phthalic acid at normal and subzero temperatures. *Chimica e l'Industria (Milan);(Italy), 73*(4).
29. Buck, R., Rondinini, S., Covington, A., Baucke, F., Brett, C. M., Camoes, M., et al. (2002). Measurement of pH. Definition, standards, and procedures (IUPAC Recommendations 2002). *Pure and applied chemistry, 74*(11), 2169-2200.
30. Sandengen, K., Kaasa, B., & Østvold, T. (2007). pH Measurements in Monoethylene Glycol (MEG) + Water Solutions. *Industrial & Engineering Chemistry Research, 46*(14), 4734-4739. doi:10.1021/ie061305a
31. Soames, A., Iglauer, S., Barifcani, A., & Gubner, R. (2018). Acid Dissociation Constant (pKa) of Common Monoethylene Glycol (MEG) Regeneration Organic Acids and Methyldiethanolamine at Varying MEG Concentration, Temperature, and Ionic Strength. *Journal of Chemical & Engineering Data, 63*(8), 2904-2913. doi:10.1021/acs.jced.8b00221
32. Roberts, J. D., & C, C. M. (1977). *BASIC PRINCIPLES OF ORGANIC CHEMISTRY* (Second ed.). Menlo Park, CA: W.A. Benjamin, Inc.
33. François, M. (2020). *Stability of dehydration glycols MEG and TEG.* NTNU,
34. Monteiro, M., Moura-Neto, M., Macedo, G., Silva, G., Silva, D., Pereira, L., et al. (2019). Thermal Degradation of Monoethylene Glycol in Aqueous Saline Solution: Evaluation by Thermogravimetric and Physicochemical Analyses. *Industrial & Engineering Chemistry Research, 58*(27), 12159-12165.
35. Crossey, L. J. (1991). Thermal degradation of aqueous oxalate species. *Geochimica et Cosmochimica Acta, 55*(6), 1515-1527. doi:https://doi.org/10.1016/0016-7037(91)90124-N
36. Dinglinger, A., & Schröer, E. (1937). The kinetics of thermal oxalic acid decomposition in solution. *Zeitschrift für Physikalische Chemie, 179A*(1), 401-426. doi:doi:10.1515/zpch-1937-17936

37. Shabaker, J. W., Huber, G. W., Davda, R. R., Cortright, R. D., & Dumesic, J. A. (2003). Aqueous-Phase Reforming of Ethylene Glycol Over Supported Platinum Catalysts. *Catalysis Letters, 88*(1), 1-8. doi:10.1023/A:1023538917186
38. Evans, W. L., & Adkins, H. (1919). THE OXIDATION OF ORGANIC COMPOUNDS WITH ALKALINE POTASSIUM PERMANGANATE. Part I.—The Oxidation of Acetaldehyde. Part II.—The Oxidation of Glycol, Glycollic Aldehyde, Glyoxal, Glycollic Acid and Glyoxalic Acid. *Journal of the American Chemical Society, 41*(9), 1385-1414.
39. Smith, W. B. (2002). Ethylene glycol to acetaldehyde-dehydration or a concerted mechanism. *Tetrahedron, 58*(11), 2091-2094.
40. Smith, W. B. (1999). Hydrogen as a migrating group in some pinacol rearrangements: a DFT study. *Journal of physical organic chemistry, 12*(10), 741-746.
41. Barth, T. (1991). Organic acids and inorganic ions in waters from petroleum reservoirs, Norwegian continental shelf: a multivariate statistical analysis and comparison with American reservoir formation waters. *Applied Geochemistry, 6*(1), 1-15.
42. Barth, T., Borgund, A. E., & Riis, M. (1990). Organic acids in reservoir waters—relationship with inorganic ion composition and interactions with oil and rock. *Organic Geochemistry, 16*(1-3), 489-496.

Chapter 6

CO_2 corrosion of carbon steel in thermally degraded Monoethylene Glycol

6.1 Abstract

The conditions for the recovery of monoethylene glycol (MEG) in the MEG recovery unit (MRU) are ambient to vacuum pressures and ambient to about 150 °C. As described in earlier chapters of this thesis, a consequence of these high temperatures is the thermal degradation of MEG, which produces organic acids. In this work, the corrosive behaviour of thermally degraded MEG under MRU conditions is studied, and the effects of produced organic acids on the CO_2 corrosion of carbon steel are explored. Electrochemical tests and corrosion analysis were conducted on carbon steel coupons in 3 wt.% NaCl 12.5M MEG solution, thermally degraded aerobically (in air-saturated conditions) and anaerobically (in oxygen-free conditions) at 140 °C. Electrochemical tests were conducted at 60 °C and 80 °C. The results from this study show that carbon steel corrosion in degraded MEG is higher than fresh MEG (before degradation) but significantly lower than corrosion in fresh MEG with added

equivalent organic acid eluding to the possible corrosion-inhibiting effect resulting from the thermal degradation of MEG.

Keywords: Monoethylene glycol, MEG regeneration Unit, CO_2 corrosion, organic acids, carbon steel

6.2 Introduction

As with any engineering operation, maintaining materials integrity is vital to oil and gas operations. Failure to maintain material integrity could result in substantial financial, environmental and safety consequences from spills and loss of production. These risks are even higher with deep-water production, where significant harm to the marine environment and repair could be considerably costly [1-2]. Accordingly, corrosion, a significant factor for the integrity of metals, must be controlled within design requirements for the pipelines and processing equipment wall metals. Construction materials must also be carefully selected to withstand operating conditions and requirements while balancing associated costs. Corrosion-resistant alloys (CRA) can offer better corrosion resistance but they can also be considerably more expensive [3-4]. Even though carbon steel is more susceptible to general corrosion, it is an economical construction material relative to corrosion-resistant alloys [4, 6]. Consequently, carbon steel is widely used in the oil and gas industry and operation [4], necessitating ongoing corrosion management.

For operations with MEG as a hydrate control, the aqueous phase downstream of the wellhead is a mixture of MEG, condensed or produced water, dissolved gases and other chemical treatment additives. This aqueous phase is carried through production pipelines and processing vessels, influencing the corrosive

behaviour and integrity of construction wall metals in its path. Oil and gas operations are predominantly oxygen-free and carbon dioxide (CO_2) rich; as a result, CO_2 corrosion of construction wall materials is prevalent compared to oxygen corrosion in such environments [5]. The influence of MEG on the CO_2 corrosion of carbon steel in oil and gas production is well researched [6-16], and it is established that MEG reduces corrosion rates, albeit this reduction cannot be relied upon as the primary corrosion mitigation method [8].

As MEG is reused, the aqueous phase is processed in the MRU to recover MEG for re-injection into the pipeline. The recovery of MEG in the MRU involves a series of steps at varying temperatures and pressure. For most MRU designs, pre-treatment of MEG to remove entrained hydrocarbon, suspended solids, and low solubility salts are typically done at ambient pressure and temperatures of about 40 °C - 60 °C [17]. In contrast, desalting and dewatering of MEG are conducted at ambient to vacuum pressures and temperatures as high as 150 °C[18]. A technical challenge for the recovery of MEG at these high temperatures is the degradation of MEG into organic acids. While the recycling of MEG is a cost-effective measure for MEG hydrate prevention operation, degradation of MEG during recycling alters its chemical properties [19-20] and corrosivity. This work explores the changes in the corrosivity of MEG upon degradation during recycling.

While research into MEG degradation products and CO_2 corrosion of carbon steel is not new [7; 9-12; 21], there are still significant gaps in this area, one of which this work targets. Organic acids have been reported as the degradation products of MEG, and existing studies on the effects of these degradation products on the corrosivity of MEG have only looked at fresh MEG with the addition of one of the expected organic acids from the degradation of MEG. Amongst their other results, Ikeh et al. (2016) reported the corrosivity of MEG with added acetic acid [9]. Similarly, Mendez et al. (2005) reported on the effects

of acetic acid and MEG on CO_2 top-of-the-line corrosion [11]. Santambrogio et al. (2016) report great work on the influence of oxalic, glycolic, acetic, and formic acids on the corrosivity of MEG [21]. However, these studies have focused on added organic acids, primarily from reservoir-produced water content, not degraded MEG nor organic acids produced from the degradation of MEG.

Among volatile fatty acids, the influences of acetic acid on carbon steel corrosion was widely studied for oil and gas operations, rightly because it is the most abundant organic acid content of reservoir-produced water. Acetic acid concentrations could vary from 0 ppm - 17 ppm (0.28 mM) [22] and 300 pm (5 mM) [23] in reservoir-produced water. Formic acid and propionic acids are also reported in reservoir-produced waters but to lower extents, up to 4 ppm (0.07mM) and 10 pm (0.13 mM), respectively [22]. However, Chapter 5 of this thesis shows that organic acid content in thermally degraded MEG varies in combination and composition and could accumulate beyond 120 mM depending on the time and oxygen content during degradation. Glycolic acid is one of the main products of MEG's thermal degradation, which is rarely found in reservoir-produced waters [22]. Soames et al. (2019) studied the corrosivity of degraded MEG samples [10]. While their work reports significant knowledge of the corrosion rates of degraded MEG with and without added corrosion inhibitors, they did not report the composition of the organic acids in the degraded MEG or the effects of these organic acids on corrosion.

Thus, it can be established that the effects of organic acids from thermally degraded MEG on metal corrosion is not well understood. In this study, MEG was thermally degraded at 140 °C for 21 days, and corrosion measurements were conducted for comparison with fresh MEG with similar organic acid contents. The rotating cylinder electrode (RCE) was used for corrosion measurements so that shear stress could be varied to investigate changes in

corrosion rate with flow pattern. Liquid flowing over a surface creates a shear proportional to its flow velocity. By varying the speed of the corroding sample on the RCE, the shear on the sample can correspond to the shear resulting from different flow regimes – laminar or turbulent [24]. Tests were conducted on low shear, characteristic of laminar flow and high shear, characteristic of turbulent flow. Understanding carbon steel's corrosive behaviour in degraded MEG will provide insight into corrosion protection measures that can be employed to achieve desired minimal corrosion rates, making carbon steel a more cost-effective construction material choice without necessarily expending the significant capital costs associated with plant construction using corrosion-resistant alloys.

6.2.1 Electrochemical techniques for Corrosion measurements

This study employed linear polarisation (LP), Tafel polarisation and electrochemical impedance spectroscopy (EIS) to study the influence of degraded MEG on carbon steel corrosion. The LP is a rapid and non-destructive electrochemical technique whereby the corrosion rate of a metal in an electrolyte is calculated by measuring the current flowing through the metal relative to an applied potential (or polarisation).

Corrosion involves two sets of simultaneous and complementary reactions - the anodic and cathodic reactions. For carbon steel corrosion in a weak acid solution, the anodic reaction is expressed as equation (6.1) while the cathodic reaction is expressed as equation (6.2); in this case, the weak acid is the source for the hydrogen ion (H^+) [25].

$$Fe \rightarrow Fe^{2+} + 2e^- \tag{6.1}$$

$$H^+ + e^- \rightarrow \frac{1}{2} H_2 \tag{6.2}$$

The anodic reaction creates a surplus of electrons at the corroding metal surface. This surplus of electrons flows to the cathodic reaction sites where the cathodic reactant consumes the electrons. This flow of electrons generates an anodic current, I_a and a corresponding cathodic current, I_c, at the anodic and cathodic sites, respectively.

At corrosion potential (E_{corr}), I_a equals I_c and both equal the corrosion current I_{corr}. During LP tests, a small direct current (DC) potential perturbation of ± 10 mV relative to the open circuit potential (OCP) is applied to the corroding metal; as the potential is applied, I_a is no longer equal to I_c, and a net current density, I, is induced between the anodic and cathodic sites. At a narrow potential region close to OCP, a relationship between potential and current is linear, the slope of which gives the corroding metal's polarisation resistance (R_P). I_{corr} is further calculated from the polarisation resistance R_P using the Stern-Geary equation (6.3) [26]

$$I_{CORR}=\frac{B}{R_P} \tag{6.3}$$

Where I_{corr} is corrosion current in A/cm^2

R_p is polarisation resistance in Ohms

B is the Stern-Geary constant and can be determined experimentally from Tafel polarisation by equation(6.4).

$$B=\frac{\beta_a\beta_c}{2.303(\beta_a+\beta_c)} \tag{6.4}$$

Where β_a and β_c are Tafel coefficients for anodic and cathodic regions, respectively.

B value of 19 mV has been reported for carbon steel corrosion in MEG [27] and have been used for all LP corrosion rate calculation in this result.

The corrosion rate is then calculated from the corrosion current using (6.5) [26]

$$CR = \frac{I_{corr} K Ew}{dA} \tag{6.5}$$

Where CR is the corrosion rate

I_{corr} is corrosion current in A/cm^2

K is the corrosion rate constant that defines the unit for the corrosion rate

Ew is the equivalent weight in grams/equivalent

d is density in g/cm^3

A is the surface area of the sample in cm^2

Values for K are 3272 for corrosion rate in mm/year and 1.288 × 10^5 for corrosion rate in mils/year[26]

While linear polarisation is non-destructive with applied potential relatively close to OCP, only ± 10 mV relative to the OCP [28], Tafel polarisation is destructive and applied potential is generally greater than ± 200 mV relative to the OCP. The LPR and Tafel polarisation are very similar techniques; however, the Tafel plots provide more insight into the anodic and cathodic reactions of the corroding system. Tafel polarisation is the most fundamental procedure for the experimental determination of I_{corr}. The Tafel coefficients β_a and β_c are determined from the slopes of the anodic and cathodic regions of the Tafel plot [29-30].

When the potential applied to a corroding metal is sufficiently higher than the OCP, the current flow away from the anodic site increases, causing anodic polarisation of the corroding metal which results in a irreversible change to the metal surfaces [28]. On the other hand, when the applied potential is sufficiently lower than the OCP the current flow away from the anodic site is reduced, causing cathodic polarisation.

An ideal Tafel plot of the log of current density vs potential is shown in Figure 6-1. The determination of corrosion parameters β_a, β_c, I_{corr} and E_{corr} for an ideal Tafel plot is illustrated in Figure 6-2. β_a is the slope of the anodic polarisation region of the Tafel plot and β_c is the slope of the cathodic polarisation region.

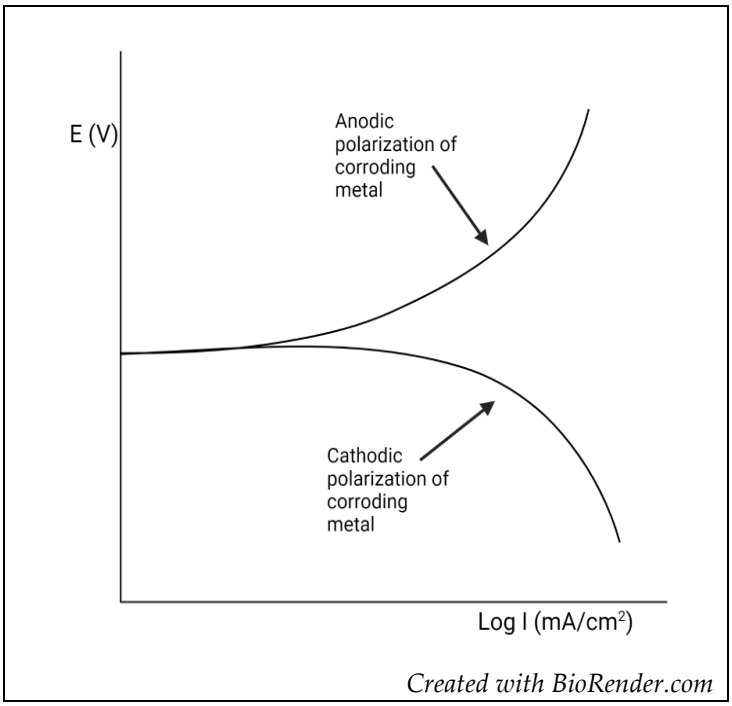

Figure 6-1: Illustration of Tafel plot

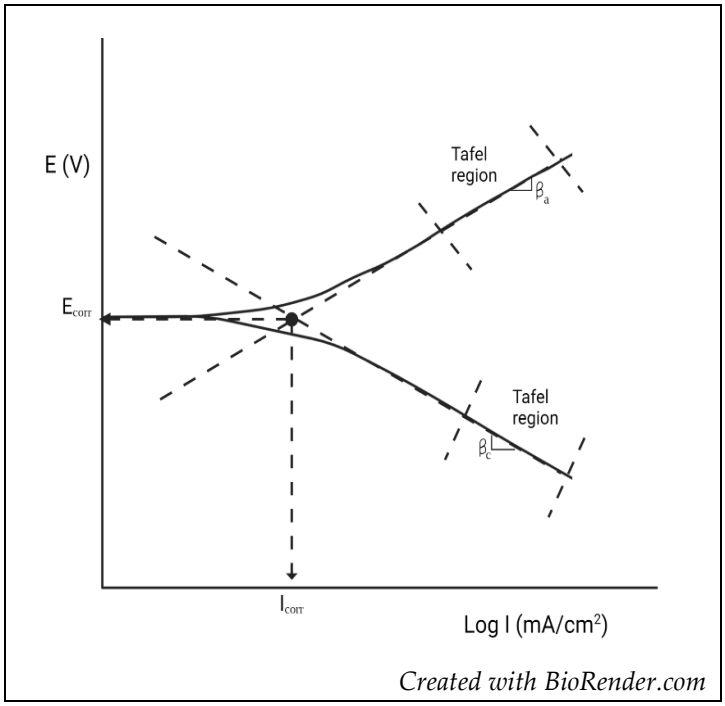

Figure 6-2: Illustration of Tafel plot showing corrosion parameters

Electrochemical impedance spectroscopy (EIS) in corrosion is a frequency domain measurement made by applying a sinusoidal voltage to the electrochemical cell and analysing the resulting impedance through the cell over a wide range of frequencies, typically 100 mHz - 100 kHz. Contrary to LP, where a small DC potential is applied, EIS measures electrochemical impedance resulting from applying an alternating current (AC) potential to an electrochemical cell [31]. Like resistance (measured in LR) is the resistance to the flow of DC, impedance (measured in EIS) is the resistance to the flow of AC. However, impedance is the total opposition to current in an AC current, which becomes a function of frequency. Consequently, impedance measurements reveal more information that can be used to differentiate electrical components in an electrical circuit. One such representation of the electrical circuit information from EIS is the Nyquist diagram. The Nyquist diagram is a complex plane plot of an EIS spectrum. It can be fitted to an equivalent electrical circuit providing information about physical processes in a corroding system as they relate to certain circuit elements like resistors,

capacitors and inductors [31]. The Bode plots are another representation of the EIS, showing changes in magnitude and phase as a function of the frequency in an AC system [32].

As earlier mentioned, impedance is the total opposition to current in an AC circuit; it is cumulative of impedance from a resistor, a capacitor, or an inductor. While inductors are not clearly defined in a chemical system like corrosion [33], the resistor and the capacitors are clearly defined. They can be attributed to the physical components in a corrosion system. For instance, a resistor can be associated with solution resistance (R_s) and charge transfer (or polarization) resistance (R_{ct}) [8; 15; 34-35]. The solution resistance is the resistance to the flow of current resulting from the physical and chemical properties of the solution in which the metal is corroding [36-37]. The charge transfer resistance is the resistance to the flow of current across the corroding metal surface resulting from the corrosion reaction kinetics [36-37]. A capacitor in a corrosion process has been attributed to the double-layer capacitance, which is an electric field at the metal-liquid interface resulting from an array of charged particles and oriented dipoles in a thin layer on the metal-liquid interface [38]. In corrosion systems, the double-layer capacitance does not behave ideally and often is presented as a constant phase element (CPE) [37]. Other components of the corrosion electrical circuit are the Warburg impedance, coating capacitance and a few others that are outside the interest of this review. A physical representation of these electrical circuit components for typical carbon steel in aqueous solution corrosion is illustrated in 6-3.These components of the electrical circuit can be identified from EIS data, as explained below.

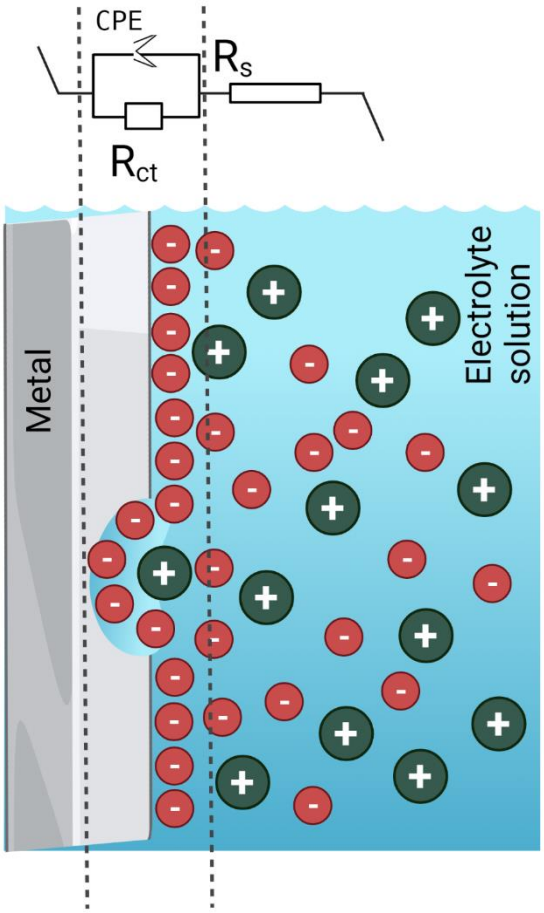

Figure 6-3: Illustration of an electrical circuit in a corrosion system

The polar form representation of impedance and the Cartesian form representation in equations (6.6) and (6.7) show a real and an imaginary component for impedance [39].

$$Z_{(\omega)} = |Z_{(\omega)}| e^{j\theta(\omega)} \tag{6.6}$$

$$Z = R + jX \tag{6.7}$$

Where $Z(\omega)$ is the impedance at radial frequency ω,
Radial frequency ω can be converted to linear frequency f as $\omega = 2\pi f$
$|Z_{(\omega)}|$ is the ratio of voltage difference amplitude V and current amplitude. I i.e $\frac{V}{I}$
Θ is the current output phase shift
R is resistance

X is reactance and
j is an imaginary unit,

$|Z_{(\omega)}|$ and jX are the imaginary components of impedance, while Z(ω) and R are the real components of impedance. The real component in impedance denoted Z', relates to resistance within the electrical system and the imaginary component, denoted Z'', relates to the reactance in the system. A plot of Z'' against Z' for each frequency point produces a Nyquist or complex plane plot. The Nyquist plot of an electrochemical test cell is analysed by fitting it to a Nyquist plot of a model circuit, thereby identifying the many characteristic features exhibited by the test cell. A commonly used electrical circuit would be Randle's circuit, shown in 6-4 with the corresponding Nyquist plot for Randle's circuit [39].

(a) (b)

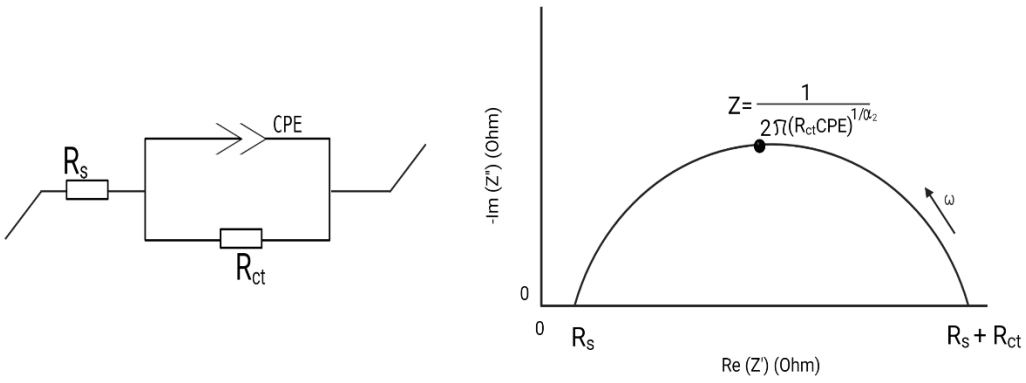

Figure 6-4: (a) Randle's circuit and (b) corresponding Nyquist plot used to model impedance spectra.
Rs is a solution resistance;
CPE is a constant phase element
R_{ct} is a polarisation resistance or a Charge transfer resistance

The Bode Plot is a combination of two plots; one is a plot of impedance magnitude against frequency, and the other bode plot is a plot of frequency phase shift against frequency. The shape of a Bode plot is an indication of the

electrical circuit components involved. An illustration of typical Bode plots showing components of an electrical circuit is shown in Figure 6-5.

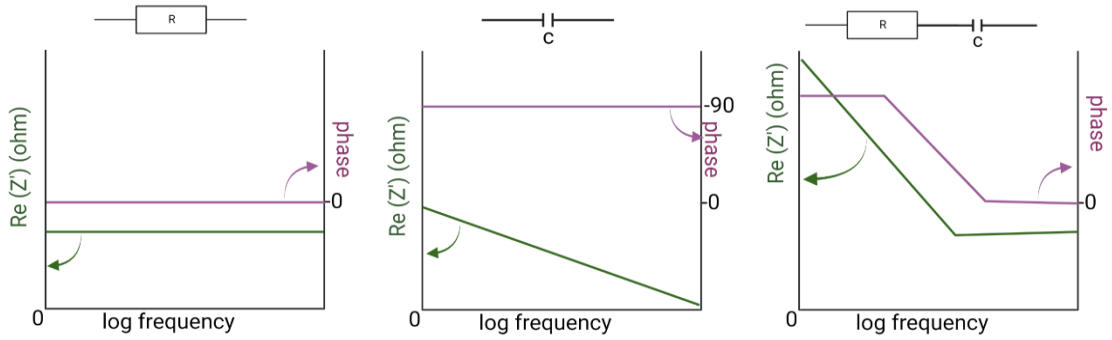

Figure 6-5: Illustration of electrical component in Bode plot. Left: resistor, middle: capacitor, and right: a resistor and a capacitor in series.

6.3 Methodology

6.3.1 Materials

Lean MEG with about 20 wt% water and 3 wt% salt is commonly used to mimic reboiler MEG stream [18] and has been used for this study. Analytical grade MEG (Rheochem Australia), analytical grade sodium chloride salt (ROWE Scientific Australia) and de-ionised water were used to prepare the MEG solutions. Analytical-grade organic acids were purchased from Sigma Aldrich. The composition of MEG solutions used in this study is presented in Table 6-1.

Table 6-1: Simulated lean MEG composition.

	12.5 mol/kg sol. MEG (0.5 mol/kg sol. ionic strength)
Monoethylene glycol (wt. %)	77.6
De-ionised water (wt. %)	19.4
Sodium chloride (wt. %)	3.0

UNS G10180 grade carbon steel from European corrosion supplies was used for the corrosion studies in this work. The chemical composition of these carbon steel electrodes is presented in Table 6-2. Nitrogen (99.999%) gas and carbon

dioxide gas (99.999%) were used for MEG degradation and for electrochemical experiments, respectively. The gases were obtained from BOC gases®.

Table 6-2: Composition of carbon steel electrodes

Element	Iron	Manganese	Silicon	Carbon	Phosphorus	Sulphur	Nickel
Content (wt. %)	98.6	0.71	0.37	0.18	0.03	0.03	0.01

6.3.2 Thermal degradation of MEG and Degradation products.

The degraded MEG solution used for this work (composition presented in Table 6-1) was thermally degraded at 140 °C for 21 days. The MEG regeneration unit is usually in a low-oxygen environment; results from the study in Chapter 5 of this thesis confirm degradation even in an oxygen-free environment. However, the presence of oxygen during degradation affects the speciation and concentration of organic acids.

This study investigated the corrosivity of both oxygen-free degraded MEG and air-saturated degraded MEG. The degradation was conducted under a nitrogen blanket for the oxygen-free degraded MEG, while air-saturated degradation was conducted with an air blanket. The method and experimental setup for degradation are the same as those presented in Chapter 5 of this thesis. After the degradation stage was completed, the MEG samples were rapidly cooled by submerging the test cell in cold water. The purpose of this step was to reduce the solution temperature and stop the degradation reaction quickly.

The pH of MEG subsamples was measured at room temperature (ca. 25 °C) in ambient air with a metro GMH 5550 pH meter and 100 BNC Standard 3 molar KCL refillable glass pH electrode. The pH electrode was calibrated for MEG

pH measurements according to the method proposed by Sandengen et. al.[40]. The calibration curve for the pH electrode used in this study is presented in Figure 5-3.

Subsamples of degraded MEG were also collected and analysed for organic acids concentration by ion chromatography according to the method described in Chapter 3 of this thesis.

6.3.3 Electrochemical experimental setup

The rotating electrode cylinder (RCE) setup was used for all electrochemical measurements and is presented in Figure 6-6 below. This setup consists of a 1-litre cylindrical cell on an IKA® RET hot plate with thermocouples to maintain the temperature between ± 1 °C of the required test temperature. Two advantages of the RCE are that it enables measurements at varying shear rates and controlled hydrodynamics at the working electrode surface [41-42]. Consequently, tests can be conducted for both low-shear rate laminar flow and high-shear rate turbulent flow.

The three-electrode configuration consists of the carbon steel RCE working electrode (WE), a graphite counter electrode (CE) and a saturated silver-silver chloride electrode (Ag/AgCl) reference electrode (RE). The 1-litre cylindrical cell was fitted with a ground glass flange and a glass lid for an airtight environment. The glass lid has six access points for the temperature probe, the reference and counter electrodes, the gas inlet and outlet, and the working electrode.

The ASTM test methods for polarisation resistance measurements G59-97 [22] and cleaning of corrosion test specimen G1-03 [24] were adopted for all tests. BioLogic VMP3 multichannel potentiostat controlled by EC-Lab® software was used for all electrochemical measurements. The Zfit analysis on the EC-Lab software was used to fit successive impedance cycles.

Tests were conducted at 60 °C and 80 °C under continuous CO_2 gas sparging at 50 mL/min. The carbon steel sample was mounted onto the working RCE electrode, as shown in Figure 6-6 a). Before testing, all carbon steel samples were prepared by successive wet polishing with 120, 320 and 600 grit silicon carbide abrasive paper and then sonicating in ethanol to clean and degrease, followed by drying with nitrogen gas.

Carbon steel samples were prepared before each experiment and immersed into a test solution less than 5 minutes after preparation. The height and diameter of the RCE samples were measured to the nearest 0.01 cm using a Mitutoyo Absolute Digimatic CD-6 CSX digital calliper, and the surface area was calculated using measured height and diameter. The test solution for each electrochemical test was heated to test temperature while sparging and held at test temperature for 4 hours before the working electrode was immersed into the solution

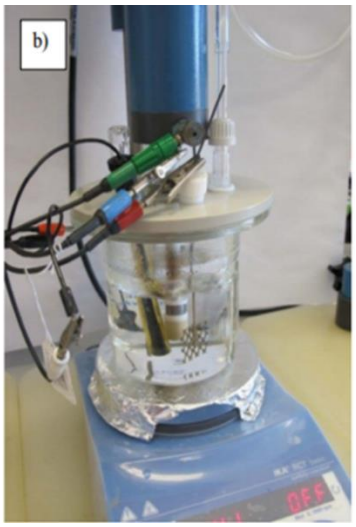

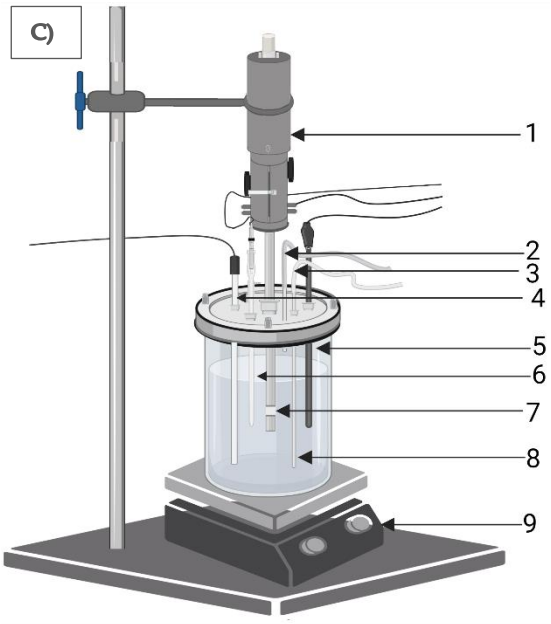

1. Rotator, 2. Gas out, 3. Gas in, 4. Temperature probe, 5. Graphite counter electrode, 6. Ag/AgCl standard electrode, 7. Working electrode, 8. Gas in, 9. Hot plate

Figure 6-6: Experimental setup for electrochemical measurements

a) *Carbon steel sample working electrode*
b) *Photo of set up*
c) *Schematic of setup*

The RCE setup was conducted at least twice per sample, results were trended, and outlier results were repeated to check for reproducibility. Measurements were considered reproduceable when there was no more than 10% variance between repeat measurements. Results presented in this work are an average of 2 reproduceable measurements. Error bars reported show the low and high measurements for each test signifying the estimated error in measurement.

6.3.4 Shear stress, Density and Viscosity

Tests were conducted at 2 rotational speeds, i.e., 100 rpm and 1500 rpm. The working electrode wall shear stress at these rotational frequencies was calculated with equations (6.8) - (6.10) [42-43]

$$\tau = 0.0079 \rho R_E^{-0.3} U^2 \tag{6.8}$$

$$R_E = U d \frac{\rho}{\mu} \tag{6.9}$$

$$U = \frac{\pi d F}{60} \tag{6.10}$$

Where τ is the wall shear stress in Pa*s
R_E is Reynolds number and
U is the linear velocity in cm/s at the outer surface of the RCE sample calculated with equation 6.7
d is the diameter of the RCE sample
μ is the solution absolute viscosity in g/cm.S
ρ is the solution density g/cm^3 and
F is the rotational frequency of the RCE sample, which is either 100 rpm or 1500 rpm in this work.

The solution density, ρ at 60 ° and 80 °C, was measured using a 10 mL Bingham pycnometer according to the ASTM D1217-20 standard method for density determination [44]. The pycnometer is a glass flask with a close-fitting ground glass stopper with a capillary hole. The capillary hole allows liquid overflow of expanding liquid with the increase in temperature. For this density measurement, the pycnometer was first cleaned with water, followed with acetone and allowed to dry completely before weighing to obtain an initial empty weight. Then the pycnometer was filled with MEG solution and inserted into a constant temperature bath set to the desired temperature. After 30 minutes in the water, the filled pycnometer was removed, carefully dried with a clean, lint-free tissue, and weighed. The density of the solution was calculated as (6.11)

$$\frac{W_f - W_e}{V} \tag{6.11}$$

Where W_f is the weight of the filled pycnometer
W_e is the weight of the empty pycnometer
V is the volume of the pycnometer

Absolute viscosity, μ, was measured using a Haake ViscoTester 550 rotational viscometer with an MV-DIN spindle and a ViscoTemp 30150 controller. To measure the viscosity, the sample was added to the ViscoTester 550 sample chamber, the desired temperature was set on the ViscoTemp 30150, and the viscosity results were displayed on the Rheowin software upon completion. The temperature accuracy for viscosity measurements was ±0.1 °C.

Density and Viscosity measurements were repeated at least twice per sample. Measurements were considered reproduceable when there was no more than 10% variance between repeat measurements. Results presented here for density

and viscosity are an average from two reproduceable measurement for each test.

6.4 Results

6.4.1 Density, viscosity, and calculated wall shear stress

As expected, viscosity for all MEG solutions reduced with an increase in temperature from 60 °C to 80 °C, as presented in Figure 6-7. Viscosities also reduced with degradation; after 21 days of air-saturated degradation, viscosity reduced by 5% at 60 °C and 6% at 80 °C. The changes in viscosity after 21 days of oxygen-free degradation were slightly lower compared to air-saturated degradation; 3% at 60 °C and 5% at 80 °C.

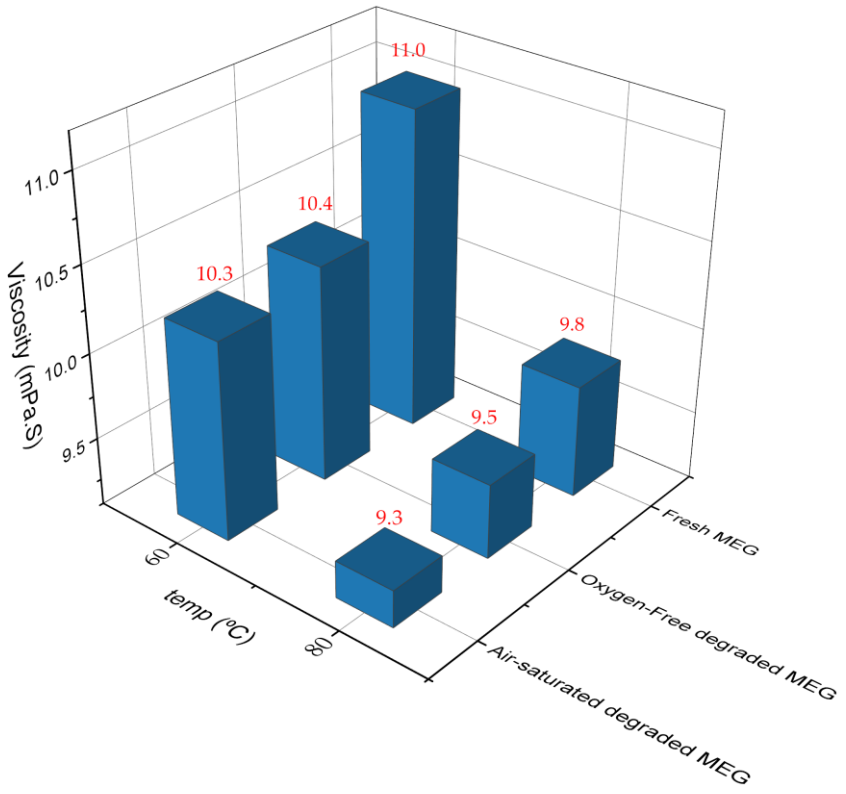

Figure 6-7: Viscosity of fresh simulated lean MEG before and after degradation for 21 days under oxygen-free and air-saturated environment.

Similar trends were also observed for densities before and after 21 days degradation, as presented in Figure 6-8. Densities decreased with temperatures and with degradation; however, the decrease was minimal; no more than 0.3% decrease in density at 60 °C and no more than 1.0% decrease at 80 °C. Air-saturated degradation has slightly lower densities. These changes in viscosities and densities concur with MEG degradation to less dense and less viscous organic acids, as well as the more progressive degradation in air-saturated degradation compared to oxygen-free degradation.

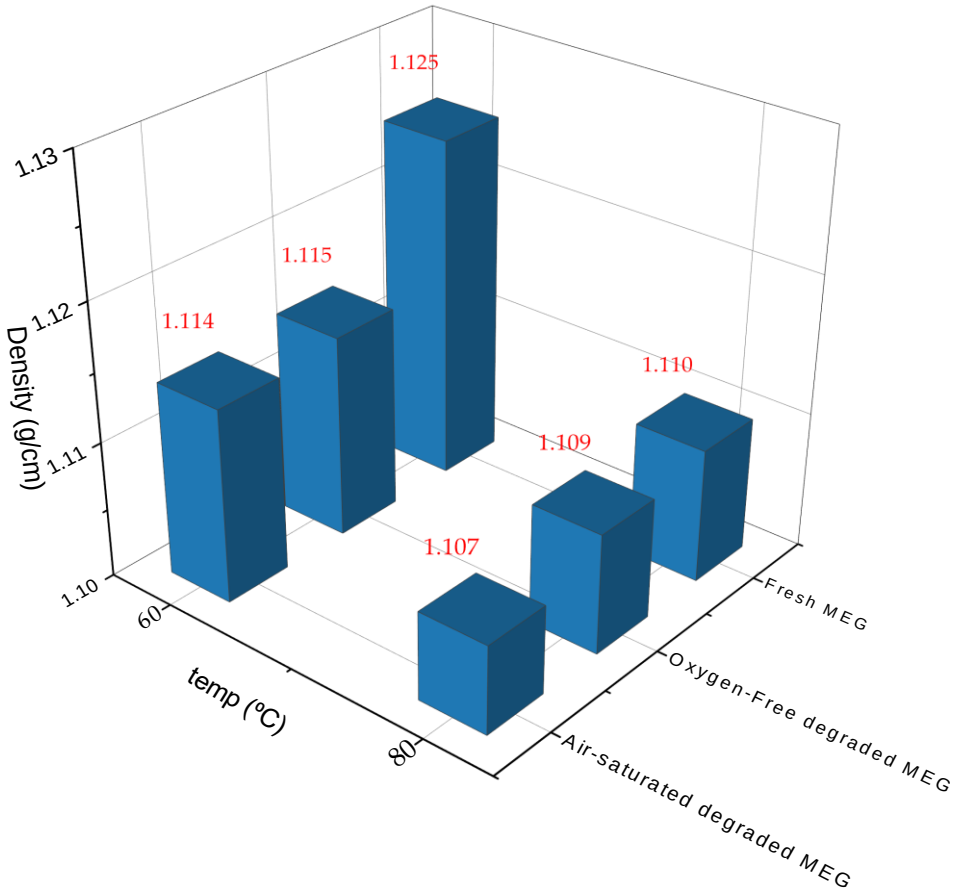

Figure 6-8: Density of fresh simulated lean MEG before and after degradation for 21 days under oxygen-free and air-saturated environment.

Calculated Reynolds number (RE) for experiments in this work are presented in Table 6-3. Turbulent flow for RCE tests occurs at Reynolds number > 200 while laminar flow occurs at Reynolds number < 200 [34]. Results in Table 6-3

show laminar flow RE for samples sheared at 100 rpm and turbulent flow RE for samples sheared at 1,500 rpm. It is apparent that the change in physical properties affect the shear stresses at the same rotational speed. Nonetheless, the change may be considered negligible (i.e., < 2%) and the difference in corrosion behaviour could be attributed to chemical aspect of the test solutions.

Table 6-3: Calculated Shear stress and Reynolds numbers at the electrode surface in fresh and degraded MEG.

		Fresh MEG		Air-saturated degraded MEG		Oxygen-Free degraded MEG	
		60 ^{0}C	80 ^{0}C	60 ^{0}C	80 ^{0}C	60 ^{0}C	80 ^{0}C
Shear Stress (mPa.S)	**100 rpm**	126	129	123	126	124	127
	1500rpm	12,568	12,898	12,313	12,611	12,404	12,670
RE	**100 rpm**	136	119	138	126	142	127
	1500rpm	2038	1787	2066	1890	2113	1907

Note: internal diameter of RCE samples was approximately 1.6cm

6.4.2 Corrosion in Fresh MEG

Corrosion rates determined from the LP technique for carbon steel in fresh MEG solutions taken at 4 h after immersion are presented in Figure 6-9. Fresh MEG, in this case, refers to MEG solutions as per compositions in Table 6-1 before degradation. The corrosion rate of carbon steel increased with increasing temperature and shear stress. This behaviour has been reported extensively for CO_2 corrosion of carbon steel in MEG [6; 8; 10; 12]

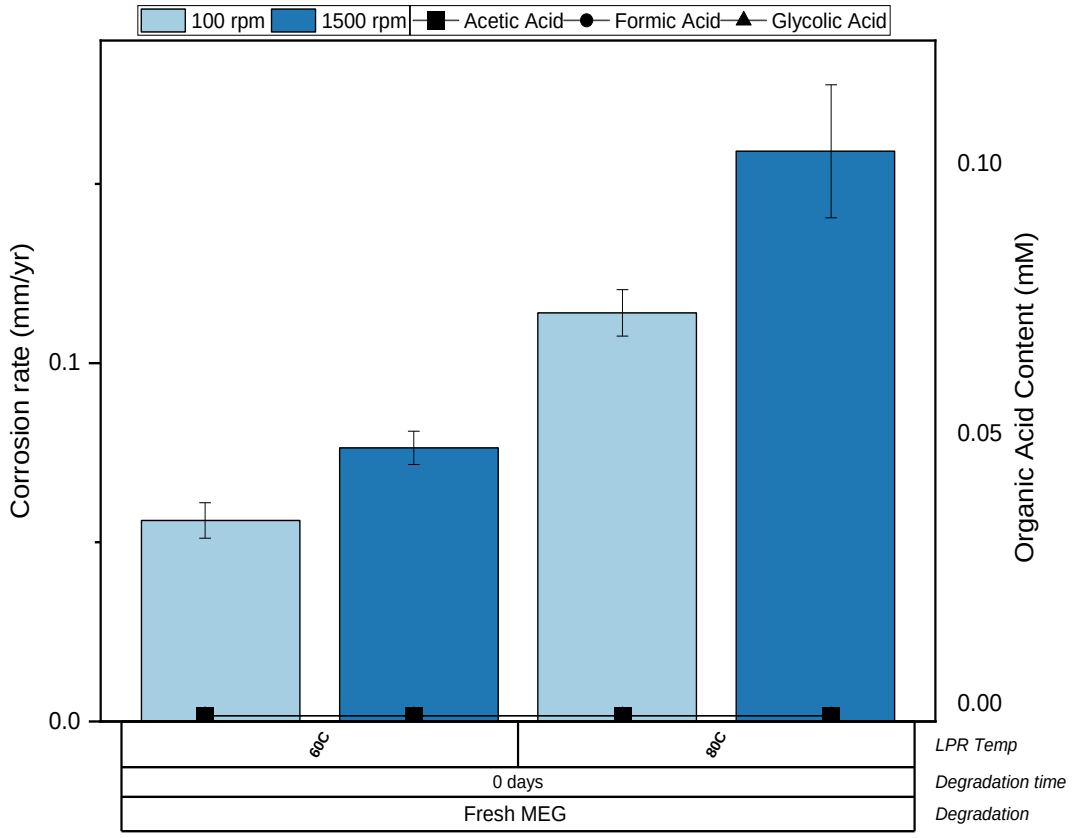

Figure 6-9: Stabilised corrosion rates (CR) for carbon steel in fresh MEG with total organic acid content (pH of fresh MEG solution measured at 25 ^{0}C in ambient air is 5.89).

The effects of shear stress and temperature on corrosion rate provide information that defines the rate control mechanism for corrosion. A 40% increase in corrosion rate was observed with a 100 times increase in shear stress from average of 128 mPa.s - 12,733 mPa.s at both 60 °C and 80 °C. This corresponding increase in corrosion rate with shear stress indicates a diffusion-controlling mechanism on carbon steel corrosion in fresh MEG. As the dominant cathodic reaction is hydrogen reduction, diffusion control behaviour is expected [45]. In a diffusion-controlled mechanism, the rate of the chemical reaction is almost spontaneous, and the rate of mass transfer of hydrogen ions within the bulk fluid becomes the rate-limiting step; this manifests as a

proportional increase in corrosion rate with an increase in shear stress and activation energy less than 20 KJ.mol^{-1} [45].

On the other hand, an activation-controlled mechanism has a relatively slow reaction rate and is not limited by diffusion within the bulk fluid; the mechanism is independent of shear stress [45]. For carbon steel corrosion in fresh simulated lean MEG solution, activation energy was calculated using Equation (6.12) where T_1 is 60 °C, and T_2 is 80 °C (both temperatures converted to absolute temperature scale K); I_{corr1} and I_{corr2} are corrosion current at temperatures T_1 and T_2 respectively; R is the ideal gas constant (= 8.3145 J/K·mol) and E_a is the activation energy

$$\ln\frac{I_{corr2}}{I_{corr1}} = \frac{E_a}{R}\left(\frac{1}{T_1} - \frac{1}{T_2}\right) \tag{6.12}$$

The calculated activation energy for fresh MEG was 34.7 KJ.mol^{-1} at 126 mPa.s and 35.9 KJ.mol^{-1} at 12,568 mPa.s. These activation energies are > 20 KJ.mol^{-1}, indicating that the corrosion mechanism in fresh MEG is neither pure diffusion controlled nor activation-controlled but follows a mixed-controlled mechanism.

6.4.3 Corrosion in oxygen-free degraded MEG

As discussed in Chapter 5, the degradation of MEG at high temperatures is a thermo-oxidative process that produces organic acids, primarily glycolic and formic acids and smaller amounts of acetic and oxalic acid. The corrosion of carbon steel in oxygen-free degraded MEG with corresponding produced organic acid content is presented in Figure 6-10. Figure 6-10 shows corrosion rates in MEG solution at varying shear stress and temperatures before and after 7 and 21 days of oxygen-free degradation, as well as organic acid composition in the MEG solutions.

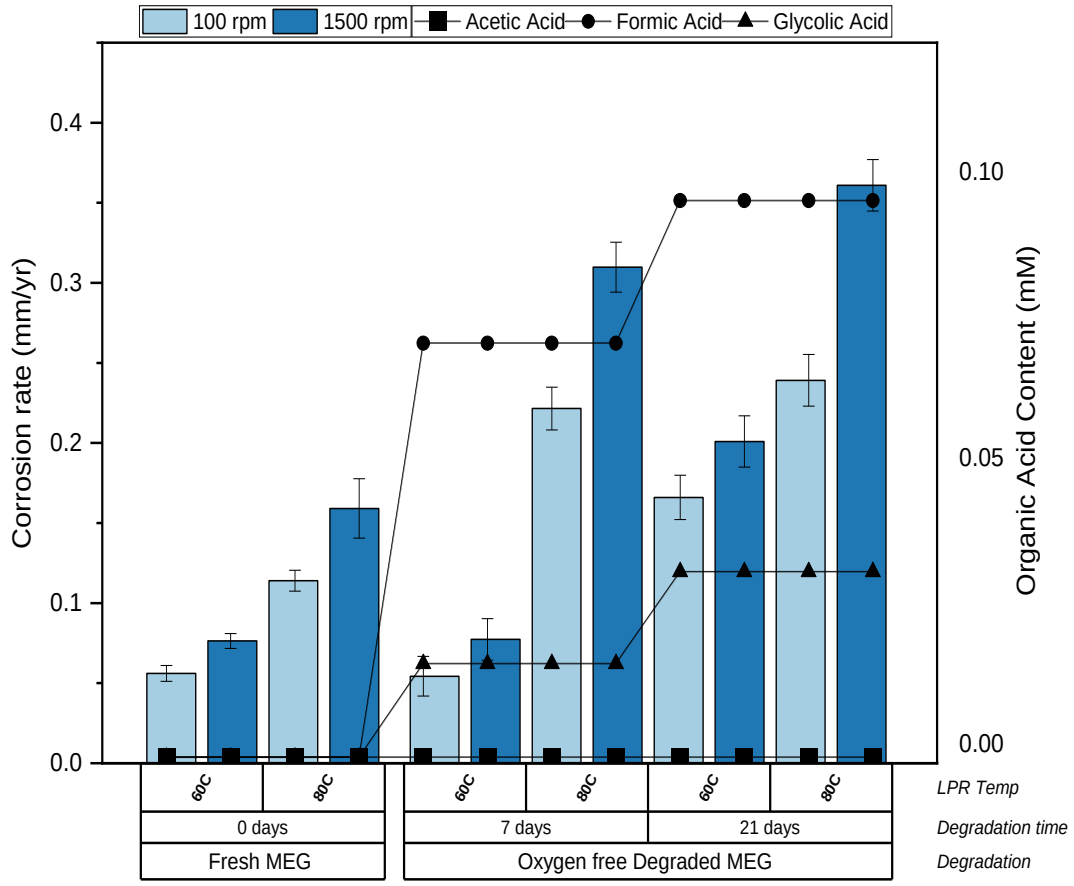

Figure 6-10: Stabilised corrosion rates (CR) for carbon steel in fresh MEG and oxygen-free degraded MEG with total organic acid content. (pH of 7-days degraded MEG measured at 25 ^{0}C is 5.3, pH of 21-days degraded MEG measured at 25 ^{0}C is 5.1)

After 7 days of degradation, oxygen-free degradation of MEG did not significantly affect the corrosion of carbon steel under mild corrosion conditions (60 °C and 123 mPa.s), with the corrosion rate remaining almost equal to that in fresh MEG. The influence of shear stress on the corrosion rate of oxygen-free degraded MEG at 60 °C and 80 °C was similar to that of fresh MEG. The corrosion rate increased by about 40% with an increase of shear stress from an average of 125 mPa.s - 12,462 mPa.s. The calculated activation energy was 68.8 KJ.mol^{-1} at 125 mPa.s and 67.9 KJ.mol^{-1} at 12,462 mPa.s. A similarly mixed control mechanism is also observed for corrosion after 7 days oxygen free degradation of MEG.

Increasing temperature increases the corrosion rate suggesting that the corrosion reaction kinetics increases with temperature as expected. Calculated activation energies for corrosion in 21 days oxygen free-degraded MEG were 19.8 KJ.mol-1 at 125 mPa.s and 28.7 KJ.mol-1 at 12,462 mPa.s. While the corrosion rate was observed to almost double with prolonged degradation at 60 °C, there was only about a 15% increase in corrosion rate at 80 °C with prolonged. At 80 °C, the change in shear stress also resulted in an almost doubling corrosion rate; this shows that the diffusion-limiting effect on corrosion was very significant at the low shear stress. With an increase in shear stress, this diffusion effect is minimised, and corrosion becomes more activation controlled.

Even though the total organic acid produced from the oxygen-free degradation of MEG was minimal, only about 0.11 mM after 21 days degradation, there was a correlation of corrosion rate with the increasing organic acid content. Corrosion rate gradually increased with prolonged degradation and increasing organic acid content, as seen in Figure 6-10.

6.4.4 Corrosion in air-saturated degraded MEG

Stabilised corrosion rates for carbon steel in air-saturated degraded MEG with corresponding produced organic acid content are presented in Figure 6-11. As discussed in chapter 5, Air-saturated degradation of MEG produces significantly more organic acid than oxygen-free degradation.

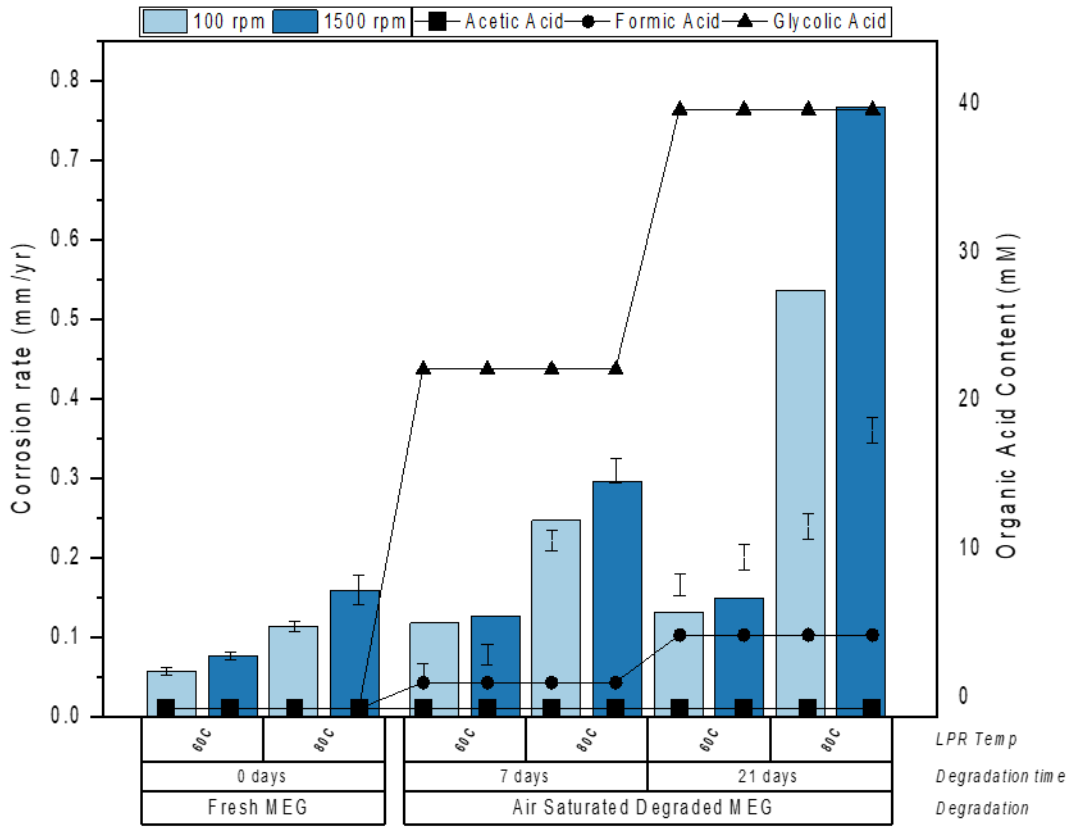

Figure 6-11: Stabilised corrosion rates (CR) for carbon steel in fresh MEG and air-saturated degraded MEG. (pH of 7-days degraded MEG is 4.4, pH of 21-days degraded MEG is 4.17)

Air-saturated degradation was seen to cause a significant increase in the corrosion rate of carbon steel in comparison with fresh MEG. After 7 days of air-saturated degradation, the corrosion rate was almost 100% increased at 60 ^{0}C and 80 ^{0}C. The effect of prolonged degradation is, however, pronounced in corrosion at 80 ^{0}C with an almost 400% increase in corrosion rate compared to fresh MEG at identical conditions.

The calculated Activation energy in 7 days of air-saturated degraded MEG was 36.1 KJ.mol^{-1} at 125 mPa.s and 41.6 KJ.mol^{-1} at 12,462 mPa.s. The activation energy was observed to increase with prolonged air-saturated degradation, increasing to 68.8 KJ.mol^{-1} at 125 mPa.s and 80.2 KJ.mol^{-1} at 12,462 mPa.s with 21 days of air-saturated degradation. This increase in activation energy has been reported for organic acid in brine [46-47]. However, the effect of increasing shear stress on corrosion rate is significantly minimised in air-

saturated degraded MEG, with only about a 10% increase in corrosion rate at 60^0C and a 20% increase in corrosion rate at 80^0C. While corrosion in degraded MEG follows a mixed control rate theory, oxygen-free degradation was more diffusion-controlled, whereas air-saturated degradation exhibited activation controlled mechanism. This shift towards activation controlled mechanism can be attributed to an abundance of organic acids in air-saturated degraded MEG, thereby minimising the effect of diffusion in solution.

It has been established that for carbon steel corrosion, organic acid dissociates in solution, releasing electrons at the cathodic sites, thereby increasing the rate of the cathodic corrosion reaction [37, 38]. The Tafel plots in Figure 6-12 show typical cathodic and anodic polarisation linear sweeps for carbon steel in oxygen-free and air-saturated degraded MEG and un-degraded MEG at 80 ^{0}C and 1500 rpm. The plots were determined potentiodynamically at a scan rate of 1 mV S^{-1} after 4 h immersion in the test solution under open circuit conditions. This plot shows that the simulated lean MEG under oxygen-free degradation affected the anodic reaction more pronouncedly than the cathodic reaction. In comparison, air-saturated degradation affected both the anodic and cathodic reactions.

Consequently, the effect of organic acids on carbon steel corrosion results in changes to the cathodic region of the Tafel plot and no changes to the anodic region of the Tafel plot for carbon steel corrosion [47]. This correlates with the findings from this work, suggesting that the corrosion rate for oxygen-free degraded MEG is not a consequence of organic acids content. The corrosion rate increases in oxygen-free degraded MEG, albeit with a minimal increase in produced organic acid. Also, the effect of organic acids content is seen in the cathodic region of the Tafel plot for the air-saturated degraded MEG (Figure 6-12).

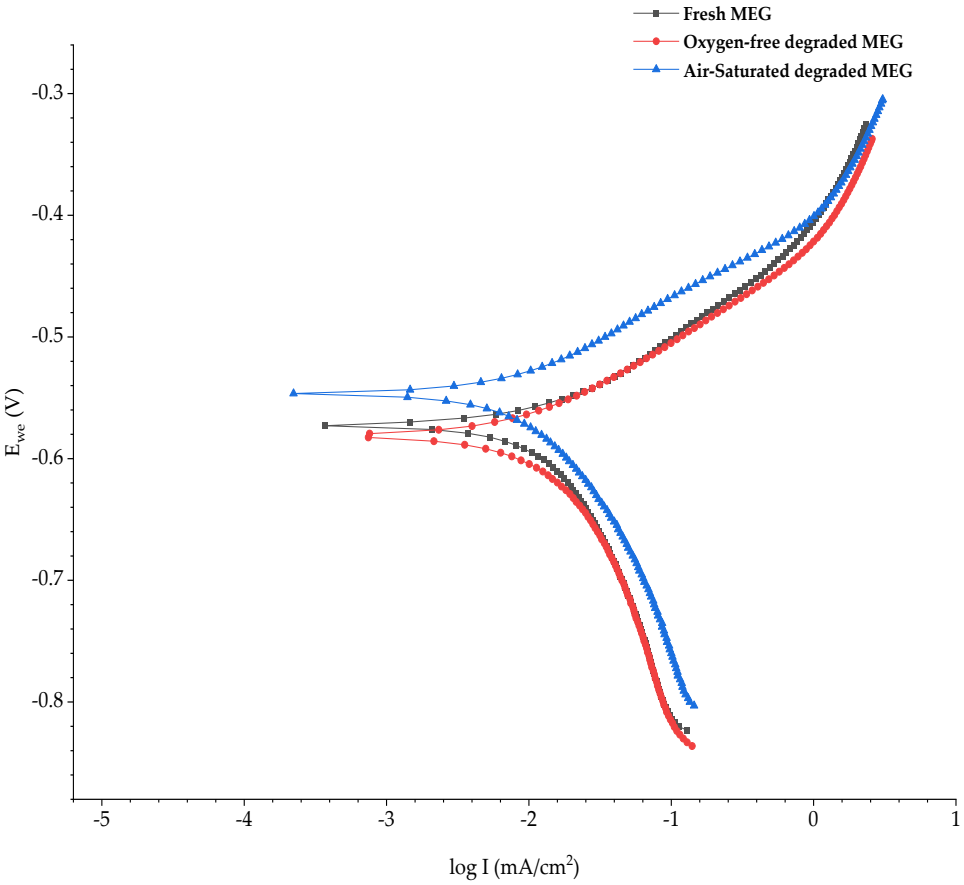

Figure 6-12: Tafel plot for carbon steel at stabilised OCP in fresh MEG and 21 days degraded MEG at 80 ⁰C and 1500 rpm.

6.4.5 Corrosion in Fresh MEG with added organic acids

As earlier mentioned, results from this work on thermally degraded MEG show that the concentration of organic acids alone could not explain the increase in corrosion rate of carbon steel in thermally degraded MEG. Corrosion rate of carbon steel increased even with oxygen-degradation MEG, wherein minimal organic acid is produced. Further tests were conducted to distinguish the influences of individual organic acids in MEG on carbon steel corrosion and to differentiate this from the effect of degradation. Experiments were conducted on fresh un-degraded MEG samples with added organic acids - 7mM of acetic and formic acid each and 50mM of glycolic acid. The concentrations selected were in the same range observed for 21 days air-saturated degradation.

Negligible amounts of oxalic acids were observed for thermal degradation of MEG at a degradation temperature of 140 °C; hence oxalic acid was not considered in these tests.

While existing literature on the influence of acetic acids on carbon steel corrosion in MEG is relatively substantial, similar literature on the influence of formic and glycolic acids is not well established. The Tafel plot for the corrosion of carbon steel in fresh MEG with each of the produced organic acids (i.e. glycolic, formic and acetic) is presented in Figure 6-13. The plots in Figure 6-13 show that under test conditions of 80 °C and 1500 rpm, corrosion current for carbon steel increases in acetic acid, with changes to both the anodic and cathodic regions of the Tafel plot. This observation concurs with existing literature [34; 46-47].

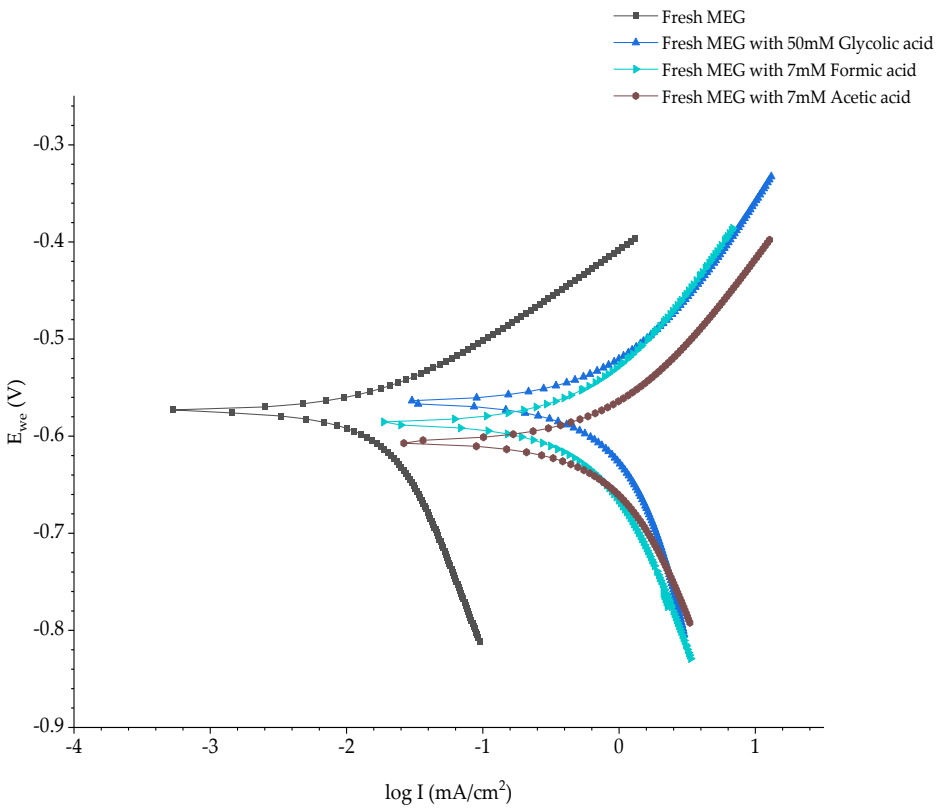

Figure 6-13: Tafel Plot for carbon steel at stabilised OCP in fresh MEG with added organic acids at 80 °C and 1500 rpm

Figure 6-13 also shows similar influences for formic and glycolic acids on carbon steel corrosion. Polarisation parameters presented in

Table 6-4 show that both cathodic and anodic currents increased with the addition of any of the three organic acids. However, the open circuit potential (OCP) remained the same for all three organic acids. These results in Figure 6-13 and

Table 6-4 indicate that adding any of these organic acids equally influences the cathodic and anodic corrosion reactions.

Table 6-4: Polarisation parameters of carbon steel in MEG with added organic acid at 80 °C and 1500rpm

Test media	Fresh MEG	7mM Acetic acid	7mM Formic acid	50mM Glycolic acid
OCP (mV)	-573.76	-605.99	-580.37	-565.06
b_a (mV)	99.1	200.1	221.7	242.6
b_c (mV)	368.1	403.3	482.4	753.6
B (V)	0.034	0.058	0.066	0.080
icorr (A/m^2)	0.07	5.37	3.07	5.07
CR (mm/yr)	0.08	4.67	3.56	5.89

In general, the corrosion rates of carbon steel with individually added organic were significantly larger than those measured in thermally degraded with similar organic acid concentrations. Even though comparable organic acid contents, corrosion rates in fresh MEG with added organic acids were almost 5 times more than corrosion rates measured in 21 days air-saturated degraded MEG. At this stage, it was unclear if the combination of acids produced during degradation affected the corrosion rate; hence more tests were conducted on carbon steel with mixtures of these organic acids. Figure 6-14 shows the Tafel plots for carbon steel corrosion in MEG solutions with added mixed organic acids, while Table 6-5 shows the polarisation parameters for carbon steel corrosion in MEG solutions with added mixed organic acids.

Significant increases in corrosion current densities were observed with the addition of mixed acids increasing corrosion rate. On the other hand, changes in OCP were not significant, and neither were b_a and b_c cumulative for the individual acids.

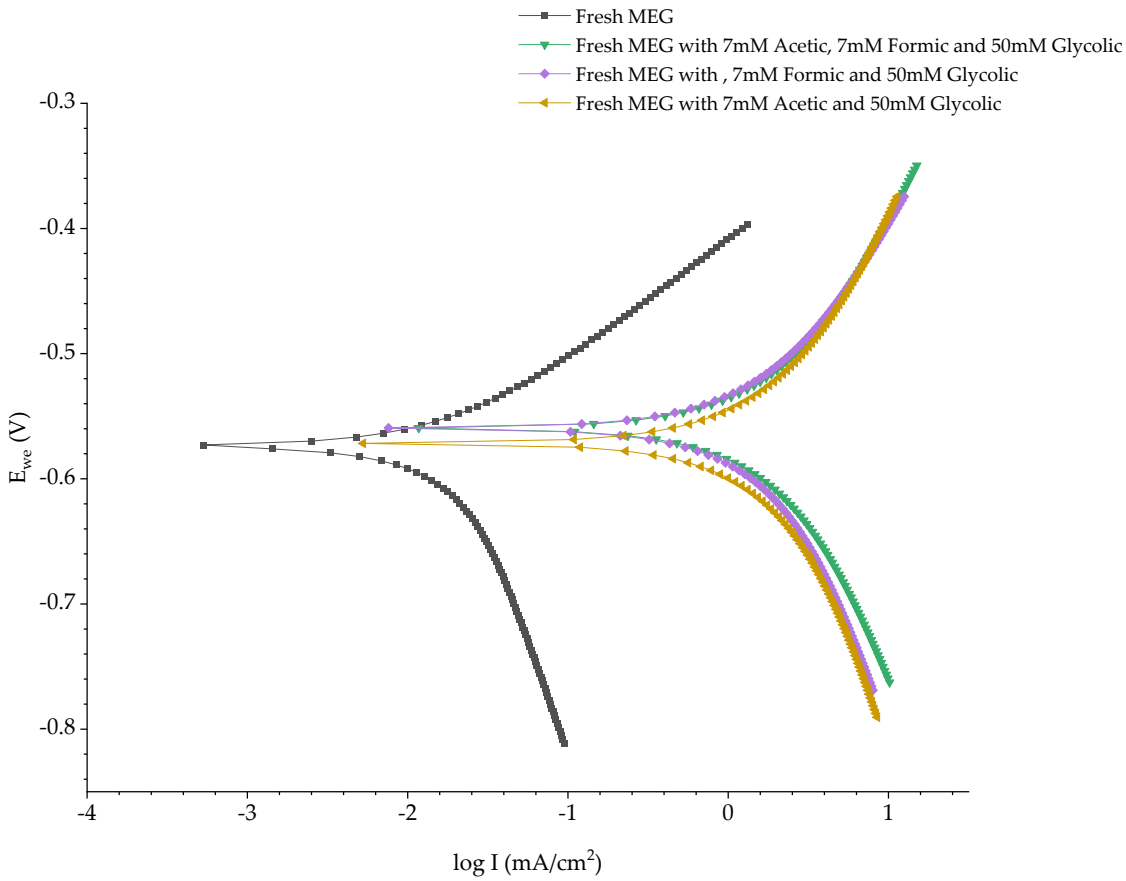

Figure 6-14: Tafel Plot for carbon steel at stabilised OCP in fresh MEG with added mixed organic acids at 80 °C and 1500 rpm

Table 6-5: Polarisation parameters of carbon steel in MEG with added mixed organic acid at 80 °C and 1500rpm

Test media	7mM Acetic and 50mM Glycolic	7mM Formic and 50mM Glycolic	7mM Acetic 7mM Formic and 50mM Glycolic
OCP (mV)	-571.54	-559.61	-559.67
b_a (mV/dec)	316.30	246.80	273.50
b_c (mV/dec)	448.30	382.90	338.00
B (V/dec)	0.0805	0.0652	0.0656
icorr (A/m2)	10.38	8.07	9.81
CR (mm/yr)	12.05	9.38	11.40

A comparison of Tafel plots for fresh MEG with and without added organic acids and degraded MEG is presented in Figure 6-15. Polarisation parameters for this comparison are presented in Table 6-6. This comparison shows that the corrosion current density for Fresh MEG with added mixed acids is much higher than those for both degraded MEG and fresh MEG, suggesting that degradation may have a slight inhibiting effect on corrosion compared to the addition of neat acids.

The Tafel plot for air-saturated degraded MEG shows an initial region of anodic dissolution where the anodic slope is similar to that of fresh MEG, followed by a sharp reduction in the anodic slope, indicating a possible passivation region. The calculated anodic Tafel slope for air-saturated degraded MEG is slightly lower than that for fresh MEG, which could be a consequence of the possible passivation effect of carbon steel during corrosion in air-saturated degraded MEG. A more positive OCP is also observed for air-saturated MEG compared to Fresh MEG with or without added organic acids. A more positive OCP indicates the formation of an oxide film on the corroding metal surface resulting in passivation of the corroding metal[48]. This passivation is not characteristic of the organic acids in corrosion, suggesting a more complex effect of degradation on carbon corrosion.

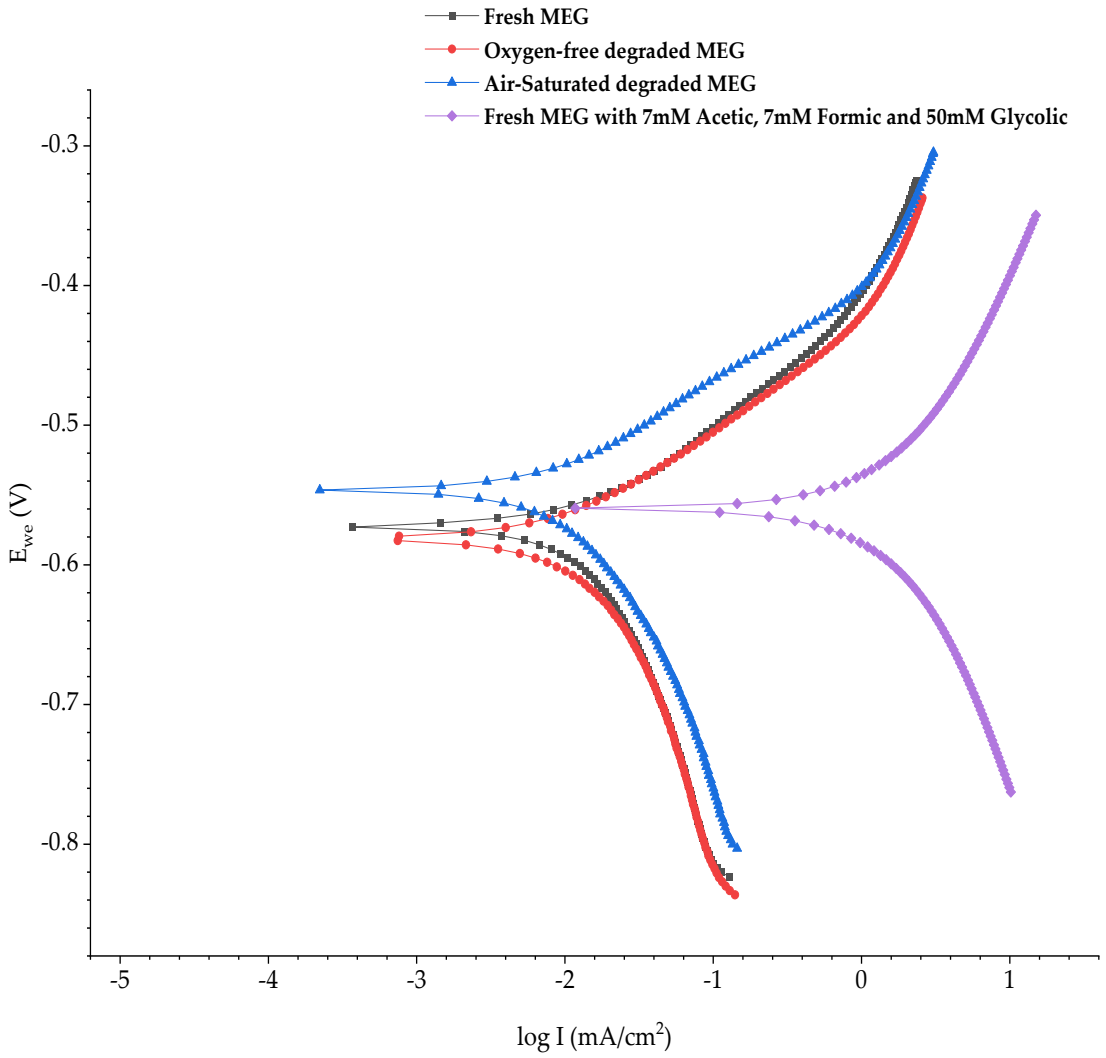

Figure 6-15: Tafel Plot for carbon steel at stabilised OCP in 21 days air-saturated degraded MEG and fresh MEG with added organic acids at 80 ºC and 1500 rpm

Table 6-6: Polarisation parameters of carbon steel in MEG with added organic acid at 80ºC and 1500rpm

Test media	Fresh MEG	Oxygen-free degraded MEG*	Air-saturated degraded MEG*	7mM Acetic 7mM Formic and 50mM Glycolic
OCP (mV)	-573.76	-583.32	-546.56	-559.67
ba (mV/dec)	99.1	95.3	86.9	273.50
bc (mV/dec)	368.1	303.6	269.0	338.00
B (V/dec)	0.034	0.0315	0.0285	0.0656
icorr (A/m2)	0.07	0.31	0.70	9.81
CR (mm/yr)	0.08	0.361	0.818	11.40

* after 21 days of degradation

EIS data were used to confirm polarisation results from the comparison of carbon steel corrosion in fresh MEG (with and without added organic acids) and degraded MEG. The EIS plots are presented in Figure 6-16; as seen in these plots, both the Nyquist and the Bode plots presented good agreements with the Randle's circuit - that is, solution resistance in series with charge transfer resistance and constant phase element as illustrated in Figures 6-3 and 6-4. The Nyquist plot presents a semi-circle with diameters decreasing with degradation. There was no significant change in solution resistance, but significant changes were evident for charge transfer resistance in fresh MEG and degraded MEG. In agreement with LP results, degraded MEG had less resistivity than fresh MEG with no organic acid but more resistivity than MEG with added organic acids. The EIS resistivity results in Figure 6-16 correlate with the corrosion current density trends from polarisation results in Figure 6-15.

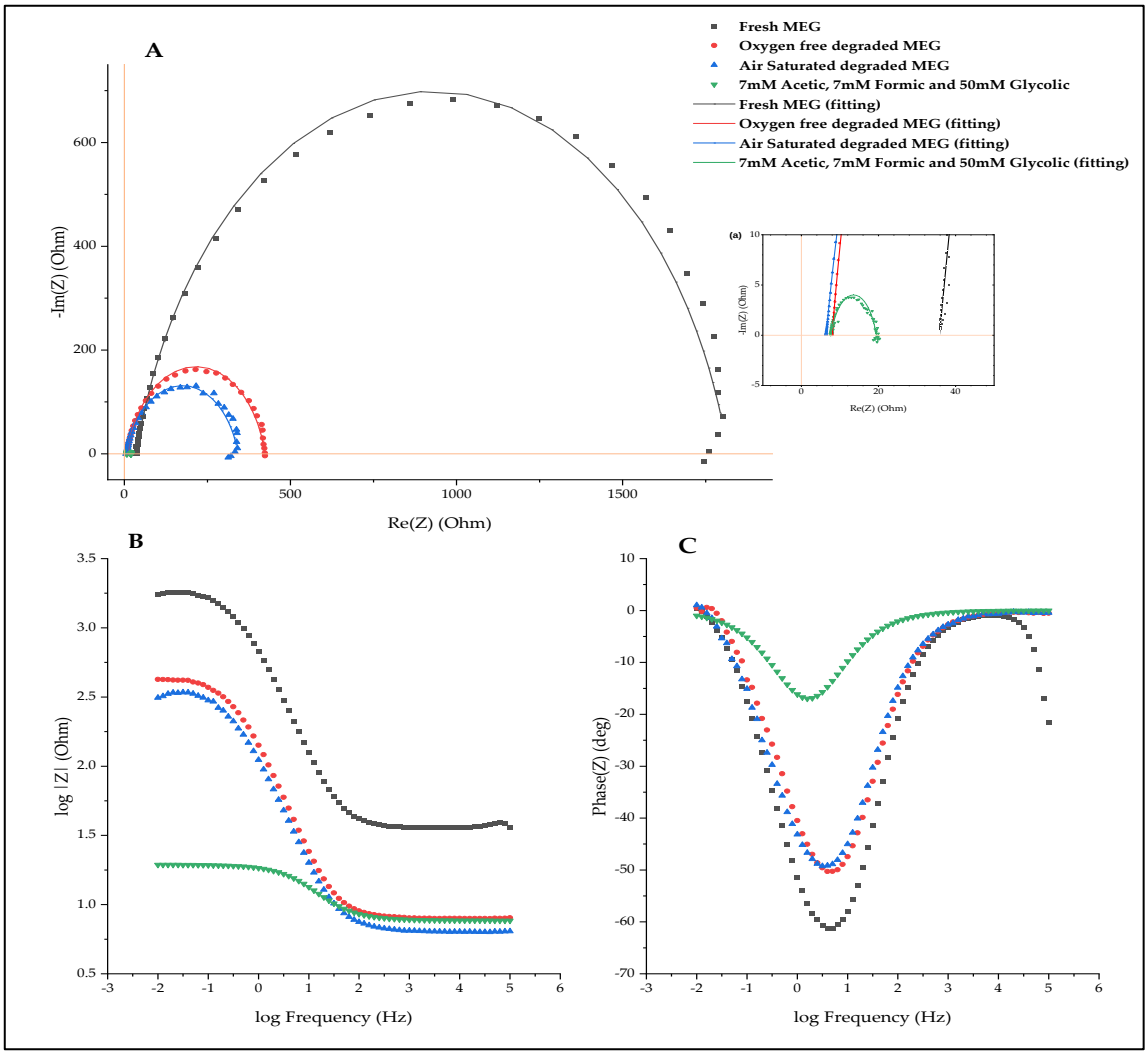

Figure 6-16: EIS Plots for carbon steel at stabilised OCP in 21 days of air-saturated degraded MEG and fresh MEG with added organic acids at 80 ^{0}C and 1500 rpm. A) Nyquist plot a) zoomed content of A. B) and C) Bode plots.

6.4.6 Further discussion

Findings from this study expand knowledge on the degradation of MEG and its effect on CO_2 corrosion of carbon steel. The study in Chapter 5 of this thesis confirms that air-saturated degradation of MEG produces more organic acids than oxygen-free degradation at 140 °C. Densities and viscosity data presented in this chapter support this increased degradation in air-saturated degradation compared to oxygen-free degradation as densities and viscosities reduced with increasing organic acids in solutions. Electrochemical data presented here also show an increasing corrosion rate for carbon steel with the degradation of MEG. However, the increase in organic acids produced by degradation does not explain the associated trends in corrosion rate for degraded MEG.

Generally, corrosion rates increased with increased temperature and shear rates, with 80 °C at 1500 rpm presenting the highest corrosion rates for all tests. While total organic acids increased only up to 0.1mM in 21 days oxygen-free degraded MEG, corrosion rates at 80 °C at 1500 rpm increased from 0.08 mm/yr to 0.36 mm/yr. This is slightly more than a 3.5-fold increase in corrosion rate. On the other hand, a 10-fold increase in corrosion rate is observed in the air-saturated degradation of MEG under the same conditions, whereas the total organic acid content in air-saturated degradation goes up to 50mM. The corrosion rate increased up to 0.8 mm/yr. in air-saturated degraded MEG.

Compared with added organic acids in fresh MEG, corrosion rates were significantly higher than in degraded MEG, even when organic acids contents were comparable, as in the 21-day air-saturated degraded MEG. The corrosion rate increased 142 folds with 64 mM total added organic acid but only 10 folds in 21 days air-saturated degraded MEG with about 50 mM total organic acid and 3.5 folds in oxygen-free degraded MEG with about 0.1 mM total organic acid.

These results suggest an inhibitive effect of thermal degradation on the CO_2 corrosion of carbon steel. It is proposed that there is an influence of MEG degradation products, other than the widely postulated organic acids, which are yet to be determined. Aldehydes are known intermediates for the production of organic acids from glycols. The summary for possible MEG degradation pathways summarised in Figure 5-13: A *suggested mechanism for the production of acetic acid from anaerobic thermal degradation of MEG.*" shows glycolaldehyde, glyoxal and acetaldehyde as intermediate products. While the corrosion-inhibition properties of these aldehydes have not been intrinsically investigated, some studies exist that elude to the corrosion-inhibitive properties of aldehydes in general.

Salix leaves water extract, consisting of 91.39% glyceraldehyde dimer, has been proposed as a novel green corrosion inhibitor for mild steel in sulphuric acid, providing up to 80% inhibition efficiency depending on concentration and temperature [49]. Wang et al. (2012) have reported excellent corrosion inhibition performance for water-soluble aldehydes for carbon steel corrosion [50]. Avdeev et al. (2012) also reported the inhibitive effect of unsaturated aldehydes on mild steel corrosion in solutions of hydrochloric and sulphuric acids [51].

6.5 Conclusion

The effect of the thermal degradation of MEG on the CO_2 corrosion of carbon steel under different conditions has been explored. In general, CO_2 corrosion of carbon steel increased with the degradation of MEG. However, the corrosion rate was significantly less than the corrosion rate for fresh MEG with added

organic acids at the same concentration. The increased corrosion rate in degraded MEG is not explained solely by the increase in produced organic acids.

These results suggest an inhibitive effect of the thermal degradation of MEG on the CO_2 corrosion of carbon steel. The inhibitive effect of small concentrations of aldehydes has been reported in literature. Therefore, it is a reasonable postulation that these aldehydes may contribute to this inhibitive effect of thermal degradation of MEG on CO_2 corrosion of carbon steel. However, this influence of aldehydes on CO_2 corrosion of carbon steel in degraded MEG cannot be concluded without further investigation. Consequently, this further investigation on the influence of aldehydes on CO_2 corrosion of carbon steel in degraded MEG is proposed for further research.

References

1. Karami, M. (2012). Review of corrosion role in gas pipeline and some methods for preventing it. *Journal of pressure vessel technology, 134*(5).
2. Akinyemi, O., Nwaokocha, C., & Adesanya, A. (2012). Evaluation of corrosion cost of crude oil processing industry. *Journal of Engineering Science and Technology, 7*(4), 517-528.
3. Wright, E. J. (2017). Materials Integrity by Design. *International Journal of Offshore and Polar Engineering, 27*(03), 239-244.
4. Gardner, L. (2005). The use of stainless steel in structures. *Progress in Structural Engineering and Materials, 7*(2), 45-55.
5. Tuttle, R. (1987). Corrosion in oil and gas production. *Journal of Petroleum Technology, 39*(07), 756-762.
6. Gonzalez, J. J., Alfonso, M. E., & Pellegrino, G. (2000). *Corrosion of Carbon Steels in Monoethylene Glycol*. Paper presented at the CORROSION 2000, Orlando, Florida. https://doi.org/
7. Halvorsen, A. M. K., Andersen, T. R., Halvorsen, E. N., Kojen, G. P., Skar, J. I., Biørnstad, C., et al. (2007). *The Relationship Between Internal Corrosion Control Method, Scale Control And Meg Handling Of A Multiphase Carbon Steel Pipeline Carrying Wet Gas With CO2 And Acetic Acid.* Paper presented at the CORROSION 2007.
8. Pojtanabuntoeng, T., Salasi, M., & Gubner, R. (2014). *The Influence of Mono Ethylene Glycol (MEG) on CO2 Corrosion of Carbon Steel at Elevated Temperatures (80 to 120oc)*. Paper presented at the CORROSION 2014, San Antonio, Texas, USA. https://doi.org/
9. Ikeh, L., Enyi, G., & Nasr, G. (2016). *Inhibition Performance of Mild Steel Corrosion in the Presence of Co 2, HAc and MEG.* Paper presented at the SPE International Oilfield Corrosion Conference and Exhibition.
10. Soames, A., Salasi, M., Barifcani, A., & Gubner, R. (2019). Corrosion of Carbon Steel during High Temperature Regeneration of Monoethylene Glycol in the Presence of Methyldiethanolamine. *Industrial & Engineering Chemistry Research, 58*(32), 14814-14822.
11. Mendez, C., Singer, M., Comacho, A., Nesic, S., Hernandez, S., Sun, Y., et al. (2005). *Effect of Acetic Acid, pH and MEG on the CO2 Top of the Line Corrosion.* Paper presented at the CORROSION 2005.
12. Ivonye, I., Wang, C., Hu, X., & Neville, A. (2013). *Corrosion Study of Carbon Steel in the Presence of Monoethylene Glycol (MEG) and Corrosion Inhibitors in Acid.* Paper presented at the CORROSION 2013.

13. Ivonye, I., Wang, C., & Neville, A. (2015). *The corrosion of carbon steel in the presence of Monoethylene glycol (MEG)–assessing the influence of an iron carbonate scale.* Paper presented at the CORROSION 2015.
14. Ekawati, D., Berntsen, T., Seiersten, M., & Hemmingsen, T. (2017). Effect of Temperature, Bicarbonate, and MEG Concentrations on CO2 Corrosion of Carbon Steels. *Corrosion, 73*(9), 1157-1167.
15. Pojtanabuntoeng, T., & Salasi, M. (2017). An electrochemical study of carbon steel CO2 corrosion in the presence of monoethylene glycol: The effects of pH and hydrodynamic conditions. *Electrochimica Acta, 258*, 442-452.
16. Islam, M. M., Pojtanabuntoeng, T., & Gubner, R. (2018). Corrosion of carbon steel under condensing water and monoethylene glycol. *Corrosion Science, 143*, 10-22.
17. Zaboon, S., Soames, A., Ghodkay, V., Gubner, R., & Barifcani, A. (2017). Recovery of mono-ethylene glycol by distillation and the impact of dissolved salts evaluated through simulation of field data. *Journal of Natural Gas Science and Engineering, 44*, 214-232. doi:https://doi.org/10.1016/j.jngse.2017.04.007
18. Zaboon, S. M. Z. (2019). *Monoethylene Glycol Distillation System Design Validation, Operation and Effluent Treatment.* Curtin University,
19. Badi, D., Al Helal, A., Lagat, C., Phan, C., & Barifcani, A. (2021). Evaluation of reboiler temperature retention time on MEG degradation products at varying MEG concentrations. *Journal of Petroleum Science and Engineering, 196*, 107735. doi:https://doi.org/10.1016/j.petrol.2020.107735
20. AlHarooni, K., Barifcani, A., Pack, D., Gubner, R., & Ghodkay, V. (2015). Inhibition effects of thermally degraded MEG on hydrate formation for gas systems. *Journal of Petroleum Science and Engineering, 135*, 608-617. doi:https://doi.org/10.1016/j.petrol.2015.10.001
21. Santambrogio, M., Perrucci, G., Trueba, M., Trasatti, S., & Casaletto, M. (2016). Effect of major degradation products of ethylene glycol aqueous solutions on steel corrosion. *Electrochimica Acta, 203*, 439-450.
22. Bostick, D. T. (2002). *Characterization of soluble organics in produced water*. Retrieved from
23. Latta, T. M., Seiersten, M. E., & Bufton, S. A. (2013). *Flow assurance impacts on lean/rich MEG circuit chemistry and MEG regenerator/reclaimer design.* Paper presented at the Offshore technology conference.
24. Gabe, D. R., Wilcox, G., Gonzalez-Garcia, J., & Walsh, F. (1998). The rotating cylinder electrode: its continued development and application. *Journal of Applied Electrochemistry, 28*(8), 759-780.
25. Tran, T. N. (2014). *Corrosion Mechanisms of Mild Steel in Weak Acids.* Ohio University,

26. ASTM G102-89 Standard Practice for Calculation of Corrosion Rates and Related Information from Electrochemical Measurements. (2015). In *ASTM G102-89(2015)e1*. West Conshohocken, PA: ASTM International,.
27. Pojtanabuntoeng, T., Kinsella, B., Ehsani, H., & McKechnie, J. (2017). Assessment of corrosion control by pH neutralisation in the presence of glycol at low temperature. *Corrosion Science, 126*, 94-103.
28. ASTM G59-97 Standard Test Method for Conducting Potentiodynamic Polarization Resistance Measurements. (2014). In. West Conshohocken, PA: ASTM International,.
29. Mansfeld, F. (2005). Tafel slopes and corrosion rates obtained in the pre-Tafel region of polarization curves. *Corrosion Science, 47*(12), 3178-3186.
30. Stern, M., & Geary, A. L. (1957). Electrochemical polarization: I. A theoretical analysis of the shape of polarization curves. *Journal of The Electrochemical Society, 104*(1), 56.
31. *Basics of electrochemical impedance spectroscopy*. (2007). Retrieved from [online] https://www.gamry.com/application-notes/EIS/basics-of-electrochemical-impedance-spectroscopy/:
32. Hahn, J., Edison, T., & Edgar, T. F. (2001). A note on stability analysis using bode plots. *Chemical Engineering Education, 35*(3), 208-211.
33. Bisquert, J., & Guerrero, A. (2022). Chemical Inductor. *Journal of the American Chemical Society, 144*(13), 5996-6009.
34. Islam, M., Gubner, R., & Pojtanabuntoeng, T. (2021). *Electrochemical Investigation into the Influence of Monoethylene Glycol on CO2 Corrosion in the Presence of Acetic Acid.* Paper presented at the CORROSION 2021.
35. Javidi, M., & Khodaparast, M. (2015). Inhibitive Performance of Monoethylene Glycol on CO2 Corrosion of API 5L X52 Steel. *Journal of Materials Engineering and Performance, 24*(4), 1417-1425. doi:10.1007/s11665-015-1415-3
36. Nahir, T. M. (2005). Fundamentals of Impedance Spectroscopy. In J. R. Macdonald, Barsoukov E (Ed.), *Impedance Spectroscopy: Theory, Experiment, and Applications,* (pp. 1-20). Hoboken, NJ: John Wiley & Sons, Inc.
37. Hernández, H. H., Reynoso, A. M. R., González, J. C. T., Morán, C. O. G., Hernández, J. G. M., Ruiz, A. M., et al. (2020). Electrochemical impedance spectroscopy (EIS): A review study of basic aspects of the corrosion mechanism applied to steels. *Electrochemical Impedance Spectroscopy*, 137-144.
38. Grahame, D. C. (1947). The electrical double layer and the theory of electrocapillarity. *Chemical reviews, 41*(3), 441-501.
39. Randles, J. E. B. (1947). Kinetics of rapid electrode reactions. *Discussions of the faraday society, 1*, 11-19.

40. Sandengen, K., Kaasa, B., & Østvold, T. (2007). pH Measurements in Monoethylene Glycol (MEG) + Water Solutions. *Industrial & Engineering Chemistry Research, 46*(14), 4734-4739. doi:10.1021/ie061305a
41. Gabe, D. R., & Walsh, F. C. (1983). The rotating cylinder electrode: a review of development. *Journal of Applied Electrochemistry, 13*(1), 3-21. doi:10.1007/BF00615883
42. Walsh, F., Kear, G., Nahle, A. H., Wharton, J., & Arenas, L. (2017). The rotating cylinder electrode for studies of corrosion engineering and protection of metals—An illustrated review. *Corrosion Science, 123*, 1-20.
43. Pine Research Instrumentation. (2006). Study of mass-transport limited corrosion using Pine rotated cylinder electrodes. An overview of theory and practice. In P. R. Instrumentation (Ed.), *Pine Research Instrumentation Technical Note* (Vol. 2006-01). 5908 Triangle Drive, Raleigh, N.C. 27617. USA: Pine Research Instrumentation.
44. ASTM D1217-20 Standard Test Method for Density and Relative Density (Specific Gravity) of Liquids by Bingham Pycnometer. (2007). In *Annual Book of Standards*. West Conshohocken, PA: ASTM International.
45. Atkins, P., Atkins, P. W., & de Paula, J. (2014). *Atkins' physical chemistry*: Oxford university press.
46. Fajardo, V., Canto, C., Brown, B., & Nesic, S. (2007). *Effect of organic acids in CO2 corrosion.* Paper presented at the CORROSION 2007.
47. Okafor, P. C., Brown, B., & Nesic, S. (2009). CO2 corrosion of carbon steel in the presence of acetic acid at higher temperatures. *Journal of Applied Electrochemistry, 39*(6), 873-877.
48. Rammelt, U., Koehler, S., & Reinhard, G. (2009). Use of vapour phase corrosion inhibitors in packages for protecting mild steel against corrosion. *Corrosion Science, 51*(4), 921-925.
49. Mahgoub, F. M., Hefnawy, A., & Hameed, E. (2020). Novel Green Corrosion Inhibitor for Mild Steel in Sulfuric Acid. *Protection of Metals and Physical Chemistry of Surfaces, 56*(2), 450-458. doi:10.1134/S2070205120020318
50. Wang, Y., Wang, T., Wang, B., Chang, W., Cao, J., Hu, L., et al. (2022). Performance Evaluation of a Novel and Effective Water-Soluble Aldehydes as Corrosion Inhibitor for Carbon Steel in Aggressive Hydrochloric Medium. *Journal of Renewable Materials, 10*(2), 301-327. doi:https://doi.org/10.32604/jrm.2021.015518
51. Avdeev, Y. G., Kuznetsov, Y. I., & Buryak, A. K. (2013). Inhibition of steel corrosion by unsaturated aldehydes in solutions of mineral acids. *Corrosion Science, 69*, 50-60. doi:https://doi.org/10.1016/j.corsci.2012.11.016

Chapter 7

Conclusions

This work sort to provide answers to several research questions by investigating the chemical interaction of MEG during high-temperature regeneration. Several findings have been made from this work, and future research prospects have been uncovered. The following conclusions can be deduced from these findings.

7.1 Conclusions

Chapter 3: A robust alternative methodology for assay of MEG samples from the MEG regeneration Unit.

- Ion chromatography can be applied to the assay of MEG samples from the MEG Recovery Unit (MRU) with spikes recovery >91% and Relative standard deviation <5.25% (n = 20) for samples from a pilot scale MRU.
- Both the Dionex™ CS16 and CS19 columns are applicable for analysing significant cations found in MRU MEG samples; however, the CS16 column is preferred when MDEA is not used for pH stabilisation corrosion mitigation.
- The simultaneous determination of MDEA and other cations in MEG MRU samples can be achieved by ion chromatography using the test

method detailed in Table 3-6: IC test method and parameters for CS19 column.

- The Dionex™ AS11 column is applicable for analysing significant cations found in MRU MEG samples.

The Cation test methods are presented in .

- Table 3-5: IC test method and parameters for CS16 column and Table 3-6: IC test method and parameters for CS19 column.
- The anion test method is presented in Table 3-13: Organic acid test method parameters.

Chapter 4: The effect of MEG on the solubility of calcium ions in the MEG regeneration Unit

- Calcium carbonate solubility decreases with temperature and reaches the minimum at 90°C. Increasing temperature beyond 90°C promotes the dissolution of $CaCO_3$.
- The presence of MEG increased the activity coefficient of calcium carbonate and calcium ions with respect to temperature.
- Above 120 C, degradation of MEG occurred leading to organic acid formation and the calcium ion solubility increasing with increasing organic acid content. There was a correlation between acetate ions (dominant degradation product under this condition) concentration and dissolved calcium concentration suggesting the chelation of the calcium ion with organic acid ions.

Chapter 5: The thermal oxidative degradation of MEG during regeneration

- The pH of the degrading MEG solution declines at a steady state in correlation with the organic acid accumulation. However, the rate of change in pH was higher for the less concentrated MEG solution, concurrent with the increase in acid dissociation constants (pKa) for these organic acids with increasing MEG mole fraction solution
- At the test temperature of 140 °C, negligible amount of oxalic was observed, glycolic acid and formic acid being the two primary organic acids produced during the degradation of MEG.
- The anaerobic degradation of MEG favoured acetic acid production at the test temperature, especially with the more concentrated MEG solution and the presence of calcium salt.

Chapter 6: The effect of thermal degradation on the CO_2 corrosion of carbon steel in the MEG regeneration unit

- CO_2 corrosion of carbon steel increased with degradation of MEG.
- Corrosion rate was significantly less than corrosion rate for fresh MEG with added organic acids.
- The increased corrosion rate in degraded MEG could not be explained solely by the increase in produced organic acid.
- Results suggested an inhibitive effect of thermal degradation of MEG on CO_2 corrosion of carbon steel.

7.2 Recommendations for future research

The following recommendations are made for future research.

- The influence of aldehydes on CO_2 corrosion of carbon steel in degraded MEG is postulated from findings in this work, however further investigation on this influence is required; electrochemical tests

can be conducted to study this inhibitive effect from aldehydes and is therefore proposed for future research.

- While aldehydes are known intermediates during the thermal degradation of MEG, the kinetics of conversion and stability of these aldehydes during thermal degradation of MEG remain unclear. Further investigation into characterisation of aldehydes species in the thermal degradation of MEG is recommended, as it will expand knowledge in this field of study.
- While chapter 4 of this thesis accurately measures the amount of $CaCO_3$ in solution for the experiments reported therein, it assumes that all the $CaCO_3$ dissolves in solution resulting in equal concentration of Ca^{2+} and CO_3^{2-} ions. This, however, does not account for the possible reaction of CO_3^{2-} ions to HCO_3^- and OH which diminishes the concentration of CO_3^{2-} ions and the activity coefficient of Ca^{2+}. The results in chapter 4 are recommended as a starting point for future study where the CO^2 partial pressure is controlled and the concentration of HCO^{3-} and CO_3^{2-} can be calculated.
- Chapter 6 of this thesis studied the corrosivity of thermally degraded MEG on carbon steel in the MEG regeneration unit and reports corrosion rates in MEG solutions, however the work did not generate sufficient data to draw conclusions concerning associated corrosion reaction mechanisms. Future research in this area could investigate the corrosion reaction mechanism for carbon steel in thermally degraded MEG.

Appendix

Copyright and permissions

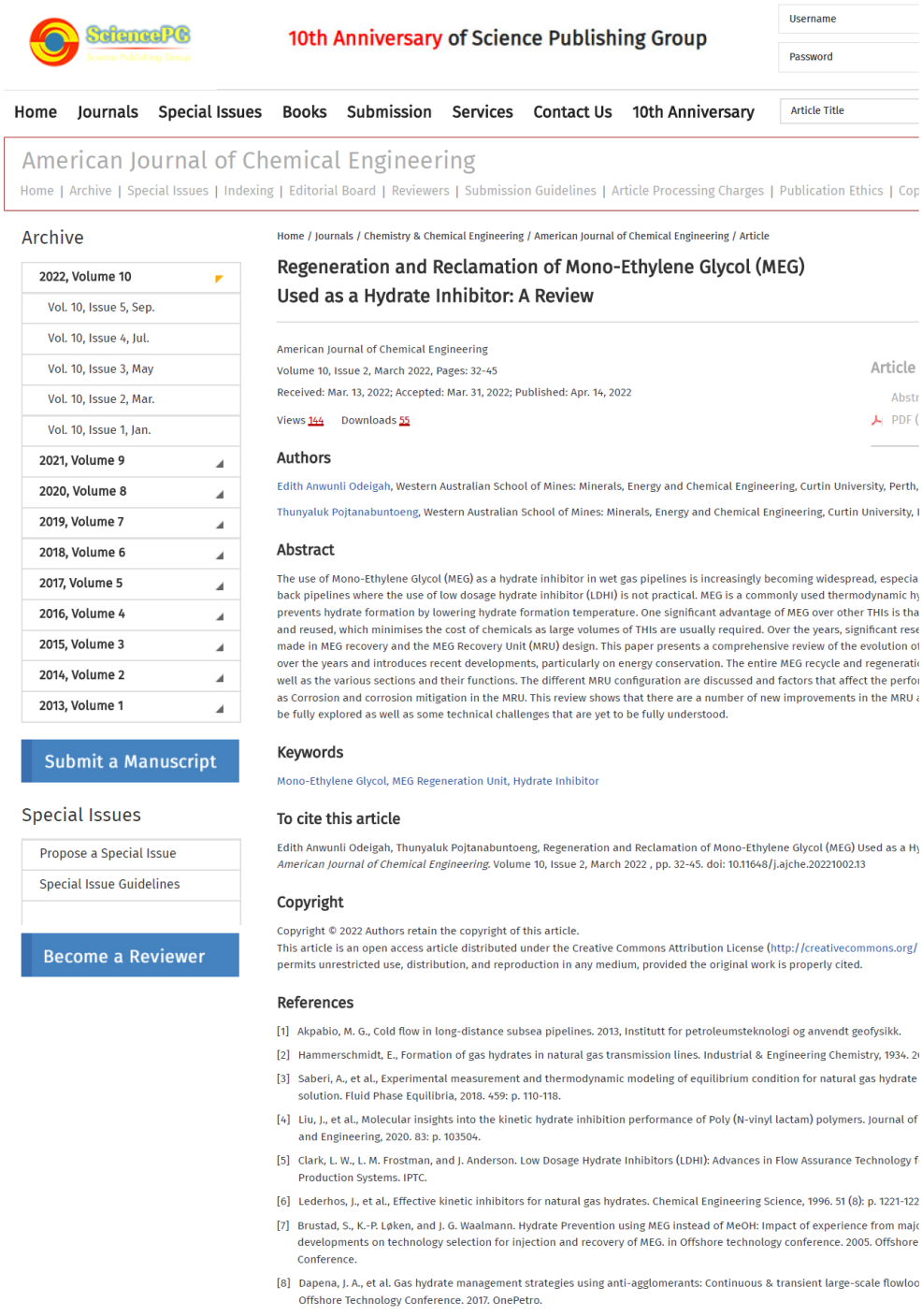

Regeneration and Reclamation of Mono-Ethylene Glycol (MEG) Used as a Hydrate Inhibitor: A Review

American Journal of Chemical Engineering
Volume 10, Issue 2, March 2022, Pages: 32-45
Received: Mar. 13, 2022; Accepted: Mar. 31, 2022; Published: Apr. 14, 2022

Authors

Edith Anwunli Odeigah, Western Australian School of Mines: Minerals, Energy and Chemical Engineering, Curtin University, Perth,

Thunyaluk Pojtanabuntoeng, Western Australian School of Mines: Minerals, Energy and Chemical Engineering, Curtin University, I

Abstract

The use of Mono-Ethylene Glycol (MEG) as a hydrate inhibitor in wet gas pipelines is increasingly becoming widespread, especia
back pipelines where the use of low dosage hydrate inhibitor (LDHI) is not practical. MEG is a commonly used thermodynamic hy
prevents hydrate formation by lowering hydrate formation temperature. One significant advantage of MEG over other THIs is tha
and reused, which minimises the cost of chemicals as large volumes of THIs are usually required. Over the years, significant rese
made in MEG recovery and the MEG Recovery Unit (MRU) design. This paper presents a comprehensive review of the evolution of
over the years and introduces recent developments, particularly on energy conservation. The entire MEG recycle and regeneratio
well as the various sections and their functions. The different MRU configuration are discussed and factors that affect the perfo
as Corrosion and corrosion mitigation in the MRU. This review shows that there are a number of new improvements in the MRU
be fully explored as well as some technical challenges that are yet to be fully understood.

Keywords

Mono-Ethylene Glycol, MEG Regeneration Unit, Hydrate Inhibitor

To cite this article

Edith Anwunli Odeigah, Thunyaluk Pojtanabuntoeng, Regeneration and Reclamation of Mono-Ethylene Glycol (MEG) Used as a Hy
American Journal of Chemical Engineering. Volume 10, Issue 2, March 2022 , pp. 32-45. doi: 10.11648/j.ajche.20221002.13

References

[1] Akpabio, M. G., Cold flow in long-distance subsea pipelines. 2013, Institutt for petroleumsteknologi og anvendt geofysikk.

[2] Hammerschmidt, E., Formation of gas hydrates in natural gas transmission lines. Industrial & Engineering Chemistry, 1934. 2

[3] Saberi, A., et al., Experimental measurement and thermodynamic modeling of equilibrium condition for natural gas hydrate solution. Fluid Phase Equilibria, 2018. 459: p. 110-118.

[4] Liu, J., et al., Molecular insights into the kinetic hydrate inhibition performance of Poly (N-vinyl lactam) polymers. Journal of and Engineering, 2020. 83: p. 103504.

[5] Clark, L. W., L. M. Frostman, and J. Anderson. Low Dosage Hydrate Inhibitors (LDHI): Advances in Flow Assurance Technology f Production Systems. IPTC.

[6] Lederhos, J., et al., Effective kinetic inhibitors for natural gas hydrates. Chemical Engineering Science, 1996. 51 (8): p. 1221-122

[7] Brustad, S., K.-P. Løken, and J. G. Waalmann. Hydrate Prevention using MEG instead of MeOH: Impact of experience from majo developments on technology selection for injection and recovery of MEG. in Offshore technology conference. 2005. Offshore Conference.

[8] Dapena, J. A., et al. Gas hydrate management strategies using anti-agglomerants: Continuous & transient large-scale flowloo Offshore Technology Conference. 2017. OnePetro.